JMT

Journal of Musculoskeletal Trauma

Vol. 39, No. 3, July 2026

JMT Journal of Musculoskeletal Trauma

Vol. 39, No. 3, July 2026

Pages 185-274

The Korean Orthopaedic Trauma Association

pISSN 3058-6267
eISSN 3058-6275

JMT

Journal of Musculoskeletal Trauma | e-jmt.org

Vol. 39, No. 3, July 2026

The Korean Orthopaedic Trauma Association

JMT Journal of Musculoskeletal Trauma

e-jmt.org

pISSN 3058-6267
eISSN 3058-6275

Vol. 39, No. 3, July 2026

Aims and Scope

The Journal of Musculoskeletal Trauma is the official publication of the Korean Orthopaedic Trauma Association. It is an international, peer-reviewed, open access journal dedicated to advancing the science, education, and clinical care of musculoskeletal trauma. The journal provides a platform for the dissemination of high-quality research, innovative techniques, and multidisciplinary approaches that improve patient outcomes in the field of orthopedic trauma and related disciplines.

As an open access journal, all articles are freely available to readers worldwide, ensuring the widest possible dissemination of knowledge and promoting collaboration among researchers, clinicians, and educators.

The scope of the journal encompasses the prevention, diagnosis, treatment, and rehabilitation of musculoskeletal injuries, including but not limited to:

- Fractures, dislocations, and soft tissue injuries of the extremities and axial skeleton
- Advances in surgical techniques, implants, and prosthetic devices
- Biomechanical and biological research related to trauma and tissue healing
- Rehabilitation strategies and innovations for functional recovery
- Clinical and translational research bridging basic science and clinical practice

The journal invites submissions of original research articles, systematic reviews, meta-analyses, technical notes, and correspondence that contribute to the advancement of musculoskeletal trauma care. Submissions are welcomed from all regions of the world, promoting a diverse and inclusive exchange of knowledge and perspectives.

The *Journal of Musculoskeletal Trauma* serves as a resource for orthopedic surgeons, trauma specialists, researchers, rehabilitation professionals, and all healthcare providers involved in the care of musculoskeletal injuries. By fostering collaboration and disseminating cutting-edge findings, the journal aims to elevate the standards of trauma care globally.

Open Access

Publisher: The Korean Orthopaedic Trauma Association
Editor-in-Chief: Jae Ang Sim

Publishing/Editorial Office
The Korean Orthopaedic Trauma Association
2F, 202-a5, 12-16, Dasanjungang-ro 146 beon-gil, Namyangju 12285, Korea
Tel: +82-31-560-2187, Email: office@e-jmt.org

Printed by M2PI
#805, 26 Sangwon 1-gil, Seongdong-gu, Seoul 04779, Korea
Tel: +82-2-6966-4930, Fax: +82-2-6966-4945, Email: support@m2-pi.com

This work is supported by the 'Lottery Fund' of the 'Ministry of Strategy and Finance' and the 'Science and Technology Promotion Fund' of the 'Ministry of Science and ICT', contributing to the realization of social value and the development of national science and technology.

Published on July 25, 2026

JMT Journal of Musculoskeletal Trauma

e-jmt.org

pISSN 3058-6267
eISSN 3058-6275

Editorial Board

JMT Journal of Musculoskeletal Trauma

e-jmt.org

pISSN 3058-6267
eISSN 3058-6275

Contents

Vol. 39, No. 3, July 2026

Review Articles

Original Articles

Case Reports

JMT Journal of Musculoskeletal Trauma

pISSN 3058-6267 · eISSN 3058-6275
J Musculoskelet Trauma 2026;39(3):185-194
https://doi.org/10.12671/jmt.2026.00150

How do we know a fracture has healed? A narrative review of radiographic bone union definitions and assessment methods

Jeong-Hyun Koh, Seungyeob Sakong

Department of Orthopedic Surgery, Ajou University School of Medicine, Suwon, Korea

Bone union is the most commonly reported primary outcome in fracture treatment trials, yet no universally accepted radiographic definition exists. The widely taught criterion of "bridging callus on 3 of 4 cortices on anteroposterior and lateral radiographs" has no clearly identifiable primary source in the indexed literature. This narrative review traces the historical origins of radiographic bone union assessment, documents the heterogeneity of definitions used in clinical studies, and provides a comparative analysis of the standardized scoring systems developed to address this problem. A systematic PubMed search using six prespecified strategies, from database inception to March 2026, supplemented by hand-searching and citation tracking, identified 2,380 records. After screening, 359 articles on long-bone fractures were included. The "3 of 4 cortices" criterion appears most plausibly to derive from Panjabi's 1985 finding that cortical continuity was the strongest radiographic predictor of fracture strength (r=0.80), but no traceable validation study was identified despite citation tracking through successive Cochrane reviews (CD008579, pub2-pub4). In their 2008 study, Corrales and colleagues documented 11 different radiographic criteria across 123 studies, finding that '3 cortices' was used in only 27%. Five standardized scoring systems (Radiographic Union Score for Tibial fractures [RUST], modified RUST [mRUST], Radiographic Union Score for Hip [RUSH], Radiographic Union Score for Humeral fractures [RUSHU], and Radiographic Humerus Union Measurement [RHUM]) have improved interobserver reliability within specific anatomical settings but remain fragmented by site and limited to secondary bone healing. A 2024 analysis by Bax et al. further illustrated that this inconsistency is not limited to fractures, documenting 13 different criteria and nine classification systems within the osteotomy literature. The most widely used radiographic union criterion likely emerged through clinical teaching rather than formal validation. A minimum reporting framework is proposed to improve standardization in future studies. Consensus definitions, cross-site validation, and more objective assessment strategies are needed to resolve this four-decade-old problem.

Keywords: Bone union; Fracture healing; Radiographic assessment; Radiography; RUST

Review Article

Received: April 2, 2026
Revised: April 15, 2026
Accepted: April 20, 2026

Correspondence to:
Seungyeob Sakong
Department of Orthopedic Surgery, Ajou University School of Medicine, 164 Worldcup-ro, Yeongtong-gu, Suwon 16499, Korea
Tel: +82-31-219-5220
Email: sgsy4040@gmail.com

Introduction

Every orthopedic surgeon knows when a fracture has healed. Or at least, every orthopedic surgeon believes they know. The determination that a fracture has achieved union—that the bone has regained sufficient structural integrity to bear physiological loads—is one of the most consequential clinical decisions in musculoskeletal medicine. It dictates when a patient may return to weight-bearing, when hardware may be removed, and when a fracture should be deemed a nonunion requiring further intervention. It is also the single most common primary or secondary outcome measure in fracture treatment trials.

Yet this foundational assessment rests on remarkably unstable ground. There is no universally accepted radiographic definition of bone union. The criterion most commonly taught—"bridging callus on 3 of 4 cortices visible on anteroposterior and lateral radiographs"—has no clearly identifiable primary source in the indexed literature. It appears in textbooks, Cochrane reviews, and institutional protocols worldwide, yet systematic citation tracking failed to locate a definitive original study. It appears to be an educational convention that emerged through clinical teaching rather than formal validation.

The consequences of this definitional vacuum are not merely academic. When Corrales et al. [1] systematically reviewed 123 clinical studies in 2008, they found 11 different radiographic criteria for union, with "3 of 4 cortices" used in only 27%. A decade and a half later, Bax et al. [2], reviewing osteotomy studies, identified 13 criteria and nine classification systems, with nearly half of reviewed studies failing to define union at all—confirming that the definitional problem extends beyond fracture healing. The problem has not been solved; it has proliferated.

In response, the period from 2010 to 2020 saw the development of five structured scoring systems—Radiographic Union Score for Tibial fractures (RUST), modified RUST (mRUST), Radiographic Union Score for Hip (RUSH), Radiographic Union Score for Humeral fractures (RUSHU), and Radiographic Humerus Union Measurement (RHUM)—each designed to standardize radiographic union assessment for a specific anatomic site. These tools represent genuine progress, yet their proliferation by anatomic site, combined with the persistent failure of clinical trials to adopt them, means that the fundamental problem remains.

The purpose of this narrative review is threefold: to trace the historical origins of radiographic bone union assessment and identify how the "3 of 4 cortices" teaching convention emerged without a published source; to document the evolution from ad hoc definitions to structured scoring systems; and to provide a comparative analysis of the RUST, mRUST, RUSH, RUSHU, and RHUM systems, evaluating their strengths, limitations, and the gaps that remain.

Ethics statement

This study was a narrative review and did not require institutional review board approval or informed consent.

Methods

This narrative review was informed by a systematic literature search strategy. Six prespecified search strings (S1–S6) were executed in PubMed, covering the period from database inception through March 2026, targeting definitions and criteria for fracture union (S1), cortical bridging terminology (S2), radiographic scoring systems (S3), observer variability and reliability (S4), nonunion definitions (S5), and historical perspectives (S6). Full search strings are provided in Supplementary S1. Three additional seminal publications predating electronic indexing [3-5] were identified through hand searching of reference lists, and six further anchor papers not captured by the database searches were identified through backward and forward citation tracking, yielding a total of nine additional records from non-database sources.

After automated deduplication, 2,380 records were screened by title (Fig. 1). The scope was limited to long bone fractures of the appendicular skeleton (femur, tibia, humerus, radius, and ulna), including methodology and definition papers applicable across sites. Pre-specified exclusion criteria (detailed in Supplementary S1) removed spine, pediatric, pelvic, tumor, drug intervention, biomechanical modeling, arthrodesis, periprosthetic, and small bone studies, among others. After screening, 359 articles were retained. Article selection for the narrative synthesis was guided by 12 anchor papers (Table 1) identified a priori based on their seminal contribution to the development, validation, or critique of radiographic union assessment methods; of these, nine were identified through hand searching and citation tracking (as above), and three were captured by the database searches [1-12]. These were supplemented by 18 Tier 1 articles scored ≥12 points on a predefined relevance rubric.

This is a narrative review, not a systematic review. No formal data extraction or risk-of-bias assessment was performed. The heterogeneity of definitions and reporting styles across the included studies, combined with the conceptual and historical nature of the research question, supported a narrative rather than quantitative synthesis.

https://doi.org/10.12671/jmt.2026.00150

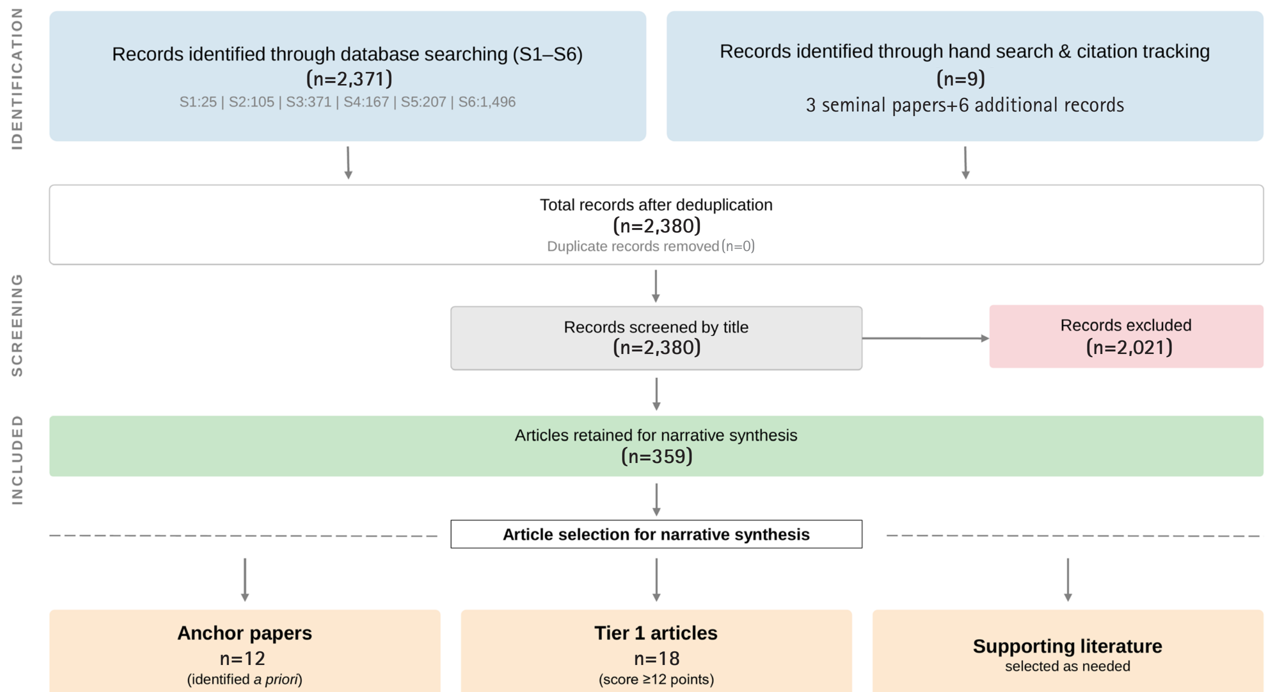

Fig. 1. Modified PRISMA flow diagram for the narrative review. Screening was performed by the principal investigator using title-based review. Article prioritization was guided by 12 anchor papers, including nine identified through hand-searching and citation tracking and three captured through database searches, together with a predefined relevance-scoring rubric (Supplementary S1). PRISMA, Preferred Reporting Items for Systematic reviews and Meta-Analyses.

Table 1. Anchor papers: foundational references for radiographic bone union assessment

No.	Study	PMID	Key contribution
1	White et al. (1977) [5]	845202	Four-stage biomechanical healing model
2	Panjabi et al. (1985) [4]	3998898	Cortical continuity r=0.80, best single predictor
3	Hammer et al. (1985) [3]	4042484	Radiographic accuracy ~50%, unreliability demonstrated
4	Corrales et al. (2008) [1]	18762645	11 Radiographic criteria, "3 cortices" only 27%
5	Whelan et al. (2002) [7]	11837825	κ=0.75 for cortical bridging, RUST motivation
6	Whelan et al. (2010) [8]	19996801	RUST development (ICC, 0.86)
7	Kooistra et al. (2010) [6]	20182243	RUST external validation (ICC, 0.84)
8	Litrenta et al. (2015) [9]	26165265	mRUST development, first union thresholds
9	Bhandari et al. (2013) [10]	23442540	RUSH development (ICC, 0.85–0.88)
10	DiSilvio et al. (2018) [12]	30882051	Any cortical bridging at 4 months predicts union
11	Ten Berg et al. (2020) [11]	31425411	68% of RCTs fail to report observer details
12	Bax et al. (2024) [2]	39534655	13 Criteria, 9 classifications, still no consensus

PMID, PubMed identifier; κ, kappa coefficient; RUST, Radiographic Union Score for Tibial fractures; ICC, intraclass correlation coefficient; mRUST, modified RUST; RUSH, Radiographic Union Score for Hip; RCT, randomized controlled trial.

The systematic search strategy was employed to ensure comprehensive identification of relevant literature and transparency regarding article selection. In addition, backward and forward citation tracking was performed to trace the origin of commonly used definitions, including tracking through successive editions of the Cochrane Collaboration's systematic review (CD008579, pub2 through pub4) [13-15]. The search strategy, screening flow diagram, and relevance scoring rubric are provided in Supplementary S1. A PRISMA-style flow diagram was used solely to enhance transparency of the search and screening process, not to imply a systematic review methodology; no duplicate records were identified across the six search strategies after automated deduplication. A limitation of this citation tracking is that non-indexed sources—including early Arbeitsgemeinschaft für Osteosynthesefragen/Association for the Study of Internal Fixation (AO/ASIF) manuals, preelectronic orthopedic textbooks, and institutional teaching handbooks—were not systematically reviewed, and therefore the possibility that the “3 of 4 cortices” criterion originated in such sources cannot be entirely excluded.

The origins of radiographic bone union assessment

The biomechanical foundation: White, Panjabi, and the four-stage model

The modern concept of radiographic union assessment can be traced to rabbit tibial osteotomy experiments conducted at Yale in the late 1970s. In 1977, White et al. [5] published a biomechanical model dividing fracture healing into four sequential stages, each defined by the relationship between radiographic appearance and mechanical stiffness. Stage III was characterized by partial cortical bridging accompanied by a marked increase in torsional rigidity. By stage IV, complete cortical remodeling had restored near-normal mechanical properties.

For the first time, this model linked specific radiographic features—particularly the degree of cortical bridging—to quantifiable mechanical endpoints. The observation that stage III, defined by partial cortical bridging, already conferred substantial mechanical strength planted the conceptual seed for what would eventually become the “3 of 4 cortices” clinical criterion. Although the 1977 study never specified a numerical threshold for cortex count, it established the principle that cortical bridging, rather than callus volume or fracture line obliteration, was the radiographic feature most closely associated with structural integrity.

Cortical continuity as the best single predictor: Panjabi 1985

Eight years later, Panjabi et al. [4] revisited this question with a more rigorous quantitative approach. They performed standardized tibial osteotomies in rabbits, allowed healing for 3 to 8 weeks, obtained orthogonal radiographs, and subjected each specimen to dynamic torsion testing. Radiographs were analyzed for five parameters: cortical continuity, callus thickness, callus diameter, fracture displacement, and callus area.

Cortical continuity emerged as the single best radiographic predictor of fracture strength (r=0.80). At the opposite end, callus area showed a correlation of only r=0.17—the weakest predictor. This finding contained a clinical paradox that remains relevant today: abundant callus formation, which is visually impressive and often intuitively reassuring, is in fact a poor indicator of mechanical strength. Conversely, the subtle finding of cortical continuity across the fracture site provides the most reliable evidence of structural healing.

If one accepts that two orthogonal radiographic views each display two cortices, and that cortical continuity is the dominant predictor of strength, then requiring bridging on “3 of 4 cortices” represents a clinical translation of Panjabi’s finding. However, these experiments were performed on rabbit tibiae with standardized transverse osteotomies, and neither White nor Panjabi ever stated a specific cortex count threshold. The extrapolation from r=0.80 to “3 out of 4 cortices” was a clinical simplification that occurred without formal validation.

The limits of radiographic assessment: Hammer 1985

In the same year, Hammer et al. [3] published a sobering counterpoint. They evaluated 127 tibial fractures treated conservatively, having seven experienced surgeons independently assess radiographs for evidence of union. The overall accuracy was approximately 50%—essentially no better than a coin toss. Even more concerning, 55% of fractures that were mechanically unstable on subsequent clinical testing had been judged as “united.” The interobserver agreement was poor.

Hammer’s findings exposed a fundamental contradiction: the specialty had adopted plain radiography as its primary tool for determining when a fracture had healed, yet the reliability of this determination was no better than chance. This should have triggered immediate efforts toward standardization. Instead, it took another 25 years before the first validated scoring system was published.

https://doi.org/10.12671/jmt.2026.00150

The era of ad hoc definitions (1990s–2000s)

Corrales 2008: quantifying the problem

The extent of definitional inconsistency was first systematically documented by Corrales et al. [1] in 2008. In a landmark systematic review of 123 clinical studies published in three major orthopedic journals between 1996 and 2006, they found 11 distinct radiographic criteria. The most commonly cited criterion was bridging by callus, bone, or trabeculae (53%), followed by bridging at three cortices (27%) and fracture line obliteration or cortical continuity (18%).

The quality reporting was equally troubling. Seventy-four percent of studies did not identify who had assessed the radiographs. Among the 26% that did, the assessors were orthopedic surgeons (19%), radiologists (2%), or both (4%). In three of the five studies that included both surgeons and radiologists, the two groups disagreed—with radiologists consistently reporting later times to union and lower union rates. Only two of the 123 studies reported any quantitative measure of interobserver reliability for their union assessment. This meant that the vast majority of fracture treatment conclusions were based on an outcome that had neither a standard definition nor a demonstrated reliability.

The “3 of 4 cortices” origin: a citation-free teaching convention

The Corrales data revealed an uncomfortable truth: the criterion most orthopedic surgeons consider “standard” was used in only 27% of studies and was not even the most common criterion. Critically, no study cited an original source for this definition [1].

This observation prompted systematic citation tracking through the Cochrane Collaboration’s review of interventions for promoting fracture healing (CD008579). This Cochrane review, published in multiple versions from 2012 through 2023 [13-15], explicitly adopted the “3 of 4 cortices” criterion, stating: “For the purpose of this review we adopted the widely accepted definitions in the literature.” However, no specific primary reference was cited for this definition. The phrase “widely accepted definitions in the literature” appeared identically in all versions from pub2 (2012) to pub4 (2023), and the reference list —while including the 2010 study by Kooistra et al. [6] for the RUST scoring system—did not contain a primary source establishing the “3 of 4 cortices” rule itself. Even the Cochrane Collaboration, regarded as the gold standard of evidence synthesis, adopted this criterion without being able to cite its origin.

This finding constitutes a central argument of the present review. The most widely recognized criterion for radiographic bone union—adopted by Cochrane and taught worldwide—has no clearly identifiable primary source in the indexed literature. It appears to be an educational convention: widely practiced, though no dedicated validation study has been identified. The most plausible genealogy is that clinicians translated Panjabi’s emphasis on cortical continuity (r=0.80) into a practical threshold based on anteroposterior (AP) and lateral radiographs. This translation occurred through clinical teaching—residency programs, conferences, and institutional protocols—rather than through a published validation study. By the time Corrales et al. [1] surveyed the literature in 2008, the “3 of 4 cortices” criterion was already established practice, yet none of those studies cited its origin because no definitive indexed primary source appears to exist.

The clinical reliability problem

Whelan et al. [7] had quantified the reliability problem in 2002. In a study of 30 tibial shaft fractures, four trauma surgeons assessed radiographs using multiple methods. The number of cortices bridged by callus achieved the highest agreement (κ=0.75), followed by visible fracture line (κ=0.70) and the surgeon’s general impression (κ=0.67). Even the best method produced only “substantial” agreement, meaning experienced trauma surgeons would disagree in approximately one of every four assessments. This established the clinical rationale for formal scoring systems.

The rise of radiographic scoring systems

RUST and mRUST

The RUST emerged directly from the 2002 reliability findings by Whelan et al. [8]. Each of four cortices visible on AP and lateral radiographs receives a score of 1 to 3 (1, fracture line, no callus; 2, visible fracture line with callus; 3, bridging callus, no fracture line), yielding a total of 4 (definitely not healed) to 12 (definitely healed). The system was designed specifically for tibial shaft fractures treated with intramedullary nailing, where the nail obscures medullary detail and only cortical assessment is possible.

In the development study, seven orthopedic reviewers—including three traumatologists, two community surgeons, and two residents—independently scored 45 sets of radiographs representing various stages of healing. Overall interobserver agreement was substantial (intraclass correlation coefficient [ICC], 0.86; 95% confidence interval [CI], 0.79–0.91), with traumatologists achieving the highest reliability (ICC, 0.86) followed by community surgeons (0.83) and residents (0.81). Intraobserver reliability was also substantial (ICC, 0.88). These values compared favorably with all previously reported methods. However, the original study was limited by a small radiograph set (n=45) and single-institution reviewers, and no union threshold was established. External validation by Kooistra et al. [6] confirmed reliability at an independent center (ICC, 0.84; 95% CI, 0.80–0.87).

The modified RUST (mRUST) expanded the scale to 4 points per cortex (adding a “remodeled” category), yielding a total of 4 to 16 [9]. In 12 experienced reviewers scoring distal femur fractures, mRUST showed higher reliability than RUST overall (ICC, 0.68 vs. 0.63), with notably better performance for nail fixation (ICC, 0.74) than plate fixation (ICC, 0.59). Prospective data from two multicenter randomized controlled trials (RCTs) provided the first data-driven union thresholds: more than 90% of reviewers considered a RUST of ≥10 and a mRUST of ≥13 to indicate union. Nails demonstrated significantly higher scores at union than plates (RUST 9.0 vs. 8.2; mRUST 12.3 vs. 10.8; P<0.01), reflecting the different biology of secondary versus primary bone healing.

RUSH

The RUSH addressed hip fractures involving both cortical and cancellous bone [10]. It incorporated cortical bridging (4–12), cortical fracture line disappearance (4–12), trabecular consolidation (1–3), and trabecular fracture line disappearance (1–3), for a total of 10 to 30. Six reviewers assessing 200 hip fracture cases achieved ICC (0.85) for femoral neck and 0.88 for intertrochanteric fractures—a dramatic improvement over the surgeon’s general impression (ICC, 0.60 and 0.50, respectively).

RUSHU and RHUM

The RUSHU extended structured assessment to humeral shaft fractures [16]. In 60 patients (40 union, 20 nonunion), interobserver ICC was 0.79. A RUSHU cutoff of <8 at 6 weeks was predictive of eventual nonunion (area under the curve, 0.84; odds ratio [OR], 12.0; 95% CI, 3.4–42.9), making it unique in its explicit focus on prediction rather than description. Subsequent prospective validation confirmed the reliability and clinical utility of the RUSHU in an independent cohort [17]. The RHUM was developed independently for nonoperatively managed humeral fractures [18], identifying cutoffs of ≤6 for nonunion risk and ≥9 for union, but was limited by a small sample (n=36) and did not report ICC values.

Comparative analysis

The proliferation of scoring systems represents genuine progress (Table 2). However, each was developed for a specific anatomic site, and none has been validated across sites. Union thresholds were established by different methodologies—consensus (RUST ≥10), reviewer percentage (mRUST ≥13), and receiver operating characteristic (ROC)

Table 2. Comparison of radiographic scoring systems for bone union

System	Target site	PMID	Scale/cortex	Total range	ICC (inter)	Union threshold[a]
RUST	Tibia (diaphyseal)	19996801	1–3	4–12	0.86	≥10 (90% agreement)
mRUST	Tibia/femur (metadiaphyseal)	26165265	1–4	4–16	0.68 (overall); 0.74 (nail)	≥13 (90% agreement)
RUSH	Hip (FN, IT)	23442540	Cortical 1–3×4+ trabecular 1–3×2	10–30	0.85 (FN); 0.88 (IT)	≥18 (suggested)
RUSHU	Humerus (shaft)	31564159	1–3	4–12	0.79	<8 nonunion risk (AUC 0.84)
RHUM	Humerus (nonoperative)	32034464	0–3	0–12	NR	≤6 nonunion/≥9 union

PMID, PubMed identifier; ICC, intraclass correlation coefficient; RUST, Radiographic Union Score for Tibial fractures; mRUST, modified RUST; RUSH, Radiographic Union Score for Hip; FN, femoral neck; IT, intertrochanteric; RUSHU, Radiographic Union Score for Humeral fractures; RHUM, Radiographic Humerus Union Measurement; NR, not reported; ROC, receiver operating characteristic.
[a]Union thresholds were derived using different methodologies: consensus (RUST), reviewer percentage agreement (mRUST), clinical suggestion (RUSH), and ROC analysis (RUSHU, RHUM).

https://doi.org/10.12671/jmt.2026.00150

analysis (RUSHU <8). The methodological limitations were systematically exposed by Ten Berg et al. [11]: 68% of recent orthopedic RCTs failed to report the specialty of the observer assessing union, and the median number of observers per trial was just one. The most recent confirmation came from Bax et al. [2], who, reviewing osteotomy studies, identified 13 criteria and nine classification systems, with 49.1% of studies failing to define union despite reporting it as an outcome—demonstrating that the problem persists across both fracture and osteotomy contexts.

Despite these differences, all five systems share a common conceptual architecture derived from Panjabi's finding that cortical continuity best predicts mechanical strength. This shared design logic can be distilled into four principles: (1) independent evaluation of discrete cortical or trabecular zones, rather than a single gestalt impression; (2) ordinal staging of each zone along a healing continuum (from no callus through bridging to remodeling); (3) summation into a composite score that allows threshold-based binary classification (union vs. nonunion); and (4) anatomic adaptation of the zone map to the specific fracture site. The five systems are therefore not five independent inventions but five site-specific implementations of a single underlying paradigm. Recognizing this shared architecture clarifies the nature of the fragmentation problem: what the field lacks is not a new conceptual model, but a unified scoring framework that can be parametrically adjusted across anatomic sites while maintaining cross-study comparability. The lack of cross-site validation and the divergence in scoring structures (3-point vs. 4-point scales, cortical-only vs. cortical-plus-trabecular components) have prevented this unification. A researcher using RUST ≥10 for tibial union and another using mRUST ≥13 for femoral union may both report "90% union at 6 months," yet the criteria are not interchangeable, and neither can be applied to a humeral fracture without adopting yet another system.

Practical considerations

For diaphyseal fractures treated with intramedullary nailing, the RUST or mRUST should be the primary assessment tool, with a mRUST ≥13 or RUST ≥10 indicating union. DiSilvio et al. [12] demonstrated that any cortical bridging at 4 months postoperatively was the most reliable early predictor of eventual union (κ=0.91)—suggesting that the simplest criterion may be the most useful for early decision-making. For hip fractures, the RUSH should be used given the dual cortical-trabecular healing pathway. For humeral shaft fractures, the RUSHU provides the only validated tool with demonstrated predictive capacity (RUSHU <8 at 6 weeks: 12-fold increased nonunion risk).

For fractures treated with compression plating, all callus-based scoring systems must be interpreted with extreme caution. Consider a simple transverse forearm fracture treated with compression plating that shows progressive fracture line obliteration at 6 months but no periosteal callus: a RUST-based assessment would yield a score of 4—formally indicating "definitely not healed"—while the fracture may have achieved solid primary union. This limitation is fundamental, not technical: current scoring systems were designed for secondary bone healing and systematically fail when applied to primary bone healing, where the absence of callus reflects the biomechanical environment rather than healing failure.

Beyond plain radiographs

The fundamental limitation of plain radiography—compressing three-dimensional anatomy into two-dimensional images—has long been recognized. Computed tomography (CT) provides cross-sectional assessment of cortical bridging around the entire circumference of the bone, and several studies have shown that CT detects bridging earlier and more accurately than plain radiographs [19]. However, its adoption as a routine union assessment tool has been limited by cost, radiation dose, metal artifact from implants, and—most critically—the absence of any standardized CT-based union scoring system. The RUST framework has not been formally adapted for CT, and no equivalent tool exists.

Ultrasound offers a non-ionizing, portable alternative capable of detecting callus earlier than radiographs [20], but remains operator-dependent and lacks standardized criteria comparable to the RUST framework. Other modalities including dual-energy X-ray absorptiometry [21], resonant frequency analysis [22], and bioimpedance monitoring [19] have shown promise in experimental settings but remain far from clinical implementation.

Perhaps most fundamentally, the conceptual framework underlying all cortex-based scoring systems—that union is defined by the presence of external callus—renders them blind to primary bone healing. When a fracture is treated with absolute stability, healing occurs through direct cortical reconstruction (Haversian remodeling) without visible callus. No modality-specific scoring system currently addresses this healing pattern, which represents not merely a technical gap but a paradigm limitation that must be addressed before any universal standard can be established.

Unresolved issues and future directions

An overarching issue underlying the definitional problem is that radiographic union is fundamentally a surrogate for clinical union—the restoration of pain-free, load-bearing function. The correlation between these two constructs has rarely been formally quantified, and clinical trials routinely treat radiographic endpoints as interchangeable with functional recovery despite incomplete evidence for this assumption. Any future consensus framework should therefore explicitly acknowledge this surrogate relationship and specify whether the intended endpoint is structural (radiographic evidence of cortical bridging), functional (return to weight-bearing or activity), or both.

Three specific areas require attention. First, a formal Delphi consensus process has never been specifically attempted for the question of radiographic bone union definition. Such a process—bringing together orthopedic traumatologists, radiologists, and clinical trialists—could establish minimum reporting standards, agree on a core set of radiographic parameters applicable across sites, and define thresholds for union and nonunion. The minimum reporting items proposed in Table 3 could serve as a starting point for such a consensus process. The Corrales-to-Bax trajectory (2008–2024) shows that the problem will not resolve spontaneously; it requires deliberate coordination.

Second, machine learning algorithms have already demonstrated high accuracy in fracture detection on plain radiographs. An artificial intelligence (AI) system trained on large datasets of serial radiographs with known clinical outcomes could potentially provide objective, reproducible union assessment, eliminating the interobserver variability that has plagued the field since the 1985 study by Hammer et al. [3]. However, AI-based assessment faces a circular problem: training an algorithm requires a ground truth label, and as this review demonstrates, there is no consensus on what that label should be. Training on RUST scores merely perpetuates the limitations of the score itself. The most promising approach may be to train AI on clinical outcomes (e.g., ability to bear weight without pain, absence of subsequent failure) rather than intermediate radiographic

Table 3. Proposed minimum reporting items for fracture union assessment in clinical studies

No.	Reporting item	Description and rationale
1	Explicit definition of union	State the radiographic criterion used to define union (e.g., bridging callus on 3 of 4 cortices, RUST score threshold, fracture line obliteration). If no validated criterion exists for the fracture type studied, this should be acknowledged.
2	Imaging modality and protocol	Specify the imaging modality (plain radiograph, CT, ultrasound), views obtained (AP, lateral, oblique), and whether standardized positioning was used.
3	Number, specialty, and experience of observers	Report how many observers assessed union, their specialty (orthopedic surgeon, radiologist, trainee), and their experience level. Corrales et al. [1] in 2008 found 74% of studies omitted this information.
4	Independence of assessment and consensus method	State whether observers assessed radiographs independently or by consensus, and describe the method for resolving disagreements (e.g., majority rule, adjudication by senior author).
5	Scoring system or assessment rule used	Identify any validated scoring system (RUST, mRUST, RUSH, RUSHU, RHUM) employed, with citation. If a non-validated criterion was used, provide its explicit definition. Report interobserver reliability (κ or ICC) when more than one observer is involved.
6	Timing of union assessment	Specify when union was assessed (e.g., fixed time point, serial assessment until endpoint, or clinician-determined). If serial, state the interval and total follow-up duration.
7	Relationship to clinical outcome	Describe whether and how radiographic union was correlated with clinical endpoints (pain-free weight-bearing, return to activity, absence of hardware failure). Radiographic union is a surrogate; its relationship to functional recovery should be made explicit.

RUST, Radiographic Union Score for Tibial fractures; CT, computed tomography; AP, anteroposterior; mRUST, modified RUST; RUSH, Radiographic Union Score for Hip; RUSHU, Radiographic Union Score for Humeral fractures; RHUM, Radiographic Humerus Union Measurement; ICC, intraclass correlation coefficient.

https://doi.org/10.12671/jmt.2026.00150

labels, thereby bypassing the definitional problem entirely.

Third, the problem extends beyond long bones. Pelvic ring fractures, periarticular fractures, and complex patterns such as segmental fractures or fractures with bone loss present assessment challenges that existing tools were not designed to handle. The next generation of union assessment tools will need to address this anatomic diversity.

Conclusions

Bone union is the most commonly reported outcome in fracture treatment research, yet the “3 of 4 cortices bridging” criterion—taught worldwide and adopted by the Cochrane Collaboration—has no clearly identifiable primary source in the indexed literature. It appears to be an educational convention born from the extrapolation of Panjabi's 1985 laboratory finding, transmitted through clinical teaching, and codified into practice without formal validation. The development of structured scoring systems (RUST, mRUST, RUSH, RUSHU, RHUM) between 2010 and 2020 improved interobserver reliability substantially, yet this progress remains fragmented by anatomic site, limited to secondary bone healing, and insufficiently adopted in clinical trials. To address these persistent gaps, we propose a set of minimum reporting items (Table 3) as a practical first step toward standardization. Until the orthopedic community agrees on what "healed" looks like on a radiograph, we cannot truly compare the outcomes of fracture treatment. This educational convention deserves formal validation, and the field urgently needs consensus definitions applicable across anatomic sites and healing patterns.

Article Information

Author contributions

Conceptualization: JHK, SS. Data curation: JHK. Investigation: JHK. Methodology: JHK, SS. Project administration: SS. Resources: JHK. Supervision: SS. Visualization: JHK.

Writing–original draft: JHK. Writing–review & editing: JHK, SS. All authors read and approved the final manuscript.

Conflicts of interest

No potential conflict of interest relevant to this article was reported.

Funding

None.

Acknowledgments

An AI-based tool (Claude, Anthropic; models used during manuscript preparation: Claude 3.5 Sonnet and Claude Opus 4) was used for language editing (grammar, clarity, and style). All content was reviewed and approved by the authors, who take full responsibility for the manuscript.

Data availability

Not applicable.

Supplementary materials

Supplementary materials related to this article can be found online at https://doi.org/10.12671/jmt.2026.00150.
Supplementary S1. Search strategy, screening flow, and article selection.

References

1. Corrales LA, Morshed S, Bhandari M, Miclau T. Variability in the assessment of fracture-healing in orthopaedic trauma studies. J Bone Joint Surg Am 2008;90:1862-8.
2. Bax EA, Harlianto NI, Custers RJ, van Egmond N, Foppen W, Kruyt MC. Radiographic assessment of bone union in proximal tibia and distal femur osteotomies: a systematic review. JBJS Open Access 2024;9:e24.00101.
3. Hammer RR, Hammerby S, Lindholm B. Accuracy of radiologic assessment of tibial shaft fracture union in humans. Clin Orthop Relat Res 1985;199:233-8.
4. Panjabi MM, Walter SD, Karuda M, White AA, Lawson JP. Correlations of radiographic analysis of healing fractures with strength: a statistical analysis of experimental osteotomies. J Orthop Res 1985;3:212-8.
5. White AA, Panjabi MM, Southwick WO. The four biomechanical stages of fracture repair. J Bone Joint Surg Am 1977;59:188-92.
6. Kooistra BW, Dijkman BG, Busse JW, Sprague S, Schemitsch EH, Bhandari M. The radiographic union scale in tibial fractures: reliability and validity. J Orthop Trauma 2010;24 Suppl 1:S81-6.
7. Whelan DB, Bhandari M, McKee MD, et al. Interobserver and intraobserver variation in the assessment of the healing of tibial fractures after intramedullary fixation. J Bone Joint

Surg Br 2002;84:15-8.
8. Whelan DB, Bhandari M, Stephen D, et al. Development of the radiographic union score for tibial fractures for the assessment of tibial fracture healing after intramedullary fixation. J Trauma 2010;68:629-32.
9. Litrenta J, Tornetta P, Mehta S, et al. Determination of radiographic healing: an assessment of consistency using RUST and modified RUST in metadiaphyseal fractures. J Orthop Trauma 2015;29:516-20.
10. Bhandari M, Chiavaras MM, Parasu N, et al. Radiographic union score for hip substantially improves agreement between surgeons and radiologists. BMC Musculoskelet Disord 2013;14:70.
11. Ten Berg PW, Kraan RB, Jens S, Maas M. Interobserver reliability in imaging-based fracture union assessment: two systematic reviews. J Orthop Trauma 2020;34:e31-7.
12. DiSilvio F, Foyil S, Schiffman B, Bernstein M, Summers H, Lack WD. Long bone union accurately predicted by cortical bridging within 4 months. JBJS Open Access 2018;3:e0012.
13. Griffin XL, Parsons N, Costa ML, Metcalfe D. Ultrasound and shockwave therapy for acute fractures in adults. Cochrane Database Syst Rev 2014;2014:CD008579.
14. Griffin XL, Smith N, Parsons N, Costa ML. Ultrasound and shockwave therapy for acute fractures in adults. Cochrane Database Syst Rev 2012;(2):CD008579.
15. Searle HK, Lewis SR, Coyle C, Welch M, Griffin XL. Ultrasound and shockwave therapy for acute fractures in adults. Cochrane Database Syst Rev 2023;3:CD008579.
16. Oliver WM, Smith TJ, Nicholson JA, et al. The Radiographic Union Score for HUmeral fractures (RUSHU) predicts humeral shaft nonunion. Bone Joint J 2019;101-B:1300-6.
17. Fordyce W, Kennedy G, Allen JR, et al. Validation of the Radiographic Union Score for HUmeral fractures (RUSHU): a retrospective study in an independent centre. Shoulder Elbow 2023;15:390-7.
18. Christiano AV, Pean CA, Leucht P, Konda SR, Egol KA. Scoring of radiographic cortical healing with the radiographic humerus union measurement predicts union in humeral shaft fractures. Eur J Orthop Surg Traumatol 2020;30:835-8.
19. Atwan Y, Schemitsch EH. Radiographic evaluations: which are most effective to follow fracture healing. Injury 2020;51 Suppl 2:S18-22.
20. Moed BR, Watson JT, Goldschmidt P, van Holsbeeck M. Ultrasound for the early diagnosis of fracture healing after interlocking nailing of the tibia without reaming. Clin Orthop Relat Res 1995;310:137-44.
21. Eyres KS, Bell MJ, Kanis JA. Methods of assessing new bone formation during limb lengthening. Ultrasonography, dual energy X-ray absorptiometry and radiography compared. J Bone Joint Surg Br 1993;75:358-64.
22. Sekiguchi T, Hirayama T. Assessment of fracture healing by vibration. Acta Orthop Scand 1979;50:391-8.

https://doi.org/10.12671/jmt.2026.00150

JMT Journal of Musculoskeletal Trauma
pISSN 3058-6267 · eISSN 3058-6275
J Musculoskelet Trauma 2026;39(3):195-204
https://doi.org/10.12671/jmt.2026.00171

Spine OpenSim models: a narrative review of the literature

Mohammad Taghi Karimi

Orthotics and Prosthetics Department, Rehabilitation Faculty of Shiraz University of Medical Sciences, Shiraz, Iran

The human spine is affected by various traumatic and pathological conditions that can impair function during daily activities. Several software programs have been developed to assess the risk of spinal injury, and OpenSim is one platform used for this purpose. Various OpenSim spine models have been developed to analyze parameters such as range of motion, moments applied to the vertebrae, muscle forces, and joint contact forces. This review aimed to compile the available OpenSim models that can be used to study the spine under normal and pathological conditions. Published studies using spine models in OpenSim were reviewed, and information on model outputs, availability, and validity was extracted. Keywords such as “spine models,” “lumbar models,” “musculoskeletal modeling,” and “trunk models” were used in combination with “OpenSim.” Eighty papers on spine models in OpenSim were identified, of which 23 were selected for final analysis. The available OpenSim models were classified as specific spine models (17 models) or full-body models (six models) that include the spine as a component. The available models can be used to assess injury risk, muscle forces, and joint contact forces in the cervical and lumbar spine. Full-body models allow examination of kinematics and joint contact forces at L5/S1, although only a limited number of muscles are represented in these models. Output validity has been evaluated in only a few models.

Keywords: Spine; Biological models; Biomechanical phenomena; Muscle strength; Computer simulation

Review Article

Received: April 13, 2026
Revised: May 2, 2026
Accepted: May 4, 2026

Correspondence to:
Mohammad Taghi Karimi
Orthotics and Prosthetics Department, Rehabilitation Faculty of Shiraz University of Medical Sciences, Sadra City Road, Shahid Doran Campus, Shiraz 7198754361, Iran
Tel: +98-71-3626-5489
Email: Mt_Karimi@Sums.ac.ir

Introduction

The performance of the musculoskeletal system influences individuals' abilities to carry out daily activities. Various diseases can impact this system’s performance, ultimately limiting daily activity. The treatment of these diseases depends on understanding their effects on kinematics, kinetics, joint contact forces, and muscle forces. While there are various methods available to determine and monitor these parameters, some can only be used in cadaveric studies. The moments and range of motion of the joints can be assessed using a motion analysis system and various approaches like inverse dynamics and inverse kinematics [1,2]. However, parameters such as joint contact forces must be evaluated based on sensor outputs inserted in the joints. These studies are often conducted on cadavers due to ethical concerns.

Now it is possible to determine joint contact forces and muscle forces using modeling approaches, which can be done with advanced software such as AnyBody and OpenSim [3]. AnyBody is commercial software, while OpenSim is free open-source software with a variety of models available.

Various models of OpenSim have been developed to analyse the motions of spine, muscle forces and also joint contact forces [4-6]. These models have been used for both normal and pathological conditions. Now use of these models is recommended to design various assistive devices, evaluation of sport activities and also to design implants. The models of the spine may include only articulated spine and also models with fully articulated thoracolumbar spine and rib cages. Depending on the models, they may include the trunk and cervical muscles. Although various models of the spine have been developed for use with OpenSim, it is not well determined which ones can be used for the cervical, lumbar, and total spine. Information regarding the validity and accuracy of the outputs of these models is not well-documented. Furthermore, it is not clear which types of these models can be used for designing assistive devices. The aim of this review was to introduce the available models of the spine that can be used in OpenSim software and to determine their validity based on available literature. Additionally, the goal was to determine the feasibility of using spine models depending on the research conducted.

Ethics statement

This study was a narrative review and did not require institutional review board approval or informed consent.

Methods

A comprehensive search was conducted in the existing literature to gather all studies on the use of OpenSim software in the analysis of spine motions in both normal and pathological conditions. The search was done in some databases including PubMed, Scopus, Web of Science, and Google Scholar. The search was done for a time period up to the end of 2025. Some keywords such as spine model, cervical model, lumbar model, musculoskeletal modeling, and trunk model were used in combination with OpenSim. The main inclusion criteria for selecting the papers were that only studies focusing on the use of spine models were included. The selection of the papers was done based on titles and abstracts. We attempted to categorize the available models of the spine based on their outputs, validity, and availability.

Results

There were 80 papers on spinal models in OpenSim software. However, only 23 papers were selected for final analysis. The models of the spine in OpenSim can be categorized into two main groups, which include (1) specific models of the spine; (2) full-body models that also include the spine.

Specific models of the spine

Musculoskeletal model of the lumbar spine

This model consists of a rigid pelvis and sacrum, five lumbar vertebrae, and torso (thoracic spine and ribcage). Each lumbar vertebra has 3 degrees of freedom (DOFs; flexion/extension, lateral bending, and axial rotation). The model has been developed to include 238 muscle fascicles which create eight muscle groups of the spine. In the newly developed model, each lumbar vertebra has 6 DOFs for both rotatory and translatory motions. The main limitation associated with this model is that it cannot be used for complex motions of the spine that involve motion across two or more planes [7]. Fig. 1 shows this model.

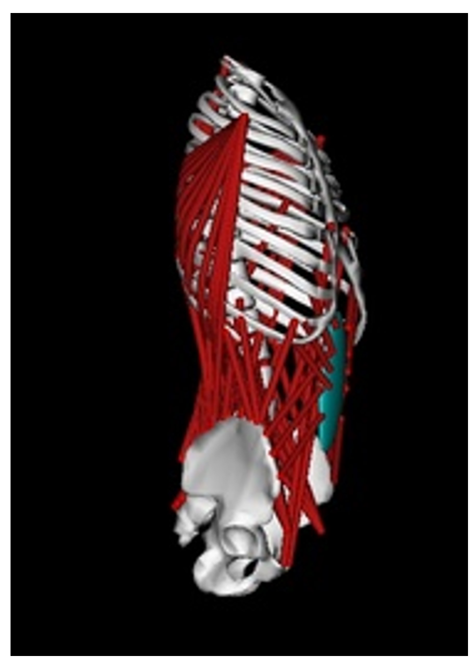

Fig. 1. Musculoskeletal model of the lumbar spine. The model includes a rigid pelvis and sacrum, five lumbar vertebrae, and the torso, including the thoracic spine and rib cage.

https://doi.org/10.12671/jmt.2026.00171

The thoracolumbar spine and rib cage model

This is fully articulated, including vertebrae from T1 to L5. It has 3 degrees of motion for rotational movement. This model also includes the head, neck, upper extremities, and most major muscles of the lumbar spine, abdomen, and intercostal muscles. There are 552 musculotendon actuators for trunk muscles and 620 actuators for the entire model, with a total of 93 DOFs in the spine. Static optimization can be used to determine muscle forces in this model, but computer muscle control cannot. The validity of the muscle forces and joint contact forces in this model was evaluated using data from the literature. This model can be used for designing exoskeletons and determining spinal loads in various lifting conditions [8]. Fig. 2 shows the thoracolumbar spine and rib cage model.

Full-body spine models with detailed thoracolumbar spine for children and adolescents

This model is a combination of articulated thoracolumbar spine and rib cage, combined head and neck with the upper and lower limb extremities. In this project, the data of 26 children and adolescents were used with ages of 6-18 years. It should be emphasized that model 2354 was used in this project [9]. The validity of the outputs of this model was evaluated with literature.

A model for estimating spinal loading during lifting and lowering tasks

A specific model (Fig. 3) was developed in this project. A fully articulated thoracolumbar model was created and validated using nine dynamic lifting tasks. Passive structures and kinematic constraints were incorporated into the model to enhance its accuracy in predicting spinal loads during dynamic tasks. The results of this study demonstrated that the model can effectively estimate spinal loads during lifting and lowering tasks, as well as perform inverse dynamics [10].

Articulated kinematic model of the thoracic and lumbar spine

This dynamic articulated model of the lumbar and thoracic spine, Fig. 4, is designed for kinematic analysis. It is a modification of Christophy's model, with the following enhancements [7].

The thoracic vertebrae in this model have been separated to increase the DOF. The pelvic section now features a custom joint that allows for translation in three-dimen-

Fig. 2. The thoracolumbar spine and rib cage model, including vertebrae from T1 to L5. It has three degrees of motion for rotational movement. This model also includes the head, neck, upper extremities, and most major muscles of the lumbar spine, abdomen, and intercostal muscles.

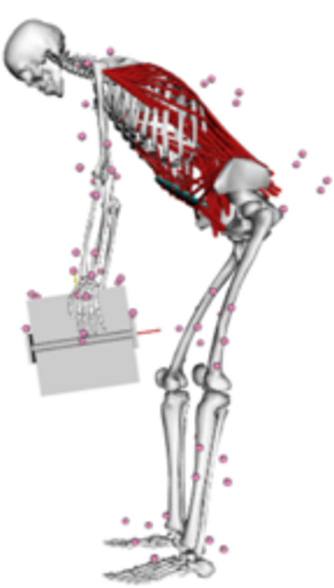

Fig. 3. Spine model for estimating spinal loading during lifting and lowering tasks. Passive structures and kinematic constraints were incorporated to improve the accuracy of spinal load prediction during dynamic tasks.

sional space. The rib cage has been removed from the previous model. This modification allows for the addition of a greater number of markers to scale the model effectively.

Lumbar spine with passive elements

In this model, the structure of the lumbar spine has been enhanced to include passive elements, particularly between L3 and S1. This model allows for the simulation of the rotational moment/force generated by the intervertebral disc, facet articulations, and ligaments [11].

London lumbar spine model

This model includes the lumbar spine and lower limbs, and was created to analyse muscle force and joint contact force during daily activities, particularly lifting. The model, Fig. 5, was constructed using magnetic resonance imaging scans of the subject. Its accuracy was verified by comparing the momentum arm of the erector spinae during forward flexion to measurements from Jorgensen's method. Various parameters, such as joint contact force and muscle forces, were assessed in this study. The results of this study based on the outputs of the model aligned well with existing literature [4].

University of Waterloo cervical spine model

This model was specifically developed to study the forces and movements of the cervical spine. It includes 218 actuators representing 58 cervical muscles. Motion data of the cervical spine and electromyography (EMG) activities of the muscles were collected from eight healthy subjects. The compressive force at C7-T1 was calculated in this model and compared to values from other models. The results revealed discrepancies between the forces in this model and those reported in existing literature, ranging from 25.5 to 368.1 N [12].

Personalized scoliotic spine models

This project aimed to create specific model of spine for scoliotic subjects. This project is a simplified model of spine adapted from Bruno et al. [13]. The model was scaled and changed based on the markers attached on the spine.

Model to determine muscle forces during sit-to-stand transfer

In this project a model was developed to analyse sit-to-stand transfer motion. The muscle forces can be determined in this task. Actually, this model consists of lower limb model 2010, musculoskeletal model of the lumbar

Fig. 4. Articulated kinematic model of the thoracic and lumbar spine. The thoracic vertebrae were modelled separately to increase the degrees of freedom.

Fig. 5. London lumbar spine model. This model includes the lumbar spine and lower limbs and was created to analyse muscle forces and joint contact forces during daily activities, particularly lifting.

https://doi.org/10.12671/jmt.2026.00171

spine, MoBL-ARMS Upper Limb Model, and head and neck musculoskeletal biomechanics model. This model has 46 DOFs with 194 actuators [14].

A model of cervical spine for injury mechanisms analysis and simulation in sport

Evaluation of the motion of the cervical spine in normal and pathological conditions can be done using advanced models of the cervical spine. There are some specific cervical models developed for this purpose, including the MASI (Fig. 6) and Rugby models. The MASI model is based on data from a healthy cadaver, which also includes the scapula and clavicle, allowing for scapular and clavicular coupled motion with respect to humeral elevation.

Rugby model

The Rugby model is another version of the MASI model used to estimate cervical spine loads in rugby and other sports activities, especially those with upper limb contacts. In the older version of this model, the internal loading of the cervical spine in non-injured activities can be evaluated. The new version of the model was developed to simulate the motions from C2-C3 to C5-C6 to simulate axial impact. Using this model, joint contact force and muscle forces can be analysed in impact activities [5,15].

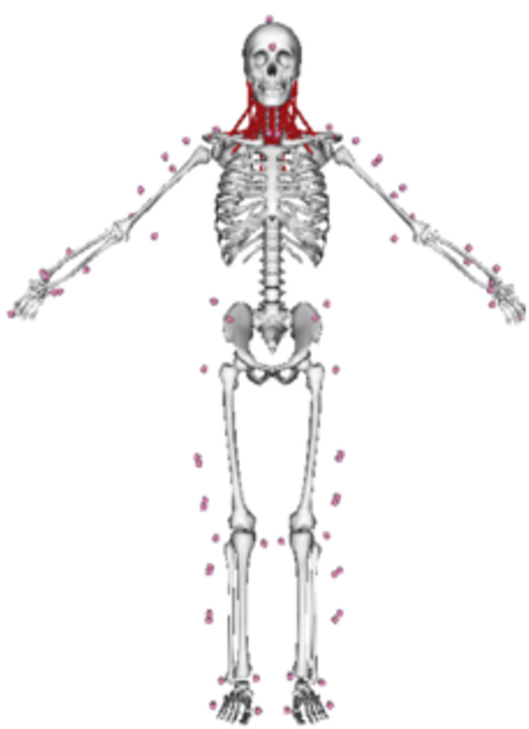

Fig. 6. MASI model of the cervical spine for injury mechanism analysis and simulation in sport. The model includes the scapula and clavicle, allowing coupled scapular and clavicular motion with humeral elevation.

The validity of both the Rugby and MASI models was established based on dynamic verification, kinematic validation, and dynamic validation. The muscle force of the cervical spine was determined using a computer muscle control approach. The results of studies based on these models support the reliability of the results. These models can be used to investigate the risks of injuries in various sports activities [15].

Full-body lifting model

This model is actually based on the full-body lumbar spine (FBLS) and was developed to estimate spinal loads during lifting. The validity of the model was assessed through various procedures, including comparisons with EMG muscle data, evaluation of intradiscal pressure, and comparison of contact forces with vertebral body implant measurements. It is important to note that this model is primarily used to determine joint loading of the lumbar spine. It appears that this model has acceptable validity for evaluating changes in lumbar loading during lifting [16].

A model to determine the role of the neck during impact loading

In this project a model of head and neck was used to determine the role of muscles and passive elements in the activities with impact loads. This model is based on works of Vasavada et al. [6] and Mortensen et al. [17]. The kinematics of head movement was evaluated in this study in various loading conditions [18,19].

Head and neck musculoskeletal biomechanics

This model of the head and neck was created based on data from five cadavers. The model includes the head, neck, scapula, and clavicle. In the first version of the model, the head had 3 DOFs (flexion/extension, abduction/adduction, and rotation) relative to the trunk. In the newer version, there were 6 DOFs (3 DOF for the motion of the skull relative to C2 and 3 DOF for the motion of C2 relative to T1). It appears that this model has a high level of validity to determine the range of motion [6].

A model to study infant head kinematics during abusive head trauma

This model was developed to determine the kinematics of head movement in infants during shaking. It is a combination of a 4.5-month-old infant model developed from computed tomography scans, and an upper body adult model [20].

Musculoskeletal model of head and neck suitable for dynamic simulations

The primary issue with previous head and neck models was their inability to calculate absolute values of moments in all directions. This was mainly due to the multi-directional moments of the cervical spine muscles. The accuracy of cervical moments has been improved by incorporating hyoid muscles into the models. This new model, known as the hyoid model, Fig. 7, can be utilized to calculate muscle forces using computer muscle control and joint contact forces using forward dynamics [17].

Full-body models

The second group of models that can be used to analyse the kinematics and kinetics of the spine is full-body models. The available full-body models can be divided into two main groups: those with detailed motions of the spine (especially for the lumbar vertebrae) and those with a combined spine (head, neck, and trunk). The second group includes models with only a link with 3 DOFs at L5/S1.

Fig. 7. Hyoid model of the cervical spine. The accuracy of cervical moment estimates was improved by incorporating the hyoid muscles into the model.

Model 1018

It is a simplified model with 10 DOFs and 18 actuators that primarily focuses on the lower extremities. This model includes a linkage with 3 DOFs between the pelvis and trunk (a combination of the head and spine). It showcases the utilization of the new Millard muscles in OpenSim. The purpose of this model is for educational, demonstrative, and initial prototyping purposes when quick simulation times are required. It can be utilized to analyse the kinematics of the trunk in relation to the pelvis. Additionally, this model can help to determine the joint contact force at L5/S1.

Model 2354

This model combines legs and trunk without upper limbs. There is a linkage between the trunk and pelvis with 3 rotational DOFs. This model consists of 23 DOFs with 54 actuators for 46 muscles. There are several trunk muscles associated with this model, including abdominal and spinal extensors. This model is mostly used for demonstration and education. It appears that this model can be used for analysing trunk kinematics relative to the pelvis [21].

Model 2392

It is a well-developed model of the lower extremity combined with a model of the trunk. While this model primarily focuses on leg muscles, it also includes a few trunk muscles. It is designed to determine the kinematics of the trunk and joint contact force at L5/S1. The model has 23 DOFs and utilizes 92 actuators for 76 muscles. Additionally, there is a link between L5/S1 with 3 DOFs in this model, allowing for the analysis of joint contact force at that specific location.

Full-body model Hamner

This is a well-developed full-body model primarily used for walking and running. It includes legs, upper limbs, and the spine. The model is also utilized to study the range of motion and moments of the joints. It is important to note that the trunk is constructed as a unit consisting of the head, neck, and spine, connecting to the pelvis at L5/S1. Several flexor and extensor muscles of the trunk are associated with this model. This model allows for the evaluation of joint contact force at L5/S1 [22].

Rajagopal model

This is another well-developed full-body model, which can

https://doi.org/10.12671/jmt.2026.00171

be used to investigate the motions of the legs, upper limb and spine at L5/S1. The muscles of trunk in this model are the same as other full-body models such as model 2392 and 2354 [23].

Full-body lumbar spine model

This is a full-body model consisting of legs, upper limbs and spine. Actually, this model is suitable to investigate the motions, muscle forces and joint contact forces of spine. The model consists of 21 segments, with 29 DOFs. There are 324 musculotendon actuators associated with this model. Each lumbar vertebra has 6 DOFs for flexion/extension, rotation and lateral bending. There are eight muscles groups of trunk which include: rectus abdominis, external obliques, internal obliques, erector spinae, multifidus, quadratus lumborum, psoas major, and latissimus dorsi. The force of muscles can be determined based on static optimization. Due to the complexity of the model, it is not possible to run computer muscle control [24].

Discussion

Now it is possible to determine the muscle forces and joint contact forces of spine during different tasks by use of motion analysis and use of some software such as AnyBody and OpenSim. However, there are some differences between these software packages. The OpenSim and AnyBody spine models are both computational tools used for musculoskeletal simulation, but they differ in focus, structure, and flexibility [25]. OpenSim is an open-source platform developed for modeling, simulating, and analysing human movement, offering a highly customizable framework with extensive community resources [3,26]. Its spine models typically emphasize biomechanical motion and inverse dynamics to study kinematics and muscle activation patterns. In contrast, the AnyBody Modelling System is a commercial software that provides a detailed, scalable representation of the musculoskeletal system, including complex spine mechanics and muscle coordination [25]. It integrates advanced optimization algorithms to estimate muscle forces and joint loads under specific conditions. While OpenSim excels in transparency, community-driven development, and flexibility for custom research, AnyBody stands out for its detailed anatomical databases, robust optimization routines, and ready-to-use parametric spine models suited for ergonomic and clinical applications [3,26].

Based on the results of this study, several models have been developed to study the motion of the spine. However, a few of them can be used to investigate the kinetics and kinematic variables of the spine. Table 1 summarizes the available models that can be used to study the motions of the spine. As can be seen from the table, there are several models of the cervical spine that can be used to evaluate kinematics, muscle forces, and joint contact forces. However, it should be noted that in most available full-body models, the spine was constructed as one component with a link at L5/S1. Therefore, most available models can be only used to determine joint contact force at L5/S1. In advanced models of the spine, only the motions of the lumbar vertebrae can be analysed in more detail, meaning that in most of them, the thoracic vertebrae were constructed as one component. The validity of the spine models is another issue that was not addressed and evaluated in most studies.

Based on the results of the available studies presented in Table 1, several models are available to investigate the research on spine which can be divided based on the regions of spine. There are six studies on model of spine in cervical regions [5,6,15,17,20]. Although all of them can be used for kinematic analysis, only four models can be used to determine the moments between cervical vertebra and also the muscle forces. The hyoid model and MASI model are the cervical models which can also be used for forward dynamics. The validity of these models was evaluated and the outputs of these models have acceptable validity to be used in the research to investigate the effects of impact in various sport activities [5,17].

There are several models of the thoracic spine that can be used to determine its range of motion. It is important to note that in most of the available models (including full-body models and spine models), the trunk is constructed as one component at the L5/S1 level. These models can be used to evaluate the motion of the trunk on the pelvis, as well as the moments applied to the connection between the trunk and pelvis. It should be noted that a few muscles are associated with full-body models.

The available models of the spine that can be used with OpenSim software can also be categorized based on the type of studies. Most of the available models of the spine (Table 1) can be used for kinematic analysis. However, depending on the structure of the models, some of the

Table 1. Various models of spine developed for OpenSim software

Model	Validity test	Output	Usage
Musculoskeletal model of the lumbar spine	No information	IK, ID	It is not suitable for complex motions of the spine that involve motion across two or more planes.
Thoracolumbar spine and rib cage model	The validity of the muscle forces and joint contact forces in this model was evaluated using data from the literature	IK, ID, SO	This model can be used for designing exoskeletons and determining spinal loading in various lifting conditions.
Full-body models with detailed thoracolumbar spine for children and adolescents	The validity of the outputs of this model was evaluated with literature.	IK, ID	This model can be used for evaluation of the motion of the spine in the subjects with age 6-18 years.
Model for estimating spinal loading during lifting and lowering tasks	The outputs of the model were validated using nine dynamic lifting tasks.	IK, ID, SO, FD	The model can effectively estimate spinal loads during lifting and lowering tasks.
Articulated kinematic model of the thoracic and lumbar spine	No information	IK, ID	This dynamic articulated model of the lumbar and thoracic spine was designed for kinematic analysis.
Lumbar spine with passive elements	No information	IK, ID	This model allows for the simulation of the rotational moment/force generated by the intervertebral disc, facet articulations, and ligaments
London lumbar spine model	The outputs of the models were validated with literature.	IK, ID	The outputs of the model regarding joint contact forces aligned well with existing literature.
University of Waterloo cervical spine model	The compressive force at C7–T1 was calculated in this model and was compared to values from other models.	IK, ID	The results revealed discrepancies between the forces in this model and those reported in existing literature, ranging from 25.5 to 368.1 N.
Personalised scoliotic spine models	No information	IK, ID	This project aimed to create specific model of spine for scoliotic subjects.
Model to determine muscle forces in sit-to-stand transfer	No information	IK, ID	In this project a model was developed to analyse sit-to-stand transfer motion and also muscle forces.
MASI cervical spine model	The validity of MASI model was established based on dynamic verification, kinematic validation, and dynamic validation.	IK, ID, CMC, FD	By use of this model, joint contact force and muscle forces can be analysed in impact activities.
Rugby cervical spine model	The validity of the Rugby models was established based on dynamic verification, kinematic validation, and dynamic validation.	IK, ID, CMC, FD	By use of this model, joint contact force and muscle forces can be analysed in impact activities.
Full-body lifting model	The validity of the model was assessed through various procedures, including comparisons with EMG muscle data, evaluation of intradiscal pressure, and comparison of contact forces with vertebral body implant measurements	IK, ID, SO	It appears that this model has acceptable validity for evaluating changes in lumbar loading during lifting.
Model of neck to determine impact loading	No information	IK, ID	The kinematics of head movement was evaluated in this study in various loading conditions.
Head and neck musculoskeletal biomechanics	No information	IK, ID	This model has a high level of validity in determining the ROM.
Infant head kinematics during abusive head trauma model	No information	IK, ID	This model was developed to determine the kinematics of head movement in infants during shaking.
Hyoid model	No information	IK, ID, CMC, FD, RRA	The accuracy of cervical moments based on this model has been improved by incorporating hyoid muscles into the models.

All listed models are publicly available in OpenSim.
IK, inverse kinematics; ID, inverse dynamics; SO, static optimization; FD, forward dynamics; CMC, computer muscle control; RRA, residual reduction algorithm; ROM, range of motion.

https://doi.org/10.12671/jmt.2026.00171

available models can be used for investigating intervertebral motions of the spine in the cervical region (Hyoid and MASI models), thoracic region (FBL model), and lumbar region. In contrast, there are a few models that can be used for evaluating joint contact forces at L5/S1 and muscle analysis during lifting [8]. There are also some full-body models that can be used for analysing motions of the spine at L5/S1 and joint contact force at this level for various research purposes (lifting, walking, etc) [21-23].

Validation of the models is another important parameter which should be considered in selection of spine models. Although there are nearly 23 models developed for vertebral column, a few of them were validated. The validity of the models was evaluated based on EMG pattern of trunk muscles, comparison between the outputs of the sensors embedded in cadavers with the outputs of the models based on forward dynamics analysis. For some model such as thoracolumbar spine and rib cage model, the output of the models was validated with the available data of literature [8]. For the cervical model developed by Waterloo University, the outputs of EMG of the muscles were compared with the pattern of activity of the muscles obtained from literature [12]. There was some discrepancy between the outputs of the models and EMG. The outputs of the Rugby and MASI models were validated based on dynamic verification [5,15]. It seems that the validity of the spine models is an important issue which should be considered in the future studies. Validation of spine models is a big challenge in the research done on spine. Inserting a sensor inside vertebra is a method to determine joint contact forces and the loads transmitted through vertebra. However, it is not practical to put sensors inside vertebra due to ethical issues. Complexity of spine structure is another important parameter which influences the validity of the outputs of spine models. Last but not least is that most of validation is based on cadaveric data which may not fully reflect living tissue behaviours.

There are some limitations associated with the available spine models. The main limitation is that only a few models can be used to determine the muscle forces and joint contact forces. Moreover, the validity of most of these models should be evaluated. It is not possible to evaluate the joint contact force and muscle forces of whole body in various tasks such as lifting. It seems that lack of studies on evaluation of the validity of the available models is the main issue which should be considered in future studies.

Conclusions

The available models of the spine can be categorized into two main groups: specific spine models and full-body models, which also include the spine with a linkage at L5/S1. Some models are designed to investigate the risk of injuries in cervical spine and can be used to determine muscle force and joint contact forces. In most full-body models, the trunk is constructed as one component linked to the pelvis at L5/S1, with a few muscles associated with the trunk in these models. It seems that a few of the available models can be used to determine muscle forces of spine and joint contact force. It is recommended that the validity of the outputs of the spine models should be evaluated in the future studies.

Article Information

Author contributions

All the work was done by Mohammad Taghi Karimi.

Conflicts of interest

No potential conflict of interest relevant to this article was reported.

Funding

None.

Data availability

Not applicable.

Acknowledgments

None.

Supplementary materials

None.

References

1. Roggio F, Ravalli S, Maugeri G, et al. Technological advancements in the analysis of human motion and posture management through digital devices. World J Orthop 2021;12:467-84.
2. Kim W, Kim M. Sports motion analysis system using wearable sensors and video cameras. In: Proceedings of the 2017 International Conference on Information and Communication Technology Convergence (ICTC); 2017 Oct; Jeju, Korea. ICTC; 2017. p. 1089-91.

3. Delp SL, Anderson FC, Arnold AS, et al. OpenSim: open-Source software to create and analyze dynamic simulations of movement. IEEE Trans Biomed Eng 2007;54:1940-50.
4. Favier CD, Finnegan ME, Quest RA, Honeyfield L, McGregor AH, Phillips ATM. An open-source musculoskeletal model of the lumbar spine and lower limbs: a validation for movements of the lumbar spine. Comput Methods Biomech Biomed Engin 2021;24:1310-25.
5. Silvestros P, Preatoni E, Gill HS, et al. Musculoskeletal modelling of the human cervical spine for the investigation of injury mechanisms during axial impacts. PLoS One 2019;14:e0216663.
6. Vasavada AN, Li S, Delp SL. Influence of muscle morphometry and moment arms on the moment-generating capacity of human neck muscles. Spine (Phila Pa 1976) 1998;23:412-22.
7. Christophy M, Faruk Senan NA, Lotz JC, O'Reilly OM. A musculoskeletal model for the lumbar spine. Biomech Model Mechanobiol 2012;11:19-34.
8. Bruno AG, Bouxsein ML, Anderson DE. Development and validation of a musculoskeletal model of the fully articulated thoracolumbar spine and rib cage. J Biomech Eng 2015;137:081003.
9. Schmid S, Burkhart KA, Allaire BT, Grindle D, Anderson DE. Musculoskeletal full-body models including a detailed thoracolumbar spine for children and adolescents aged 6-18 years. J Biomech 2020;102:109305.
10. Akhavanfar M, Mir-Orefice A, Uchida TK, Graham RB. An enhanced spine model validated for simulating dynamic lifting tasks in OpenSim. Ann Biomed Eng 2024;52:259-69.
11. Wang K, Wang L, Deng Z, Jiang C, Niu W, Zhang M. Influence of passive elements on prediction of intradiscal pressure and muscle activation in lumbar musculoskeletal models. Comput Methods Programs Biomed 2019;177:39-46.
12. Barrett JM, McKinnon CD, Dickerson CR, Callaghan JP. An electromyographically driven cervical spine model in OpenSim. J Appl Biomech 2021;37:481-93.
13. Bruno AG, Burkhart K, Allaire B, Anderson DE, Bouxsein ML. Spinal loading patterns from biomechanical modeling explain the high incidence of vertebral fractures in the thoracolumbar region. J Bone Miner Res 2017;32:1282-90.
14. Caruthers EJ, Thompson JA, Chaudhari AM, et al. Muscle forces and their contributions to vertical and horizontal acceleration of the center of mass during sit-to-stand transfer in young, healthy adults. J Appl Biomech 2016;32:487-503.
15. Cazzola D, Holsgrove TP, Preatoni E, Gill HS, Trewartha G. Cervical spine injuries: a whole-body musculoskeletal model for the analysis of spinal loading. PLoS One 2017;12:e0169329.
16. Beaucage-Gauvreau E, Robertson WSP, Brandon SCE, et al. Validation of an OpenSim full-body model with detailed lumbar spine for estimating lower lumbar spine loads during symmetric and asymmetric lifting tasks. Comput Methods Biomech Biomed Engin 2019;22:451-64.
17. Mortensen JD, Vasavada AN, Merryweather AS. The inclusion of hyoid muscles improve moment generating capacity and dynamic simulations in musculoskeletal models of the head and neck. PLoS One 2018;13:e0199912.
18. Kuo C, Fanton M, Wu L, Camarillo D. Spinal constraint modulates head instantaneous center of rotation and dictates head angular motion. J Biomech 2018;76:220-8.
19. Kuo C, Sheffels J, Fanton M, Yu IB, Hamalainen R, Camarillo D. Passive cervical spine ligaments provide stability during head impacts. J R Soc Interface 2019;16:20190086.
20. Lintern TO, Nash MP, Kelly P, Bloomfield FH, Taberner AJ, Nielsen PMF. Probabilistic description of infant head kinematics in abusive head trauma. Comput Methods Biomech Biomed Engin 2017;20:1633-42.
21. Hoy MG, Zajac FE, Gordon ME. A musculoskeletal model of the human lower extremity: the effect of muscle, tendon, and moment arm on the moment-angle relationship of musculotendon actuators at the hip, knee, and ankle. J Biomech 1990;23:157-69.
22. Hamner SR, Seth A, Delp SL. Muscle contribution to propulsion and support during running. J Biomech 2010;43:2709-16.
23. Rajagopal A, Dembia CL, DeMers MS, Delp DD, Hicks JL, Delp SL. Full-body musculoskeletal model for muscle-driven simulation of human gait. IEEE Trans Biomed Eng 2016;63:2068-79.
24. Raabe ME, Chaudhari AMW. An investigation of jogging biomechanics using the full-body lumbar spine model: model development and validation. J Biomech 2016;49:1238-43.
25. Damsgaard M, Rasmussen J, Christensen ST, Surma E, de Zee M. Analysis of musculoskeletal systems in the AnyBody Modeling System. Simul Model Pract Theory 2006;14:1100-11.
26. Seth A, Hicks JL, Uchida TK, et al. OpenSim: Simulating musculoskeletal dynamics and neuromuscular control to study human and animal movement. PLoS Comput Biol 2018;14:e1006223.

https://doi.org/10.12671/jmt.2026.00171

JMT Journal of Musculoskeletal Trauma
pISSN 3058-6267 · eISSN 3058-6275
J Musculoskelet Trauma 2026;39(3):205-215
https://doi.org/10.12671/jmt.2026.00087

Current concepts and applications of internal fixation for forearm diaphyseal fractures

Sung Yoon Jung[1], Min Kyun Cho[1], Dong-hee Kim[2], Sang Hyun Lee[3]

[1]Department of Orthopedic Surgery, Dong-A University Hospital, Dong-A University School of Medicine, Busan, Korea
[2]Department of Orthopedic Surgery, Samsung Changwon Hospital, Sungkyunkwan University School of Medicine, Changwon, Korea
[3]Department of Orthopedic Surgery, Medical Research Institute, Pusan National University Hospital, Pusan National University School of Medicine, Busan, Korea

Adult diaphyseal fractures of the forearm functionally behave as intra-articular injuries because forearm rotation depends on accurate restoration of length, axial alignment, rotation, and the native radial bow. This narrative review summarizes contemporary surgical options for adult forearm shaft fractures, including 3.5-mm plate osteosynthesis, dual mini-plate fixation, interlocking intramedullary nailing, and minimally invasive plate osteosynthesis (MIPO). Compression plating with 3.5-mm plates remains the reference standard for most fracture patterns, whereas other techniques should be regarded as selective, emerging, or salvage options according to their indication spectrum and evidence base. Mini-fragment dual plating may be useful for short segments or thin soft-tissue envelopes, although the supporting clinical evidence remains limited and meticulous biomechanical execution is essential. Interlocking intramedullary nailing is a viable alternative for carefully selected simple fracture patterns or soft-tissue-compromised situations, offering less invasive exposure but a narrower indication spectrum. MIPO may be considered for selected comminuted or soft-tissue-compromised diaphyseal fractures; however, its use in adult forearm fractures remains constrained by the high functional requirement for precise restoration of length, rotation, and the radial bow. To improve transparency, this review explicitly distinguishes established, evidence-supported methods from techniques supported mainly by limited retrospective data or institutional experience. A pattern-based pragmatic algorithm and expanded comparison table are provided to guide fixation selection according to the bone involved, fracture location, fracture morphology, soft-tissue condition, and evidence tier while minimizing complications such as nonunion, infection, nerve injury, refracture after plate removal, and radioulnar synostosis.

Keywords: Forearm injuries; Internal fracture fixation; Bone plates; Radius fractures

Review Article

Received: January 30, 2026
Revised: May 8, 2026
Accepted: May 11, 2026

Correspondence to:
Sang Hyun Lee
Department of Orthopedic Surgery, Medical Research Institute, Pusan National University Hospital, Pusan National University School of Medicine, 179 Gudeok-ro, Seo-gu, Pusan 49241, Korea
Tel: +82-51-240-8718
Email: handsurgeon@pusan.ac.kr

Introduction

Forearm diaphyseal fractures disrupt the radius-ulna unit, a functional ring whose coordinated rotation enables pronation-supination and positions the hand in space. A classic cadaveric biomechanical study about the biomechanics of forearm diaphysis stated that small errors in length, rotation, or the magnitude and location of the radial bow translate directly into motion loss and anatomical reduction is necessary in forearm diaphyseal fractures [1]. Several studies demonstrated clinically important reductions in forearm rotation with angular and rotational deformity and showed that restoration of the native radial bow correlates with functional recovery after fixation [1-3]. These biomechanical imperatives underpin contemporary surgical goals: accurate restoration of length and rotation, anatomic recreation of the radial bow (particularly in the radius), stable fixation matched to fracture morphology, and early motion. These biomechanical demands explain why forearm fracture fixation demands substantial rigidity and precise anatomical restoration for full pronation-supination, which clarifies the functional rationale for treatment selection for non-specialist readers. Open reduction and internal fixation using small-fragment plates has historically been the standard for adult both-bone forearm fractures. Landmark series reported high union rates and satisfactory motion with compression plating, and later cohort studies reinforced plating as the benchmark against which alternatives are compared [4-7]. Locking compression plates (LCP) are widely used; however, comparative series suggest broadly similar union and function between LCP and nonlocking compression plates when interfragmentary compression principles are respected [8-10]. Conversely, purely locking, noncompressive constructs may increase nonunion risk in some settings, underscoring that compression across simple fracture lines remains more important than plate technology itself. Interest in lower-profile implants and biologic fixation has expanded the contemporary armamentarium. Mini-fragment dual plating aims to reduce implant prominence and facilitate fixation in short segments or narrow corridors, but evidence remains limited and technique sensitivity is high [11,12]. Interlocking intramedullary (IM) nails have evolved to improve rotational and length control compared with historical flexible pins, and may be considered in selected simple patterns or soft-tissue-compromised situations, although recreating the radial bow—especially in the radius—remains challenging [13-21]. Selective application of minimally invasive plate osteosynthesis (MIPO) has also been reported for diaphyseal forearm fractures in comminuted patterns or compromised soft tissue; nonetheless, the forearm's high functional demand yields limited tolerance for malrotation or inadequate radial bow restoration [21]. In previous literature, "hybrid fixation" of the forearm typically refers to using different implant types in different bones (e.g., plating the radius and nailing the ulna). In contrast, placing a plate over an IM nail within the same bone is best termed a nail-plate construct (NPC) and should be viewed as a rare salvage strategy with limited supporting evidence. This review compares contemporary fixation options—3.5-mm plating, mini-fragment dual plating, interlocking IM nailing, selective MIPO, NPC, and wiring-assisted plating—integrating indications, technical pearls, outcomes, limitations, and complication avoidance. A practical, pattern-based decision algorithm is proposed to assist operative strategy selection.

Ethics statement

This study was a narrative review and did not require institutional review board approval. Informed consent was obtained for publication of clinical images.

Literature search strategy

This narrative review was informed by a structured search of PubMed/MEDLINE, Embase, Scopus, Google Scholar, and the Cochrane Central Register of Controlled Trials (CENTRAL), covering from inception through December 2025. Search terms included combinations of: "adult forearm fracture," "both-bone forearm fracture," "diaphyseal radius fracture," "diaphyseal ulna fracture," "plate fixation," "locking compression plate," "dynamic compression plate," "mini-plate," "2.7 mm plate," "intramedullary nail," "interlocking nail," "MIPO forearm," "radial bow," "radioulnar synostosis," and "refracture plate removal." Priority was given to adult clinical studies, comparative cohorts, systematic reviews/meta-analyses, and biomechanical studies directly relevant to fixation stability. Pediatric populations, metaphyseal-only fracture studies, isolated case reports lacking transferable technical relevance, and non-English reports with equivalent English evidence were excluded. A Preferred Reporting Items for Systematic Reviews and Meta-Analyses (PRISMA)-style flow diagram was added to enhance transparency regarding screening and inclusion (Fig. 1). In this review framework, 312 records were identified, 74 duplicates were removed, 238 titles/abstracts were screened, 54 full-text reports were assessed, and 25 studies were included in the final narrative synthesis.

https://doi.org/10.12671/jmt.2026.00087

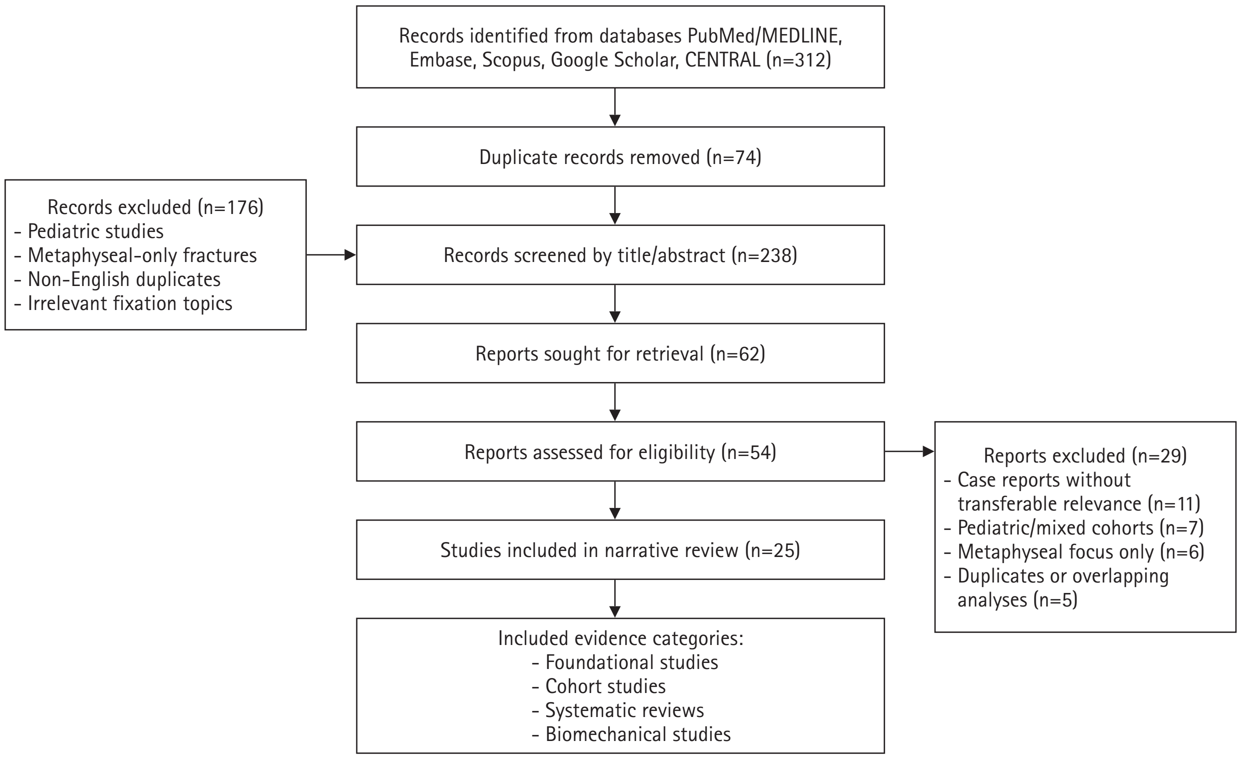

Fig. 1. PRISMA-style flow diagram showing literature identification, screening, eligibility assessment, and study inclusion for this narrative review.

Surgical options and techniques

Plate osteosynthesis with 3.5-mm plates

Indications

Plate fixation using 3.5-mm systems remains the reference standard for most adult forearm diaphyseal fractures, including the majority of simple and wedge patterns (AO/OTA 22-A/B) and many complex patterns (22-C) that permit anatomic reconstruction [4-7]. In both-bone injuries, plating is particularly advantageous because it most reliably enables restoration of length, rotational alignment, and the native radial bow, which is a critical determinant of functional recovery [1-3].

Key technical points

From a technical standpoint, separate surgical approaches to the radius and ulna are generally preferred to protect the interosseous membrane and mitigate the risk of radioulnar synostosis [22]. In many cases, the ulna is addressed first to re-establish length and serve as a template, after which the radius is reduced and contoured to restore both the magnitude and apex location of the radial bow (Fig. 2) [1-3]. For simple fracture lines, interfragmentary compression and absolute stability should be prioritized. Adequate fixation typically requires at least three bicortical screws (≥6 cortices) in each main fragment with an appropriate working length [7,9]. During proximal radial exposure and drilling through anterior (Henry approach), meticulous protection of the posterior interosseous nerve (PIN) is essential, including full supination and careful dissection.

Clinical outcomes

Large clinical series have consistently demonstrated high union rates and reliable functional recovery when anatomic and biomechanical principles are respected [4-7].

Level of evidence

Overall, the evidence supporting 3.5-mm plating is the strongest among available techniques, consisting of multiple foundational and contemporary cohort studies [4-7].

Mini-fragment dual plating (2.4–2.7 mm)

Indications

Mini-fragment dual plating has been introduced as a lower-profile strategy intended to reduce implant prominence and facilitate fixation in anatomically constrained corridors. In adult forearm diaphyseal fractures, this approach may be considered selectively in short proximal radius segments where achieving secure purchase with a single 3.5-mm plate is difficult, in patients with thin soft-tissue envelopes at risk for symptomatic prominence, or in peri-articular/metaphyseal-diaphyseal junctional extensions [11,12].

Fig. 2. A 40-year-old male patient with a radial shaft fracture. (A) Preoperative anteroposterior and lateral radiographs demonstrating a diaphyseal radial fracture. (B) Immediate postoperative radiographs after open reduction and internal fixation using a 3.5-mm plate.

Key technical points

Mechanically, dual-plate constructs—often arranged orthogonally—can distribute screw density and improve torsional resistance while maintaining a lower profile (Fig. 3) [11,12]. Similarly, during the anterior approach for proximal radial fractures, drilling beyond the far cortex can endanger the PIN. In that case, orthogonal dual-plate fixation with unicortical screws can avoid this complication.

Fig. 3. A 62-year-old male patient with a radial shaft fracture. (A) Preoperative anteroposterior and lateral radiographs showing a diaphyseal radial fracture. (B) Immediate postoperative radiographs after mini-fragment dual plating with 2.4–2.7-mm plates.

https://doi.org/10.12671/jmt.2026.00087

Clinical outcomes and limitations

Biomechanical studies suggest that well-executed 2.7-mm constructs can approach the stability of 3.5-mm plating in selected patterns [11,12,23]. Nevertheless, the clinical evidence base is smaller and heterogeneous. This technique should be clearly framed as a selective or emerging option rather than equivalent to standard 3.5-mm plating. Risks include mechanical insufficiency, loss of alignment, and nonunion when stability principles are compromised [11,12].

Level of evidence

The evidence supporting mini-fragment dual plating is limited, consisting primarily of small retrospective series and biomechanical studies [11,12,23].

Interlocking intramedullary nailing

Indications

Modern interlocking IM nails have evolved to improve rotational and length control compared with historical flexible pins and may offer advantages of smaller incisions and reduced periosteal stripping [13-18]. In adult forearm diaphyseal fractures, interlocking IM nailing can be considered selectively for simple transverse or short-oblique patterns where rotational control and length restoration can be reliably achieved. It may also be attractive in soft-tissue-compromised situations (including selected open injuries after adequate debridement) and in selected polytrauma scenarios where minimizing operative time and dissection is desirable [13-21].

Situations to avoid or use with caution

Despite these potential benefits, indications are constrained by the forearm's unique functional demand—particularly the need to recreate the radial bow and avoid rotational malalignment.

Key technical points

Technically, accurate entry point selection and high-quality reduction are essential, and rotational alignment and length should be confirmed intraoperatively using fluoroscopy with the shoulder abducted and elbow flexed to 90°, comparing with the contralateral limb. Even with multiplanar interlocking, bow recreation in the radius is often less predictable than with plating, and this limitation should be explicitly acknowledged when counseling patients and selecting cases (Fig. 4). Intraoperative strategies to mitigate malalignment include careful fluoroscopic assessment of the radial bow profile in the anteroposterior view, provisional reduction with external manipulation or pointed reduction forceps, and confirmation of rotational alignment by comparing cortical thickness patterns with the contralateral side.

Clinical outcomes

Systematic reviews and comparative series suggest that interlocking IM nails can achieve union with accept-

Fig. 4. A 38-year-old male patient with both-bone forearm shaft fractures treated with interlocking intramedullary nailing. (A) Preoperative radiographs. (B) Immediate postoperative radiographs after interlocking intramedullary nail fixation.

able complication profiles in carefully selected indications, sometimes with shorter operative time, although high-quality randomized data remain limited [14-16].

Level of evidence

Moderate evidence base consisting of systematic reviews, meta-analyses, and comparative cohort studies [13-16].

NPC within the same bone

Terminology clarification

Terminology in this area requires precision. In established orthopedic trauma usage, "hybrid fixation" generally refers to applying different implant types to different bones (e.g., plating the radius and nailing the ulna). In contrast, applying a plate over an IM nail within the same bone is best termed an NPC and should be framed as a rare salvage strategy with limited supporting evidence.

Indications

NPC may be considered in exceptional situations such as severe comminution or revision nonunion where long-span plating alone is judged biologically or mechanically unfavorable, or in selected atypical ulnar fractures requiring additional internal support and load sharing.

Key technical points and limitations

However, the technique carries important hazards. Bicortical screw purchase around a nail within the narrow ulnar canal can be technically demanding and may risk screw-nail interference, iatrogenic fracture, or compromised fixation if executed improperly. For these reasons, NPC should not be presented as a routine alternative to standard plating. In typical execution, a prebent flexible nail is inserted—commonly via proximal ulnar/olecranon entry—to provide internal support and load sharing, after which a plate is applied to provide rotational and bending stability (Fig. 5). Variable-angle locking may facilitate screw placement around the nail, and cancellous grafting may be considered in revision nonunion settings according to biological risk.

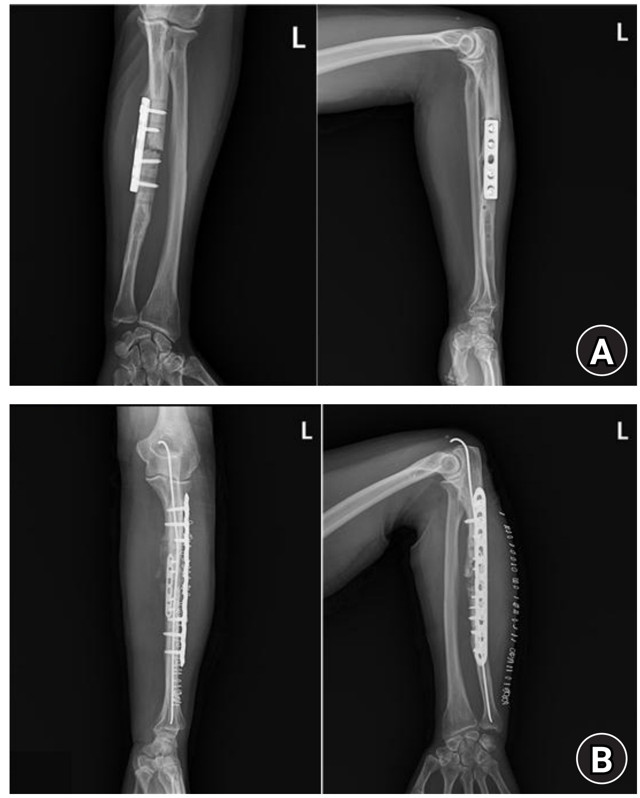

Fig. 5. A 65-year-old female patient with established nonunion after prior ulnar fixation. (A) Preoperative radiographs. (B) Immediate postoperative radiographs after revision fixation using a nail-plate construct.

Level of evidence

Overall, published clinical evidence remains limited, and NPC should be reserved for carefully selected salvage indications rather than generalized indications. Statements based on institutional experience should be clearly distinguished from evidence-based conclusions.

Transosseous wiring-assisted plate fixation

Indications

Simple transverse diaphyseal fractures require absolute stability, yet do not reliably permit interfragmentary lag-screw compression in the same manner as oblique patterns. In selected transverse diaphyseal fractures where lag-screw fixation is not feasible and maintaining compression during plating is challenging, transosseous wiring may serve as an adjunct to facilitate interfragmentary compression and reduction control [24].

Key technical points and limitations

This technique should be explicitly framed as adjunctive

https://doi.org/10.12671/jmt.2026.00087

only and should not be used as standalone definitive fixation in adult diaphyseal forearm fractures (Fig. 6).

Clinical outcomes and level of evidence

Evidence supporting this method remains limited to small retrospective reports [24]. The main value of wiring is as a technical adjunct to achieve compression and maintain reduction during plating, rather than as an independent fixation strategy. This technique represents an application of principles from the authors' institutional experience and should be used judiciously in appropriately selected cases.

Minimally invasive plate osteosynthesis

Indications

MIPO aims to preserve fracture biology via indirect reduction and bridge-plating principles while providing relative stability. In adult forearm diaphyseal fractures, its role remains selective because the forearm has limited tolerance for malrotation or inadequate radial bow restoration, particularly in the radius [21]. MIPO may be considered in comminuted or segmental diaphyseal fractures where bridge-plating principles are appropriate, and in soft-tissue-compromised situations including selected open injuries after adequate debridement (Fig. 7) [21].

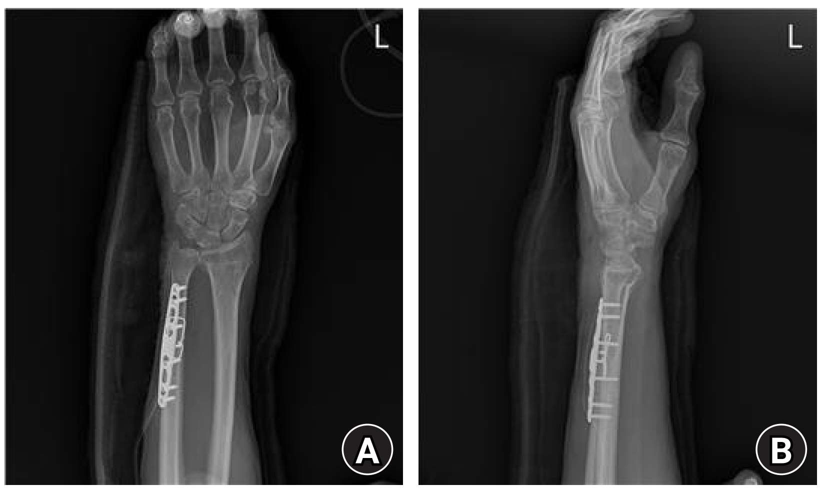

Fig. 6. A 63-year-old male patient. Immediate postoperative (A) anteroposterior and (B) lateral radiographs after transosseous wiring-assisted plate fixation.

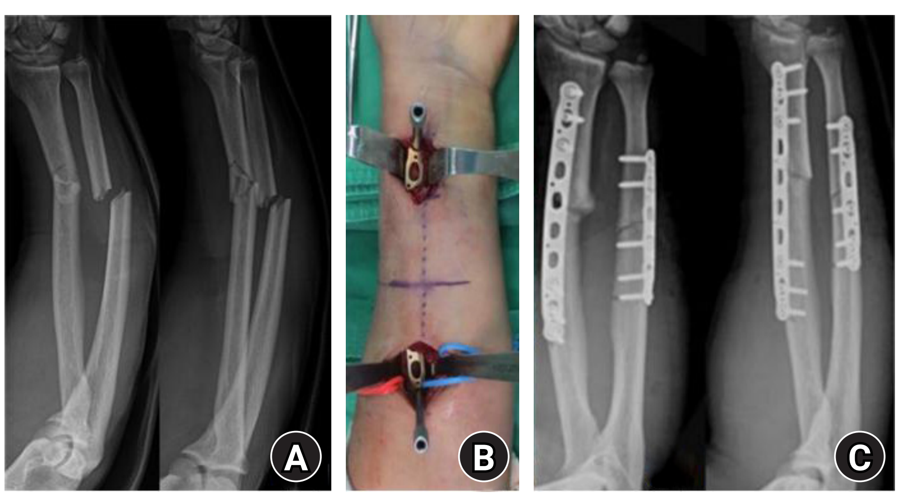

Fig. 7. A 43-year-old female patient with a comminuted radial shaft fracture treated with minimally invasive plate osteosynthesis. (A) Preoperative radiographs. (B) Intraoperative clinical photograph demonstrating external distractor-assisted indirect reduction. (C) Immediate postoperative radiographs after bridge plating using minimally invasive plate osteosynthesis.

Situations to avoid or use with caution

Conversely, MIPO should be avoided or used with extreme caution in the following situations: simple fractures where compression and absolute stability are required; cases where acceptable restoration of rotational alignment and radial bow cannot be confidently achieved by indirect means—especially in radius fractures; early learning curve cases without reliable fluoroscopic reduction control; and proximal third radius fractures with high risk of rotational malalignment.

Key technical points

Key technical considerations include meticulous intraoperative assessment of length, rotation, and overall alignment, with explicit confirmation that the radius demonstrates an acceptable radial bow restoration under fluoroscopy (Fig. 7). Specific intraoperative strategies to mitigate malalignment include: (1) use of external distractor or manual traction to restore length, (2) fluoroscopic comparison of radial bow with contralateral side, (3) assessment of rotational alignment by comparing cortical symmetry, (4) judicious use of percutaneous pointed reduction forceps, (5) careful screw placement with heightened awareness of PIN risk during proximal radius fixation.

Clinical outcomes and limitations

Clinical series suggest that union can be achieved at rates comparable to open plating in carefully selected patterns, but the evidence base remains limited and largely retrospective [21].

Level of evidence

Limited evidence base consisting primarily of retrospective comparative studies [21].

Taken together, these six fixation strategies illustrate the spectrum of contemporary approaches to adult forearm diaphyseal fractures, each with distinct indications, strengths, and limitations. A comparative overview of these techniques is provided in Table 1 [4-7,11-16,21,24,25].

Complications and avoidance

Complications following operative management of adult forearm diaphyseal fractures are strongly influenced by mechanical execution and soft-tissue condition. Nonunion or delayed union is multifactorial, reflecting biological

Table 1. Summary of fixation techniques for adult forearm diaphyseal fractures

Technique	Best indications	Key advantages	Primary caveats	Evidence tier/quantitative note
3.5-mm LCP plating	Simple or wedge diaphyseal patterns; most both-bone fractures; cases requiring precise restoration of the radial bow	Enables anatomic reduction and strong rotational control; has the strongest evidence base	Requires soft-tissue stripping; may cause implant prominence; carries a risk of refracture after implant removal [4-7,25]	Tier 1; nonunion, 2%–10%; infection, 1%–6%
Mini-plate/dual-plate fixation (2.4–2.7 mm)	Narrow corridors, short segments, thin soft-tissue envelopes, or situations requiring a lower-profile construct	Provides a low-profile construct and contouring versatility; can distribute fixation through orthogonal dual plates	Supported by limited clinical evidence; may be mechanically insufficient if fixation principles are not respected [11,12]	Tier 2; no robust pooled benchmark
Interlocking IM nailing	Simple transverse or short-oblique patterns; soft-tissue compromise; polytrauma	Requires less dissection and shorter incisions; may reduce operative time	Recreation of the radial bow and rotational control remain challenging; careful patient selection is required [13-16]	Tier 2; acceptable union in selected cases
NPC (same-bone fixation)	Severe comminution, revision nonunion, or selected salvage situations	Provides internal support and load sharing in complex cases	Supported by limited clinical evidence; technically demanding; risk of screw-nail interference	Tier 3; no published comparative outcome data
Transosseous wiring plus plate fixation	Simple transverse fractures without a lag-screw option	Facilitates interfragmentary compression as an adjunctive technique	Adjunctive technique only; excessive wiring may compromise periosteal blood supply [24]	Tier 3; small retrospective reports only
MIPO (bridge plating)	Comminuted or segmental fractures; soft-tissue-compromised injuries	Preserves fracture biology and reduces soft-tissue disruption	Limited capacity for precise rotational control and radial bow restoration [21]	Tier 2; retrospective evidence only

LCP, locking compression plate; IM, intramedullary; NPC, nail-plate construct; MIPO, minimally invasive plate osteosynthesis.

https://doi.org/10.12671/jmt.2026.00087

compromise, instability, and patient factors. Reported rates of nonunion after plate fixation range from 2% to 10% in large series [6,7]. Infection rates range from 1% to 6%, implant prominence or irritation from 10% to 30%, radioulnar synostosis from 2% to 6%, nerve injury from 1% to 5%, and refracture after plate removal from 4% to 12% [6,7,22,25]. These complication rates provide a unified risk-benefit framework across techniques.

Pattern-based practical algorithm

A pattern-based decision algorithm is proposed to assist selection of fixation strategies according to the bone involved, fracture morphology, fracture location, and soft-tissue condition. The primary objective is restoration of forearm function through accurate reconstruction of length, rotational alignment, and, particularly in radius fractures, the native radial bow (Fig. 8).

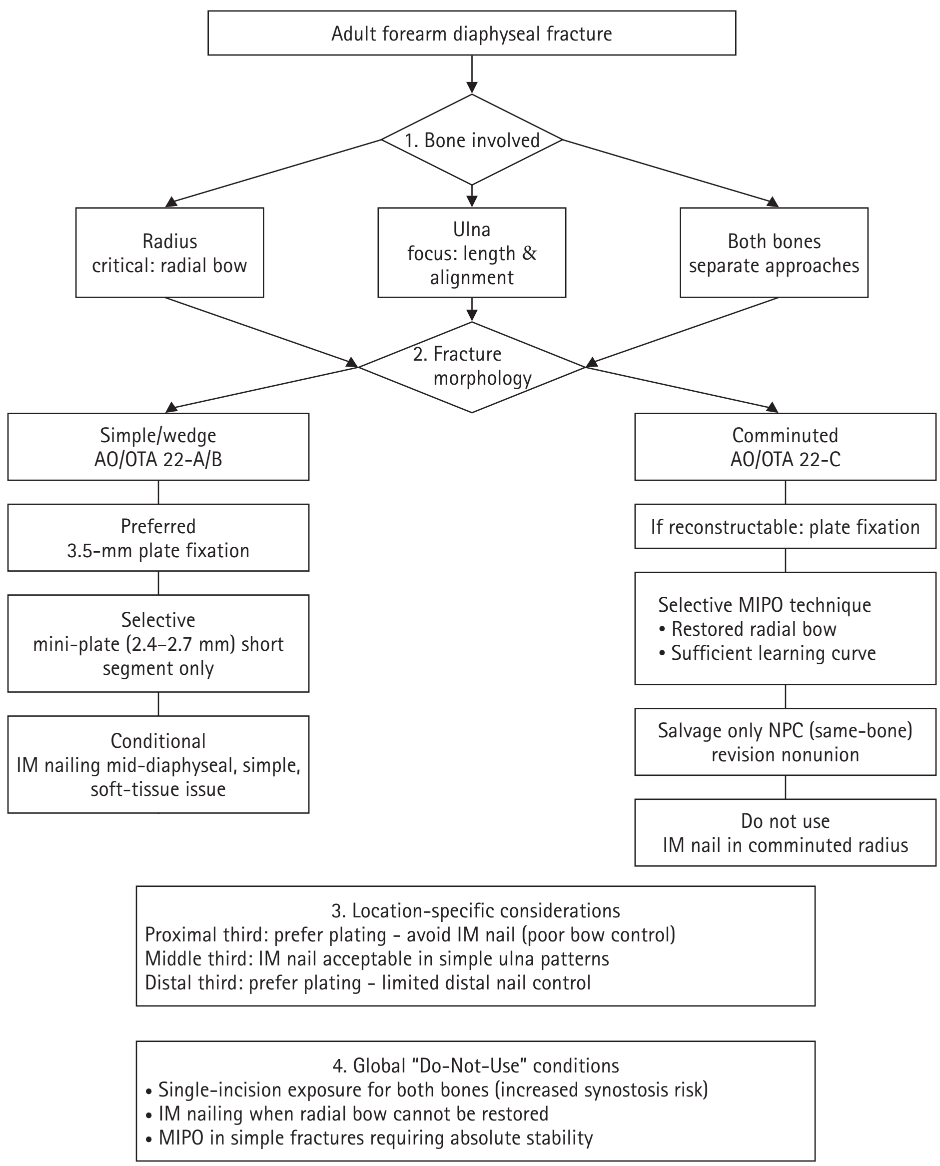

Fig. 8. Pattern-based decision-tree flowchart for fixation selection in adult forearm diaphyseal fractures, incorporating the bone involved (radius vs. ulna), fracture location (proximal, middle, or distal third), fracture morphology, and explicit contraindications. MIPO, minimally invasive plate osteosynthesis; IM, intramedullary; NPC, nail-plate construct.

The algorithm incorporates six techniques—3.5-mm plating, mini-fragment dual plating, interlocking IM nailing, NPC, transosseous wiring-assisted plating, and MIPO—and to incorporate fracture pattern, bone quality, soft-tissue condition, and surgeon experience rather than generic branching alone.

Conclusions

Regardless of implant selection, successful treatment of adult forearm diaphyseal fractures fundamentally depends on accurate restoration of length, rotation, axial alignment, and—particularly for the radius—the native radial bow. Compression plate osteosynthesis using 3.5-mm plates remains the most dependable treatment for adult diaphyseal forearm fractures because it most reliably restores anatomy and provides stable fixation across a wide range of patterns.

Contemporary alternatives—including mini-fragment dual plating, interlocking IM nailing, MIPO, transosseous wiring-assisted plating, and rare NPCs—may broaden options in carefully selected scenarios, but their indications are narrower and their evidence base is generally more limited. These techniques should be clearly presented as selective, emerging, adjunctive, or salvage options, and claims regarding their efficacy should be calibrated to the available evidence.

Article Information

Author contributions

Conceptualization: SYJ, DK. Data curation: SYJ. Formal analysis: MKC, DK, SHL. Supervision: SHL. Writing–original draft: SYJ, MKC. Writing–review & editing: MKC, DK, SHL. All authors read and approved the final manuscript.

Conflicts of interest

No potential conflict of interest relevant to this article was reported.

Funding

None.

Data availability

Not applicable.

Acknowledgments

None.

Supplementary materials

None.

References

1. Matthews LS, Kaufer H, Garver DF, Sonstegard DA. The effect on supination-pronation of angular malalignment of fractures of both bones of the forearm. J Bone Joint Surg Am 1982;64:14-7.
2. Tarr RR, Garfinkel AI, Sarmiento A. The effects of angular and rotational deformities of both bones of the forearm: an in vitro study. J Bone Joint Surg Am 1984;66:65-70.
3. Schemitsch EH, Richards RR. The effect of malunion on functional outcome after plate fixation of fractures of both bones of the forearm in adults. J Bone Joint Surg Am 1992;74:1068-78.
4. Anderson LD, Sisk D, Tooms RE, Park WI. Compression-plate fixation in acute diaphyseal fractures of the radius and ulna. J Bone Joint Surg Am 1975;57:287-97.
5. Chapman MW, Gordon JE, Zissimos AG. Compression-plate fixation of acute fractures of the diaphysis of the radius and ulna. J Bone Joint Surg Am 1989;71:159-69.
6. Stern PJ, Drury WJ. Complications of plate fixation of forearm fractures. Clin Orthop Relat Res 1983;175:25-9.
7. Droll KP, Perna P, Potter J, Harniman E, Schemitsch EH, McKee MD. Outcomes following plate fixation of fractures of both bones of the forearm in adults. J Bone Joint Surg Am 2007;89:2619-24.
8. Saikia K, Bhuyan S, Bhattacharya T, Borgohain M, Jitesh P, Ahmed F. Internal fixation of fractures of both bones forearm: comparison of locked compression and limited contact dynamic compression plate. Indian J Orthop 2011;45:417-21.
9. Azboy I, Demirtas A, Uçar BY, Bulut M, Alemdar C, Ozkul E. Effectiveness of locking versus dynamic compression plates for diaphyseal forearm fractures. Orthopedics 2013;36:e917-22.
10. Kim SB, Heo YM, Yi JW, Lee JB, Lim BG. Shaft fractures of both forearm bones: the outcomes of surgical treatment with plating only and combined plating and intramedullary nailing. Clin Orthop Surg 2015;7:282-90.
11. Wahbeh JM, Kelley BV, Shokoohi C, et al. Comparison of a 2.7-mm and 3.5-mm locking compression plate for ulnar

 https://doi.org/10.12671/jmt.2026.00087

fractures: a biomechanical evaluation. OTA Int 2023;6:e278.
12. Justice W, Adams A, Kasper A, Takagi-Stewart J, Ilyas AM. Forearm fracture fixation with locking plates: does size matter. J Hand Surg Glob Online 2024;6:319-22.
13. Lari A, Hassan Y, Altammar A, et al. Interlocking intramedullary nail for forearm diaphyseal fractures in adults: a systematic review and meta-analysis of outcomes and complications. J Orthop Traumatol 2024;25:16.
14. Box MW, Stegelmann SD, Domingue GA, et al. Intramedullary nail fixation versus open reduction and internal fixation for treatment of adult diaphyseal forearm fractures: a systematic review and meta-analysis. J Orthop Surg Res 2024;19:719.
15. Zhao L, Wang B, Bai X, Liu Z, Gao H, Li Y. Plate fixation versus intramedullary nailing for both-bone forearm fractures: a meta-analysis of randomized controlled trials and cohort studies. World J Surg 2017;41:722-33.
16. Kale SY, Singh SD, Samant P, Bukalsaria D, Chaudhari P, Ghodke RJ. Treatment of diaphyseal forearm fracture with interlocking intramedullary nailing: a pilot study. J Clin Orthop Trauma 2021;17:195-200.
17. Köse A, Aydın A, Ezirmik N, Topal M, Can CE, Yılar S. Intramedullary nailing of adult isolated diaphyseal radius fractures. Ulus Travma Acil Cerrahi Derg 2016;22:184-91.
18. Blažević D, Benčić I, Ćuti T, et al. Intramedullary nailing of adult forearm fractures: results and complications. Injury 2021;52 Suppl 5:S44-8.
19. Lee SK, Kim KJ, Lee JW, Choy WS. Plate osteosynthesis versus intramedullary nailing for both forearm bones fractures. Eur J Orthop Surg Traumatol 2014;24:769-76.
20. Lee YH, Lee SK, Chung MS, Baek GH, Gong HS, Kim KH. Interlocking contoured intramedullary nail fixation for selected diaphyseal fractures of the forearm in adults. J Bone Joint Surg Am 2008;90:1891-8.
21. Kang HT, Jo YH, Kang HJ. Comparison of minimally invasive plate osteosynthesis (MIPO) and open reduction and internal fixation (ORIF) for the treatment of radial shaft fractures: a retrospective study. BMC Musculoskelet Disord 2025;26:320.
22. Abdul Azeem M, Alhojailan K, Awad M, Khaja AF. Post-traumatic radioulnar synostosis: a retrospective case series of 10 patients in Kuwait. J Shoulder Elbow Surg 2022;31:1595-602.
23. Crow BD, Mundis G, Anglen JO. Clinical results of minimal screw plate fixation of forearm fractures. Am J Orthop (Belle Mead NJ) 2007;36:477-80.
24. Choi SJ, Jung SY, Kim MB. Transosseous wiring method for simple transverse shaft fracture of the upper extremity. Arch Hand Microsurg 2024;29:34-9.
25. Beaupre GS, Csongradi JJ. Refracture risk after plate removal in the forearm. J Orthop Trauma 1996;10:87-92.

JMT Journal of Musculoskeletal Trauma

pISSN 3058-6267 · eISSN 3058-6275
J Musculoskelet Trauma 2026;39(3):216-226
https://doi.org/10.12671/jmt.2026.00073

Postoperative sagittal alignment and reoperation predict late outcomes after plate fixation of AO/OTA 33C distal femur fractures: a retrospective cohort study

Hee Gon Park

Department of Orthopedic Surgery, Dankook University College of Medicine, Cheonan, Korea

Background: Intra-articular distal femoral fractures are associated with high complication rates and variable late outcomes. Although the AO Foundation/Orthopaedic Trauma Association (AO/OTA) classification system is useful for describing injury severity and anticipating complications, whether fracture subtype alone determines clinically relevant late outcomes remains unclear. This study aimed to evaluate postoperative complications and late outcomes following plate fixation of intra-articular distal femoral fractures and to identify factors independently associated with final clinical outcomes.

Methods: This retrospective cohort study was conducted at a regional Level I trauma center. Patients with AO/OTA 33C intra-articular distal femoral fractures who underwent plate fixation and were followed for at least 12 months were included. Radiographic parameters reflecting coronal and sagittal alignment were assessed using standardized measurement methods. Postoperative complications and reoperation were recorded as intermediate events. Clinically relevant late outcomes included final knee range of motion (ROM), leg length discrepancy, and radiographic osteoarthritis severity, assessed as the difference in Kellgren-Lawrence grade. Multivariable linear regression analyses were performed to identify factors independently associated with late outcomes.

Results: The 33C3 group (n=33) had significantly higher rates of open fracture (54.5%), nonunion (39.4%), and reoperation (45.5%) than the 33C1–2 group (n=49). At the final follow-up, 33C3 fractures were associated with lower mean ROM ($P<0.001$) and greater osteoarthritis progression ($P<0.001$). However, multivariable analysis showed that sagittal malalignment (Δ anatomical posterior distal femoral angle: $\beta=-2.35$, $P=0.001$) and reoperation ($\beta=-17.5$, $P=0.001$), rather than AO/OTA subtype itself, were independent predictors of final ROM.

Conclusions: Although fracture subtype according to the AO/OTA classification was associated with predictable complication patterns, clinically relevant late outcomes following intra-articular distal femoral fractures were more closely associated with postoperative alignment quality and the treatment course than with fracture classification alone. These findings highlight the importance of optimizing radiographic alignment and preventing complications that lead to reoperation to improve long-term outcomes after plate fixation.

Level of evidence: III.

Keywords: Femur; Femoral fractures; Intra-articular fractures; Bone plates; Treatment outcome

Original Article

Received: January 27, 2026
Revised: May 4, 2026
Accepted: May 11, 2026

Correspondence to:
Hee Gon Park
Department of Orthopedic Surgery, Dankook University College of Medicine, 119 Dandae-ro, Dongnam-gu, Cheonan 31116, Korea
Tel: +82-41-550-6290
Email: osdku@dankook.ac.kr

Introduction

Background

Intra-articular distal femur fractures are complex injuries associated with substantial morbidity and functional impairment. Although relatively uncommon, these fractures present significant treatment challenges due to articular surface involvement, metaphyseal comminution, and the frequent coexistence of patient- and injury-related risk factors. Despite advances in fixation techniques, postoperative complications and inferior long-term outcomes remain common [1-3].

The AO Foundation/Orthopaedic Trauma Association (AO/OTA) classification system is widely used to describe fracture morphology and severity in distal femur fractures. Intra-articular fractures classified as AO/OTA type 33C encompass a broad spectrum of injury patterns, ranging from relatively simple articular fractures (C1 and C2) to highly complex multifragmentary fractures (C3) [4]. Previous studies have demonstrated that more complex fracture patterns are associated with higher rates of nonunion, fixation failure, and reoperation [5-7]. However, it remains unclear whether fracture subtype alone determines clinically relevant late outcomes.

In clinical practice, patients with intra-articular distal femur fractures frequently experience late problems such as limitation of motion (LOM), leg length discrepancy (LLD), and progressive post-traumatic osteoarthritis, even in the absence of overt fixation failure [8-10]. These observations raise an important question: are clinically relevant late outcomes primarily dictated by fracture classification, or are they more closely associated with modifiable factors such as postoperative alignment, reduction quality, and subsequent treatment course?

Objectives

Therefore, this study aimed to evaluate postoperative complications and clinically relevant late outcomes following plate fixation of intra-articular distal femur fractures, investigating their associations with fracture subtype, radiographic parameters, and postoperative events. We hypothesized that while fracture subtype would be associated with predictable complication patterns, final clinical outcomes would be more closely related to radiographic alignment and the occurrence of reoperation than to fracture classification alone.

Methods

Ethics statement

This study was approved by the Institutional Review Board (IRB) of Dankook University Hospital (IRB No. DKUH 2025-12-003). The requirement for informed consent was waived by the IRB due to its retrospective design.

Study design

This was a retrospective cohort study conducted in accordance with the Strengthening the Reporting of Observational Studies in Epidemiology (STROBE) guidelines for observational studies.

Setting

This retrospective cohort study was conducted at the Department of Orthopedic Surgery of Dankook University Hospital, a regional Level I trauma center in Cheonan, Korea. Consecutive adult patients who underwent plate fixation for AO/OTA 33C intra-articular distal femur fractures between 2004 and 2024 were identified. Outcomes were assessed using postoperative and follow-up clinical and radiographic data, with a minimum follow-up of 12 months.

Participants

We identified all consecutive patients who underwent operative treatment for intra-articular distal femur fractures at our regional Level I trauma center between 2004 and 2024. By including every patient who met the predefined inclusion criteria during this 20-year period, we aimed to minimize selection bias and ensure that the cohort reflects the true clinical spectrum of AO/OTA 33C fractures treated at our institution. Eligible patients were adults with unilateral AO/OTA type 33C intra-articular distal femur fractures treated with plate fixation, including cases in which accessory screws were used to facilitate articular reduction. Patients with a minimum follow-up of 12 months were included. Patients with pathologic, periprosthetic, or stress fractures, those requiring additional soft-tissue reconstructive procedures, and those treated without plate fixation were excluded. Given the institutional role as a Level I trauma center, patients with polytrauma were not excluded. A total of 242 patients were screened, of whom 174 had AO/OTA type 33C fractures. After excluding patients who did not meet the eligibility criteria (n=55), those treated without plate fixation (n=26), and those with a follow-up of less than 12 months (n=11), 82 patients were included in the final analysis (Fig. 1).

Variables

Study outcomes included postoperative complications and clinically relevant late outcomes. Postoperative complications were nonunion, deep infection, and implant failure, and reoperation was defined as any subsequent surgical intervention performed due to these complications. Late outcomes assessed at the final follow-up were final knee range of motion (ROM, degrees), LOM (ROM <90°), LLD (measured on standing scanograms), and radiographic osteoarthritis severity, quantified as the difference in Kellgren-Lawrence grade between the injured and contralateral knee (ΔK-L) at final follow-up. Conversion to total knee replacement arthroplasty (TKRA) was also recorded as a late clinical endpoint.

Data sources

Data sources were obtained retrospectively from institutional electronic medical records and the radiology archive at Dankook University Hospital. Baseline demographics, injury characteristics, operative details, postoperative complications, reoperations, and clinical follow-up data (including knee ROM) were abstracted from medical charts.

Measurements

Fractures were classified by two or more orthopedic surgeons using preoperative radiographs and computed tomography (CT) scans according to the AO/OTA classification system. Representative preoperative and postoperative radiographs of each AO/OTA 33C subtype are shown in Fig. 2. Injury mechanisms were classified into high-energy

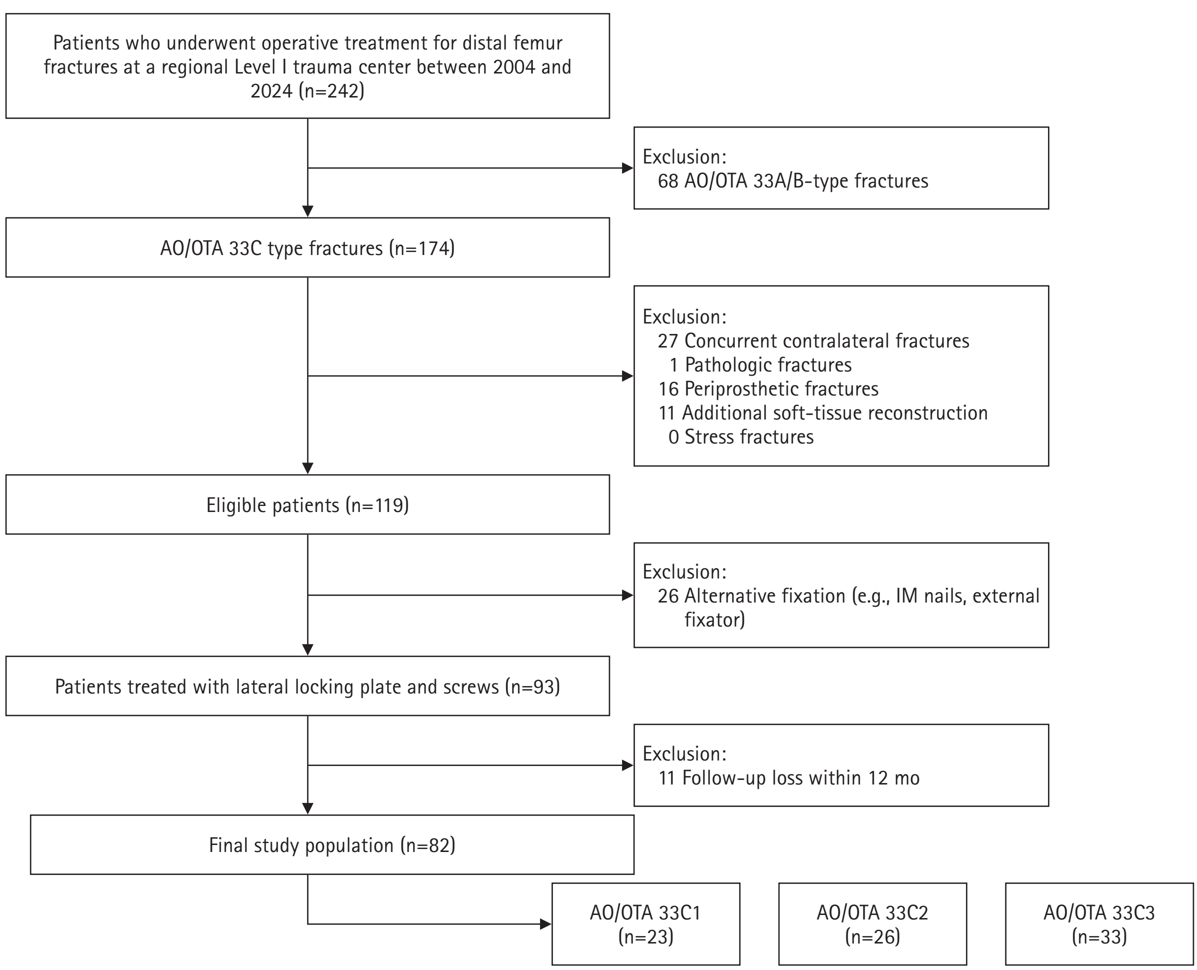

Fig. 1. Study enrollment and patient selection flowchart. AO/OTA, AO Foundation/Orthopaedic Trauma Association; IM, intramedullary.

https://doi.org/10.12671/jmt.2026.00073

Fig. 2. Representative preoperative and postoperative radiographs of AO Foundation/Orthopaedic Trauma Association (AO/OTA) 33C fracture subtypes. For each subtype, preoperative (a) anteroposterior and (b) lateral radiographs are followed by immediate postoperative (c) anteroposterior and (d) lateral radiographs after plate fixation. (A) AO/OTA 33C1 type fracture. (B) AO/OTA 33C2 type fracture. (C) AO/OTA 33C3 type fracture.

and low-energy injuries. High-energy injuries were defined as motor vehicle accidents (including car, motorcycle, and pedestrian accidents) and falls from a height of >3 m. Conversely, low-energy injuries were defined as falls from a standing height (slip down). In our cohort, slip downs were the only mechanism classified as low-energy injuries.

Radiographic assessment

Radiographic parameters were assessed using immediate postoperative and follow-up radiographs. To ensure the reliability of radiologic assessments, inter-observer reliability was evaluated. A subset of cases was randomly selected, and fracture classification and radiographic parameters—including anatomical lateral distal femoral angle (aLDFA), anatomical posterior distal femoral angle (aPDFA), hip-knee-ankle (HKA) angle, mechanical lateral distal femoral angle (mLDFA), LLD, and Kellgren-Lawrence (K-L) grades—were independently measured by two board-certified orthopedic surgeons who were blinded to the clinical outcomes. Reliability was assessed using the intraclass correlation coefficient (ICC) for continuous variables. The ICC was 0.71 (95% confidence interval [CI], 0.65–0.78), indicating substantial inter-observer agreement. Measurement methods are illustrated in Fig. 3. On anteroposterior knee radiographs of both limbs, the aLDFA was measured as the lateral angle between the anatomical axis of the femur and the distal femoral joint line (Fig. 3A). In the presence of fracture-related angulation, the femoral anatomical axis was determined using the proximal shaft segment (Fig. 3B). On standing full-length anteroposterior radiographs (whole lower extremity scanograms), overall lower-limb alignment was evaluated by measuring the HKA angle. The mLDFA and LLD were also measured according to standard definitions (Fig. 3C) [11-13].

Outcome measures

Postoperative articular reduction quality was evaluated on immediate postoperative radiographs and CT scans according to established criteria for complex intra-articular fractures. Reduction was classified as anatomical (articular step-off or gap <2 mm), good (step-off 2–5 mm), or poor (step-off >5 mm). This classification system is widely accepted for highly comminuted AO/OTA 33C3 fractures, where a 2-mm threshold represents a clinically acceptable limit for joint congruity. Postoperative complications included nonunion, infection, and implant failure. Reoper-

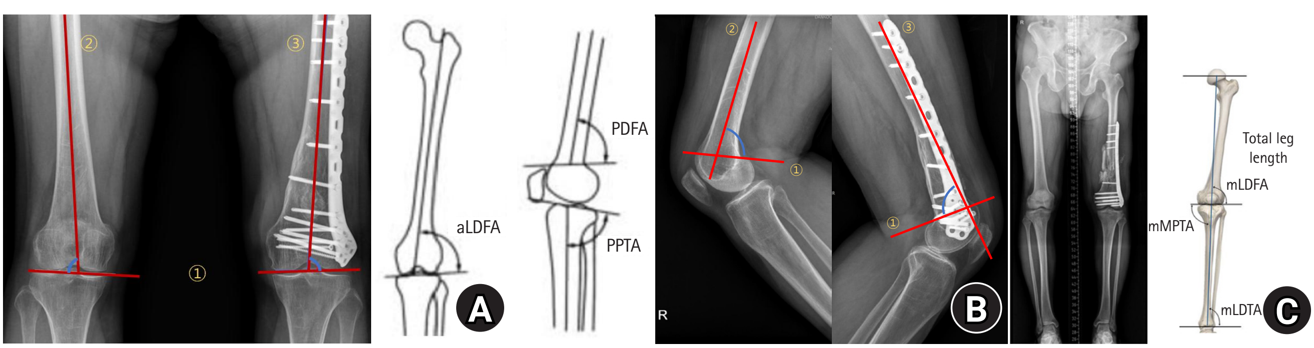

Fig. 3. (A) The aLDFA was measured as the lateral angle between the distal joint line, defined as a line tangent to the most distal points of the medial and lateral condyles (①), and the anatomical axis of the femoral shaft (②). Coronal alignment was assessed as the angle between the anatomical axis of the proximal shaft fragment (③) and the distal joint line of the condylar fragment (①). (B) The aPDFA was measured between the reference line connecting the anterior and posterior junctions where the femoral metaphysis meets the condyles (①) and the anatomical axis of the femoral shaft (②). Sagittal angulation was assessed as the angle between the anatomical axis of the proximal shaft fragment (③) and the distal junctional line of the condylar fragment (①). The degree of deformity was calculated as the angular difference between the fractured side and the intact contralateral side. (C) Limb length discrepancy was measured as the absolute difference in total leg length between the two sides. Total leg length was defined as the distance from the highest point of the femoral head to the center of the ankle joint, corresponding to the midpoint of the tibial plafond. The hip-knee-ankle angle was defined as the angle formed by the mechanical axis of the femur, extending from the center of the femoral head to the center of the knee, and the mechanical axis of the tibia, extending from the center of the knee to the center of the ankle. aLDFA, anatomical lateral distal femoral angle; PDFA, posterior distal femoral angle; PPTA, proximal posterior tibial angle; mLDFA, mechanical lateral distal femoral angle; mMPTA, mechanical medial proximal tibial angle; mLDTA, mechanical lateral distal tibial angle.

https://doi.org/10.12671/jmt.2026.00073

ation was defined as any subsequent surgical intervention performed due to postoperative complications. Clinically relevant late outcomes included final knee ROM, LOM (ROM<90°), LLD, and conversion to TKRA. To account for individual anatomical variations, radiographic parameters were assessed by comparing the injured limb to the uninjured contralateral limb, which served as the patient-specific anatomical reference. Rather than relying on population-based normal ranges, we focused on the restoration of symmetry. Coronal alignment was expressed as ΔaLDFA, defined as the absolute difference between the affected and contralateral sides. Similarly, sagittal plane alignment was evaluated using the difference in aPDFA. A deviation of greater than 5° from the contralateral side was defined as malalignment, a threshold previously identified as clinically significant for joint loading and functional outcomes. Radiographic osteoarthritis severity was assessed using the K-L grading system. To ensure an accurate evaluation of joint space narrowing and degenerative changes, all follow-up radiographs, including standing anteroposterior views and full-length scanograms, were obtained in a weight-bearing position. The progression of osteoarthritis was defined as the ΔK-L between the injured knee and the uninjured contralateral knee at the final follow-up. Using the contralateral limb as a patient-specific control allowed us to account for preexisting degenerative changes. Conversion to TKRA was performed in patients who met both radiographic and clinical criteria for end-stage post-traumatic osteoarthritis. Radiographic indication was defined as progression to K-L grade 3 or higher. Clinical indications included refractory pain with a visual analog scale score of ≥7 despite more than six months of conservative management and significant functional impairment hindering activities of daily living.

Bias

To minimize selection bias, we included all consecutive eligible patients treated during the study period using predefined inclusion/exclusion criteria. To reduce measurement bias, radiographic outcomes were assessed using standardized measurement protocols; key imaging variables were independently measured by two board-certified orthopedic surgeons blinded to clinical outcomes, and inter-observer reliability was quantified using the ICC. Potential confounding was addressed by multivariable regression including clinically relevant covariates, although residual confounding inherent to retrospective studies may remain.

Study size

The sample size was justified by an observations-per-variable ratio of 20.5:1, which is adequate for multivariate regression analysis. Additionally, a post-hoc power analysis confirmed a statistical power of >0.80.

Statistical methods

Continuous variables are presented as mean±standard deviation, and categorical variables as number (%). Comparisons between groups were performed using Student t-test or Mann-Whitney U test for continuous variables and chi-square or Fisher exact test for categorical variables, as appropriate. Multivariable linear regression analyses were conducted to identify factors associated with clinically relevant late outcomes, including final ROM, LLD, and ΔK-L. Fracture subtype, radiographic alignment parameters, and postoperative events were included as explanatory variables based on clinical relevance. To control for potential confounding factors, all multivariable models were adjusted for baseline clinical covariates, including injury mechanism (high- vs. low-energy), open fracture status, and treatment era. Missing data were addressed using complete-case analysis, and standard regression diagnostics were performed using IBM SPSS ver. 20.0 (IBM Corp.). A $P<0.05$ was considered statistically significant.

Results

Participants

A total of 82 patients were included (23 with type 33C1, 26 with 33C2, and 33 with 33C3). Baseline demographic and injury-related characteristics according to AO/OTA 33C subtype are summarized in Table 1. Compared to the 33C1-2 group, patients with 33C3 fractures significantly more often sustained high-energy injury mechanisms and open fractures (54.5% vs. 21.7%–42.3%). Regarding radiographic outcomes, the 33C3 group demonstrated inferior immediate postoperative articular reduction quality (anatomical reduction: 9.1% vs. 73.5%, $P<0.001$) and greater deviations in sagittal (ΔaPDFA, $P=0.014$) and coronal (ΔaLDFA, $P=0.006$) alignment. Complication rates were significantly higher in the 33C3 group, including nonunion (39.4% vs. 14.3%, P=0.020), infection (15.2% vs. 0%, P=0.009), and reoperation (45.5% vs. 20.4%, P=0.030).

Radiographic parameters following surgery

Postoperative complications and subsequent interven-

Table 1. Baseline characteristics according to the AO/OTA 33C subtype

Variable	Total	C1 (n=23)	C2 (n=26)	C3 (n=33)
Age (yr)	55.4±16.3	55.1±16.4	59.8±15.0	52.1±16.8
Male sex	50 (61.0)	10 (43.5)	17 (65.4)	23 (69.7)
Follow-up (mo)	28.2±18.1	30.7±20.4	25.1±14.3	28.8±19.2
Mechanism of injury				
In-car accident	30 (36.6)	4 (17.4)	12 (46.2)	14 (42.4)
Motorbike accident	12 (14.6)	0 (0.0)	5 (19.2)	7 (21.2)
Pedestrian accident	9 (11.0)	4 (17.4)	2 (7.7)	3 (9.1)
Fall down	10 (12.2)	5 (21.7)	2 (7.7)	3 (9.1)
Slip down[a]	21 (25.6)	10 (43.5)	5 (19.2)	6 (18.2)
Open fracture	34 (41.5)	5 (21.7)	11 (42.3)	18 (54.5)
Diabetes mellitus	13 (15.9)	7 (30.4)	1 (3.8)	5 (15.2)
Osteoporosis	27 (32.9)	8 (34.8)	11 (42.3)	8 (24.2)

Values are presented as mean±standard deviation or number (%).
AO/OTA, AO Foundation/Orthopaedic Trauma Association.
[a]Slip down was the only low-energy injury mechanism.

Table 2. Radiographic reduction quality and alignment parameters

Variable	Total (n=82)	C1–2 (n=49)	C3 (n=33)	P-value
Articular reduction quality				<0.001
Anatomical	39 (47.6)	36 (73.5)	3 (9.1)	
Good	35 (42.7)	13 (26.5)	22 (66.7)	
Poor	8 (9.8)	0 (0.0)	8 (24.2)	
Sagittal alignment (ΔaPDFA, °)	4.0±3.6	3.2±2.8	5.3±4.2	0.014
Coronal alignment (ΔaLDFA, °)	1.3±3.0	0.5±2.8	2.5±3.1	0.006
HKA (°)	1.5±4.4	1.0±4.3	2.3±4.5	0.170
mLDFA (°)	88.9±2.7	88.5±2.7	89.5±2.7	0.091
ΔmLDFA (°)	1.9±2.7	1.5±2.7	2.5±2.7	0.091

Values are presented as number (%) or mean±standard deviation. Δ indicates the difference between the affected and contralateral limb.
aPDFA, anatomical posterior distal femoral angle; aLDFA, anatomical lateral distal femoral angle; HKA, hip-knee-ankle angle; mLDFA, mechanical lateral distal femoral angle.

Table 3. Postoperative complications and subsequent interventions according to the AO/OTA 33C subtype

Variable	Total (n=82)	C1–2 (n=49)	C3 (n=33)	P-value
Nonunion	20 (24.4)	7 (14.3)	13 (39.4)	0.020
Infection	5 (6.1)	0 (0.0)	5 (15.2)	0.009
Implant failure	6 (7.3)	3 (6.1)	3 (9.1)	0.681
Reoperation[a]	25 (30.5)	10 (20.4)	15 (45.5)	0.030

Values are presented as number (%).
AO/OTA, AO Foundation/Orthopaedic Trauma Association.
[a]Reoperation was defined as a subsequent surgical intervention performed due to postoperative complications.

Table 4. Clinically relevant late outcomes according to the AO/OTA 33C subtype

Variable	Total (n=82)	C1–2 (n=49)	C3 (n=33)	P-value
Final ROM (°)	107.7±27.6	119.5±24.2	89.7±22.3	<0.001
LOM (ROM <90°)	13 (15.9)	4 (8.2)	9 (27.3)	0.029
ΔK-L grade	0.5±0.7	0.1±0.4	0.9±0.7	<0.001
LLD (cm)	0.7±0.8	0.4±0.5	1.3±0.9	<0.001
TKRA	7 (8.5)	3 (6.1)	4 (12.1)	-

Values are presented as mean±standard deviation or number (%).
AO/OTA, AO Foundation/Orthopaedic Trauma Association; ROM, range of motion; LOM, limitation of motion; K-L, Kellgren-Lawrence; LLD, leg length discrepancy; TKRA, total knee replacement arthroplasty.

https://doi.org/10.12671/jmt.2026.00073

tions, and clinically relevant late outcomes are summarized in Tables 2–4. Radiographic parameters reflecting reduction quality and alignment are presented in Table 2. Immediate postoperative articular reduction quality differed according to fracture subtype, with inferior reduction quality observed more frequently in AO/OTA 33C3 fractures. Sagittal plane alignment, assessed using the aPDFA, and coronal alignment, assessed using ΔaLDFA, also demonstrated greater deviation in 33C3 fractures compared with 33C1–2 fractures. In contrast, differences in overall lower-limb alignment assessed at 1 year were less pronounced between groups. Postoperative complications and subsequent interventions are summarized in Table 3. Patients with AO/OTA 33C3 fractures experienced higher rates of nonunion and reoperation compared with those with 33C1–2 fractures. All infections occurred in the 33C3 group. Among patients who developed infection, four of five cases (80.0%) occurred in the setting of open fractures, while 15 of 20 nonunion cases (75.0%) were associated with open injuries. Clinically relevant late outcomes are summarized in Table 4. Patients with AO/OTA 33C3 fractures demonstrated lower final knee ROM, a higher incidence of LOM, greater radiographic osteoarthritis severity, and larger LLD compared with those with 33C1–2 fractures. Conversion to TKRA occurred in seven patients (8.5%).

Late outcomes

At the final follow-up, the 33C3 group showed significantly worse late outcomes than the 33C1–2 group: lower mean ROM (89.7 vs. 119.5, P<0.001), greater radiographic osteoarthritis progression (ΔK-L grade: 0.9 vs. 0.1, P<0.001), and larger LLD (1.3 cm vs. 0.4 cm, P<0.001). Factors independently associated with clinically relevant late outcomes are summarized in Table 5. Multivariable linear regression analysis revealed that the independent predictors of late outcomes were specific surgical and clinical parameters rather than the fracture subtype itself. Specifically, final knee ROM was independently associated with sagittal malalignment (ΔaPDFA: β=–2.35, P=0.001) and the occurrence of reoperation (β=–17.5, P=0.001). LLD was also independently predicted by sagittal malalignment (ΔaPDFA: β=0.08, P<0.001).

Discussion

Key results

The primary finding of this study is that AO/OTA 33C3 fractures are associated with significantly higher complication rates and poorer functional outcomes compared to 33C1–2 subtypes. This is largely attributable to the high prevalence of open injuries (54.5%) and high-energy trauma mechanisms observed in the 33C3 group, which frequently lead to compromised soft-tissue envelopes and precarious vas-

Table 5. Multivariable linear regression analysis for clinical and radiographic outcomes

Variable	β[a] (95% CI)	P-value
Factors associated with final knee ROM		
Age (yr)	–0.24 (–0.52 to 0.03)	0.084
Sagittal malalignment (ΔaPDFA, °)	–2.35 (–3.73 to –0.98)	0.001
Coronal malalignment (ΔaLDFA, °)	0.08 (–2.01 to 2.18)	0.938
Reoperation (yes)	–17.5 (–27.8 to –7.1)	0.001
Factors associated with LLD		
Sagittal malalignment (ΔaPDFA, °)	0.08 (0.04 to 0.12)	<0.001
Coronal malalignment (ΔaLDFA, °)	–0.01 (–0.08 to 0.05)	0.670
HKA (°)	0.00 (–0.04 to 0.05)	0.913
Factors associated with radiographic osteoarthritis severity (ΔK-L)[b]		
Age (yr)	–0.008 (–0.016 to –0.001)	0.027
HKA (°)	–0.024 (–0.059 to 0.012)	0.185
ΔmLDFA (°)	0.039 (–0.017 to 0.095)	0.169
Follow-up (mo)	0.001 (–0.006 to 0.008)	0.757

CI, confidence interval; ROM, range of motion; aPDFA, anatomical posterior distal femoral angle; aLDFA, anatomical lateral distal femoral angle; LLD, leg length discrepancy; HKA, hip-knee-ankle angle; K-L, Kellgren-Lawrence grade; mLDFA, mechanical lateral distal femoral angle.
[a]Negative β indicates decreased ROM; positive β for LLD indicates increased LLD. [b]ΔK-L represents injured minus contralateral knee.

cularity at the fracture site.

Interpretations/comparison with previous studies

Consistent with previous reports [2,3,5-7], more complex fracture subtypes (AO/OTA 33C3) in our cohort were associated with inferior immediate postoperative radiographic findings and higher complication rates, including a marked increase in nonunion (39.4%), infection (15.2%), and reoperation. This highlights the inherent biological and mechanical challenges of treating comminuted intra-articular fractures, while also supporting the clinical utility of fracture classification for early risk stratification and predicting postoperative complications. However, the present study demonstrates that clinically relevant late outcomes following intra-articular distal femur fractures are not solely determined by the initial fracture subtype; rather, they are more closely associated with radiographic alignment parameters and the postoperative treatment course.

Crucially, when fracture subtype was adjusted for as an explanatory variable in our multivariable regression models, it did not emerge as a significant independent predictor of late functional outcomes. This approach allowed identification of factors that are independently associated with late outcomes after accounting for fracture-related risk stratification. In these analyses, sagittal plane alignment of the distal femur, assessed using the aPDFA, demonstrated a consistent association with both final knee ROM and LLD. Additionally, the occurrence of reoperation was independently associated with inferior functional outcomes, reflecting the cumulative impact of postoperative complications and alterations in the treatment course.

Radiographic osteoarthritis severity was also associated with postoperative alignment parameters, reinforcing the concept that coronal and sagittal alignment influence joint loading and degenerative changes beyond the fracture healing period [11-13]. Taken together, these results support the notion that postoperative alignment does not represent a static parameter, but rather a key determinant of long-term joint health.

Intriguingly, our multivariable analysis revealed that sagittal malalignment (ΔaPDFA), rather than the AO/OTA classification itself, was an independent predictor of both final ROM and LLD. While sagittal alignment did not reach statistical significance as an independent predictor in the final ΔK-L model, it demonstrated a clear trend toward greater radiographic changes at final follow-up. A deviation in the aPDFA alters the knee's axis of rotation and the quadriceps moment arm, leading to abnormal contact stresses across the patellofemoral and tibiofemoral joints [10]. Our results, showing a β-coefficient of –2.35 for ROM and 0.08 for LLD, suggest that even minor sagittal deviations can lead to cumulative joint degeneration and functional impairment over time. Although sagittal malalignment was not identified as a definitive independent predictor of the severity of joint degeneration (ΔK-L grade) in our model, these altered biomechanics may still potentially predispose the joint to early degenerative changes. This emphasizes that surgeons should prioritize restoring the sagittal profile as meticulously as coronal alignment. Another critical finding was the profound negative impact of reoperation on final knee ROM. The occurrence of a reoperation was associated with an average decrease of 17.5° in ROM (β=–17.5, P=0.001), which is a clinically significant loss that often hinders activities of daily living. Repeated surgical trauma likely exacerbates intra-articular adhesions and periarticular fibrosis, creating a cycle of stiffness that is difficult to reverse. Therefore, achieving definitive stability during the index surgery to minimize the need for subsequent interventions is paramount for optimizing patient prognosis.

Reoperation represents a major alteration in the treatment course and often reflects the cumulative impact of complications such as nonunion, implant failure, or infection. While fracture subtype was associated with higher rates of reoperation, the present analyses suggest that the occurrence of reoperation itself is more closely related to inferior functional and structural outcomes than fracture classification alone. This highlights the clinical significance of preventing complications that necessitate reoperation, particularly in patients with complex fracture patterns. To address the potential confounding effect of reoperations on clinical outcomes, we performed a thorough analysis incorporating 'reoperation' as a key independent variable in our multivariable models. Rather than excluding these cases—which represent a significant clinical reality in complex AO/OTA 33C fractures—including them allowed us to quantify their impact directly. Our analysis identified that undergoing a reoperation was a significant independent predictor of poorer functional outcomes (P<0.05). The inclusion of these cases ensures that our findings reflect the

https://doi.org/10.12671/jmt.2026.00073

true clinical burden and challenges associated with these high-energy injuries, rather than presenting an idealized outcome. From a clinical perspective, these results emphasize that efforts to improve outcomes after intra-articular distal femur fractures should focus on modifiable surgical and postoperative factors. While fracture classification provides valuable information regarding injury severity and anticipated complications, optimizing reduction quality, maintaining appropriate alignment, and preventing complications that lead to reoperation may have a greater impact on long-term functional and structural outcomes.

Limitations

Several limitations of this study should be acknowledged. The retrospective design introduces inherent limitations, including potential selection and information bias. Follow-up duration varied among patients, although this variability was explicitly examined when evaluating radiographic osteoarthritis progression. The study was conducted at a single Level I trauma center, which may limit generalizability to other practice settings. In addition, this study did not perform a detailed subgroup analysis based on the specific anatomical locations of concomitant fractures, such as the ipsilateral hip, tibial plateau, or ankle. Concomitant fractures in the same limb—often described as 'floating knee' injuries—are associated with significantly higher morbidity and poorer functional recovery compared to isolated fractures. Demirtas et al. [14] emphasized that the presence of multi-level fractures complicates the early rehabilitation protocol and negatively impacts the final clinical scores. Similarly, Hierholzer et al. [6] highlighted that complex fracture patterns involving adjacent joints present unique biological and mechanical challenges that can compromise both reduction quality and ROM. Given the heterogeneity of these associated injuries, future research with larger cohorts is warranted to categorize how specific concomitant fracture patterns independently influence long-term outcomes.

The precise mechanism of LLD could not be definitively categorized into structural bone shortening, sagittal bowing, or functional shortening due to joint contracture. Because our radiographic assessment of LLD relied on standing anteroposterior (AP) scanograms without corresponding lateral views, we could not fully account for the influence of sagittal plane deformities or knee flexion contractures on the final limb length. Although our multivariable analysis suggested an association between sagittal malalignment (ΔaPDFA) and LLD, these findings are limited by the two-dimensional nature of the imaging. Moreover, it is worth noting that the mean LLD in our cohort was relatively small (approximately 1.3 cm). While statistically significant within our regression model, this magnitude of limb shortening remains below the threshold typically considered clinically symptomatic or disabling. Future studies utilizing three-dimensional CT reconstruction or bilateral lateral scanograms are warranted to differentiate these complex mechanisms of limb shortening following AO/OTA 33C fractures.

Finally, the minimum follow-up duration of 12 months is a clear limitation of this study, particularly for the definitive assessment of post-traumatic osteoarthritis. While our data captured significant early degenerative changes (ΔK-L grade), which may be attributed to the rapid progression of osteoarthritis following high-energy intra-articular trauma in AO/OTA 33C fractures, this duration is likely insufficient to determine the true long-term incidence of symptomatic osteoarthritis or late conversion to TKRA. Consequently, our findings should be interpreted as early to mid-term outcomes, and further studies with longer follow-up are required to evaluate the final structural and functional status of the joint.

Despite these limitations, the present study provides clinically relevant insights by integrating fracture classification, radiographic parameters, postoperative complications, and late outcomes within a unified analytical framework. By shifting the focus from fracture subtype alone to modifiable factors and treatment course, this study offers a practical perspective for improving long-term outcomes following intra-articular distal femur fractures.

Conclusions

Postoperative complications following intra-articular distal femur fractures demonstrated predictable patterns according to AO/OTA fracture subtype, confirming the relevance of fracture classification in anticipating complication risk. However, final outcomes such as knee ROM, LLD, and radiographic osteoarthritis were associated not only with fracture pattern but also with radiographic alignment parameters and the occurrence of reoperation. These findings emphasize that while fracture classification provides an important framework, active efforts to prevent complications and optimize alignment during treatment are critical to improving long-term outcomes after plate fixation.

Article Information

Author contributions

All the work was done by Hee Gon Park.

Conflicts of interest

No potential conflict of interest relevant to this article was reported.

Funding

This research was supported by the Dankook University College of Medicine Research Fund in 2025 (Grant No. R202501235).

Data availability

Contact the corresponding author for data availability.

Acknowledgments

None.

Supplementary materials

None.

References

1. Ehlinger M, Ducrot G, Adam P, Bonnomet F. Distal femur fractures. Orthop Traumatol Surg Res 2013;99:353-60.
2. Henderson CE, Lujan TJ, Kuhl LL, Bottlang M, Fitzpatrick DC, Marsh JL. Healing complications are common after locked plating for distal femur fractures. Clin Orthop Relat Res 2011;469:1757-65.
3. Ricci WM, Loftus T, Cox C, Borrelli J. Locked plates combined with minimally invasive insertion technique for the treatment of periarticular fractures of the knee. J Orthop Trauma 2004;18:659-66.
4. Meinberg EG, Agel J, Roberts CS, Karam MD, Kellam JF. Fracture and dislocation classification compendium-2018. J Orthop Trauma 2018;32 Suppl 1:S1-170.
5. Zlowodzki M, Williamson S, Cole PA, Zardiackas LD, Kregor PJ. Biomechanical evaluation of fixation of distal femur fractures. J Orthop Trauma 2004;18:494-502.
6. Hierholzer C, von Ruden C, Potzel T, Woltmann A, Buhren V. Outcome analysis of retrograde nailing and less invasive stabilization system in distal femoral fractures: a retrospective analysis. Indian J Orthop 2011;45:243-50.
7. Elsoe R, Ceccotti AA, Larsen P. Population-based epidemiology of distal femur fractures. Int Orthop 2018;42:191-6.
8. Martinet O, Cordey J, Harder Y, Maier A, Buhler M, Barraud GE. The epidemiology of fractures of the distal femur. Injury 2000;31(Suppl 3):C62-3.
9. Pritchett JW. Supracondylar fractures of the femur. Clin Orthop Relat Res 1984;(184):173-7.
10. Kook I, Kim KY, Hwang KT. The impact of medial-first dual plating for reduction of distal femoral fractures: a retrospective comparative cohort study. Sci Rep 2025;15:15454.
11. Sharma L, Song J, Felson DT, Cahue S, Shamiyeh E, Dunlop DD. The role of knee alignment in disease progression and functional decline in knee osteoarthritis. JAMA 2001;286:188-95.
12. Brouwer GM, van Tol AW, Bergink AP, et al. Association between knee alignment and osteoarthritis progression. Arthritis Rheum 2007;56:1204-11.
13. Kellgren JH, Lawrence JS. Radiological assessment of osteo-arthrosis. Ann Rheum Dis 1957;16:494-502.
14. Demirtas A, Azboy I, Alemdar C, et al. Functional outcomes and quality of life in adult ipsilateral femur and tibia fractures. J Orthop Transl 2018;16:53-61.

https://doi.org/10.12671/jmt.2026.00073

JMT Journal of Musculoskeletal Trauma

pISSN 3058-6267 · eISSN 3058-6275
J Musculoskelet Trauma 2026;39(3):227-235
https://doi.org/10.12671/jmt.2026.00101

Open reduction and internal fixation for distal humerus fractures in older adults: a retrospective comparative study by osteoporosis status

Tong Joo Lee, Hee Beom Shin, Yongseok Lee

Department of Orthopedic Surgery, Inha University Hospital, Incheon, Korea

Background: Distal humerus fractures in older patients, particularly those with osteoporosis, pose substantial treatment challenges because of increased fracture complexity and compromised bone stock. Open reduction and internal fixation (ORIF) is the preferred treatment but may be complicated by fixation failure. This study investigated the outcomes of ORIF in older osteoporotic and nonosteoporotic patients with complete articular distal humerus fractures.

Methods: This retrospective study included 19 patients with Arbeitsgemeinschaft für Osteosynthesefragen/Orthopaedic Trauma Association (AO/OTA) 13C distal humerus fractures who underwent surgical treatment between 2012 and 2024. The mean patient age was 79.1 years. Patients were divided into osteoporotic (n=11) and nonosteoporotic (n=8) groups based on the lowest recorded dual-energy X-ray absorptiometry T-score at the femoral neck or lumbar spine. Osteoporosis was defined as a T-score of –2.5 or lower, and the nonosteoporotic group included patients with osteopenia. All fractures were treated with ORIF using bicolumnar plating. All included patients completed 12 months of clinical follow-up for visual analog scale (VAS) and Mayo Elbow Performance Score (MEPS) assessments. Radiographic follow-up was recorded separately and continued until union was confirmed; imaging follow-up extended to 12 months or longer in 14 patients and was limited to 6 months in five asymptomatic patients after confirmed union.

Results: Both groups showed significant within-group improvement in pain, as assessed using the VAS, and function, as assessed using the MEPS, over time. Between-group comparisons at each follow-up time point showed no statistically significant differences in VAS or MEPS. No radiographic nonunion was observed during the available imaging follow-up, and complications were limited to one case of screw pullout/loosening and one case of postoperative stiffness.

Conclusions: ORIF provides reliable outcomes for older patients with complex distal humerus fractures, regardless of osteoporosis status, when stable reconstruction is achievable. These findings suggest that ORIF remains a viable treatment option, with satisfactory functional recovery and low complication rates in this population.

Level of evidence: III.

Keywords: Distal humerus fractures; Internal fracture fixation; Osteoporotic fractures; Aged; Bone plates

Original Article

Received: February 15, 2026
Revised: May 6, 2026
Accepted: May 11, 2026

Correspondence to:
Tong Joo Lee
Department of Orthopedic Surgery, Inha University Hospital, Incheon 22332, Korea
Tel: +82-32-890-3662
Email: TJLee@inha.ac.kr

Introduction

Distal humerus fractures are relatively uncommon, accounting for approximately 1%–2% of adult fractures, yet they can result in substantial functional impairment because elbow stiffness and pain may markedly limit activities of daily living (ADL)—especially in older patients [1,2]. These injuries show a bimodal distribution, with high-energy trauma predominating in younger patients and low-energy falls predominating in older, often osteoporotic patients; consequently, the incidence of distal humerus fractures in the geriatric population is expected to rise as the population ages [1,2]. Complete articular fractures (Arbeitsgemeinschaft für Osteosynthesefragen/Orthopaedic Trauma Association [AO/OTA] type 13C) are frequently encountered in elderly patients and are commonly associated with severe intra-articular comminution and compromised bone stock, making stable reconstruction particularly challenging [1,3]. As osteoporosis is highly prevalent among older adults, particularly in women, the burden of fragility fractures in the elderly population has been steadily increasing [4].

Importantly, osteoporosis appears not only to increase fracture complexity but also to adversely influence fixation outcomes. In a multicenter study of patients >65 years treated with plate fixation for distal humerus fractures, osteoporosis was identified as the main predictor of failure, increasing the risk of combined clinical and radiological failure regardless of the construct or hardware used [5]. Open reduction and internal fixation (ORIF) with bicolumnar plating remains a principal reconstructive strategy for intra-articular distal humerus fractures, aiming to restore the articular surface and provide sufficient stability to permit early motion [1,2]. With contemporary anatomic locking plate constructs, ORIF for AO/OTA 13C fractures in older adults has been reported to yield satisfactory patient-reported outcomes (Oxford Elbow Score, Mayo Elbow Performance Score [MEPS], and Quick Disabilities of the Arm, Shoulder and Hand [Quick DASH]), although revision surgery remains a relevant concern [3]. Nevertheless, even with modern implants, complex complete articular fractures continue to be associated with complications such as fixation failure or nonunion, reflecting the inherent severity of intra-articular comminution in osteoporotic bone [1,5].

Total elbow arthroplasty (TEA) has also been advocated as an alternative primary option for selected elderly patients with highly comminuted or "unreconstructible" distal humerus fractures [1,2]. Good to excellent short-term clinical results after primary TEA have been reported in elderly Asian patients with distal humerus fractures, and some authors have suggested that arthroplasty may provide more predictable early outcomes than ORIF in carefully selected patients; however, the optimal strategy remains debated [6,7].

A comparative systematic review and meta-analysis of elderly distal humerus fractures reported that while TEA may yield a greater flexion-extension arc and lower rates of reoperation and postoperative stiffness, functional outcome scores (e.g., MEPS and DASH) were overall similar between ORIF and TEA [2,8]. Evidence stratified by osteoporosis status in elderly patients undergoing ORIF for complete articular distal humerus fractures remains scarce. Therefore, the purpose of the present study was to compare the radiographic and clinical outcomes of ORIF between osteoporotic and nonosteoporotic elderly patients [2,3].

Methods

Ethics statement

The study was approved by the Institutional Review Board (IRB) of Inha University Hospital (IRB No. 2025-08-001-000) and performed in accordance with the principles of the Declaration of Helsinki. The need for written informed consent was waived because of its retrospective design by the IRB.

Study design and setting

This retrospective study was conducted at Inha University Hospital and included 19 patients who underwent ORIF for complete articular distal humerus fractures (AO/OTA 13C) after low-energy falls between 2012 and 2024. All surgeries were performed by a single experienced surgeon, who maintained consistent surgical principles, exposure strategy, and bicolumnar fixation concept throughout the study period, although minor temporal changes in implants or perioperative care may still have occurred.

Participants

The cohort consisted of five males and 14 females, with a mean age of 79.1 years at the time of injury.

All fractures were classified as AO/OTA 13C type, repre-

 https://doi.org/10.12671/jmt.2026.00101

senting complex distal humeral fractures. Inclusion criteria were age ≥75 years, AO/OTA 13C distal humerus fracture, treatment with ORIF, and availability of at least 12 months of clinical follow-up for VAS and MEPS assessment. Exclusion criteria were patients managed nonoperatively, patients treated with strategies other than ORIF, fracture patterns other than AO/OTA 13C (including extra-articular fractures), and cases without at least 12 months of clinical follow-up.

Bias

Treatment-selection bias cannot be excluded because the analysis was restricted to ORIF-treated cases deemed suitable for reconstruction.

Variables

Group classification was based on the lowest recorded dual-energy X-ray absorptiometry T-score at the femoral neck or lumbar spine. Osteoporosis was defined as a T-score of –2.5 or lower at either site, whereas nonosteoporotic status was defined as a T-score greater than –2.5; therefore, the nonosteoporotic group included patients with osteopenia.

Union was defined as progressive reduction of the fracture gap and evidence of osteogenesis with cortical continuity or bridging trabecular bone across the fracture site on serial radiographs compared with prior images, together with maintained alignment. Nonunion was defined as absence of progressive healing on serial radiographs, persistent fracture gap or implant-related instability, or the need for additional surgery because of failure of union. Radiographs and postoperative complications were assessed by the treating surgeon during outpatient follow-up and were reviewed retrospectively from the stored images and clinical records.

Data sources and measurement

Clinical evaluations were conducted at approximately 3 months, 6 months, and 12 months, and functional outcomes, including the MEPS, VAS, and range of motion (ROM), were reviewed. In this study, the minimum follow-up criterion referred to clinical follow-up: all included patients completed clinical follow-up through 12 months for VAS and MEPS assessment.

Radiographic evaluation was performed with serial anteroposterior and lateral elbow radiographs to assess fracture healing, alignment, and complications. In clinically asymptomatic patients in whom union had already been confirmed, further radiographic follow-up was not routinely continued; accordingly, radiographic follow-up was limited to 6 months in five patients, whereas the remaining patients had radiographic follow-up to 12 months or longer (up to 3 years).

Statistical methods

Statistical analysis was performed using Python ver. 3.6.2 (Python Software Foundation). Continuous variables were expressed as mean±standard deviation, and categorical variables were presented as frequencies and percentages. Within-group changes over time were assessed using Friedman tests followed by Wilcoxon signed-rank tests with Bonferroni correction. Between-group comparisons at each time point were performed using Mann-Whitney U tests, and $P<0.05$ was considered statistically significant.

Rehabilitation protocol

Postoperatively, patients were initially placed in a posterior long-arm splint to immobilize the elbow joint and protect the surgical site for the first 2 weeks. After 2 weeks, the splint was removed, stitch removal was performed, and a hinged elbow brace was applied to control the ROM within a safe arc. This brace was maintained for an additional 2 weeks to allow for controlled early motion. From 1 month postoperatively, passive ROM exercises were initiated to prevent stiffness and promote joint mobility. Initially, these exercises were passive, and patients were encouraged to perform them under the guidance of a trained physical therapist. After 3 months, patients were gradually allowed to return to ADL, with increasing levels of strength and functional activity. At this point, the rehabilitation protocol transitioned from passive ROM exercises to active exercises aimed at strengthening the elbow and regaining full function. Throughout the rehabilitation process, patients were monitored closely to ensure appropriate healing, and the therapy was adjusted based on individual progress and complications.

Results

Participant flow and baseline characteristics

Nineteen patients met the inclusion criteria, including 14 females (73.7%) and five males (26.3%). The mean age at injury was 79.1±3.9 years (range, 75–88 years). All injuries resulted from low-energy falls. All fractures were classified as complete articular distal humerus fractures (AO/OTA 13C). Fracture subtypes included 13C1 in eight patients (42.1%), 13C2 in five (26.3%), and 13C3 in six (31.6%). Patients were stratified into a nonosteoporotic group (n=8) and an osteoporotic group (n=11) based on bone mineral density (BMD). The osteoporotic group had a lower mean BMD T-score than the nonosteoporotic group (−3.29±0.71 vs. −1.24±0.48). All 19 patients completed clinical follow-up through 12 months for VAS and MEPS assessment. Radiographic follow-up was continued until union was confirmed; therefore, imaging follow-up was limited to 6 months in five asymptomatic patients after confirmed union and extended to 12 months or longer (up to 3 years) in 14 patients. Accordingly, any shorter follow-up duration shown in the demographic data refers to radiographic rather than clinical follow-up. Baseline characteristics are summarized in Table 1.

Table 1. Baseline demographics by osteoporosis status

Variable	Nonosteoporotic group	Osteoporotic group	P-value
No. of patients	8	11	
Age at injury (yr)	77.0 (75.0 to 78.0)	80.0 (77.5 to 82.0)	0.113
Female sex	4 (50.0)	10 (90.9)	0.111
BMI (kg/m^2)	24.5 (22.1 to 27.1)	24.5 (22.8 to 26.9)	0.821
BMD T-score	−1.2 (−1.6 to −0.8)	−3.2 (−3.6 to −2.8)	
Radiographic follow-up (mo)	21.0 (6.0 to 25.5)	12.0 (12.0 to 16.5)	0.387
Olecranon osteotomy approach	7 (87.5)	8 (72.7)	0.603
ER visit	8 (100.0)	7 (63.6)	0.103
AO/OTA subtype			
13C1	3 (37.5)	5 (45.5)	
13C2	2 (25.0)	3 (27.3)	
13C3	3 (37.5)	3 (27.3)	

Values are presented as median (interquartile range, IQR) for continuous variables and number (%) for categorical variables. P-values were calculated using the Mann-Whitney U test for continuous variables and the Fisher exact test for categorical variables (two-sided). BMD T-score was used to define group allocation; therefore, no statistical comparison was performed for this variable.
BMI, body mass index; BMD, bone mineral density; ER, emergency room; AO/OTA, Arbeitsgemeinschaft für Osteosynthesefragen/Orthopaedic Trauma Association; IQR, interquartile range.

Surgical and treatment characteristics

An olecranon osteotomy was performed to facilitate intra-articular exposure in 15/19 cases (78.9%), including 7/8 (87.5%) in the nonosteoporotic group and 8/11 (72.7%) in the osteoporotic group. A posterior approach without osteotomy was used in 4/19 cases (21.1%). All fractures were treated with ORIF using bicolumnar (dual-plate) constructs; parallel dual-plate fixation supplemented with cannulated screw fixation was documented in 13/19 patients (68.4%) [9-12].

Clinical and functional outcomes: within-group analysis

Mean group trajectories for pain (VAS) and function (MEPS) are shown in Figs. 1 and 2, respectively. VAS scores decreased over time in both groups. In the nonosteoporotic group, mean VAS decreased from 3.38±0.74 at 3 months to 1.25±1.39 at 6 months and 0.62±1.41 at 12 months. In the osteoporotic group, mean VAS decreased from 4.64±1.96 at 3 months to 1.18±0.98 at 6 months and 0.18±0.40 at 12 months. Within-group improvement over time was statistically significant for both the nonosteoporotic group (Friedman P=0.002) and the osteoporotic group (Friedman P<0.001). Post hoc Wilcoxon signed-rank tests showed significant reductions from 3 to 6 months and from 3 to 12 months in both groups (Bonferroni-adjusted P<0.05); the 6- to 12-month interval did not reach significance in the nonosteoporotic group for VAS (Bonferroni-adjusted P=0.307).

MEPS increased over time in both groups. In the nonosteoporotic group, mean MEPS improved from 74.38±8.63 at 3 months to 83.12±5.94 at 6 months and 90.62±4.17 at 12 months. In the osteoporotic group, mean MEPS improved from 65.00±13.78 at 3 months to 83.18±8.15 at 6 months and 92.27±4.67 at 12 months. Within-group improvement over time was significant for both the nonosteoporotic group (Friedman P<0.001) and the osteoporotic group (Friedman P<0.001). Post hoc Wilcoxon signed-rank tests demonstrated significant improvements across all intervals for MEPS in both groups after Bonferroni correction (all adjusted P<0.05).

Comparative analysis: between-group outcomes

Between-group comparisons at each time point did not show statistically significant differences in VAS (3 months, P=0.124; 6 months, P=0.931; 12 months, P=0.684) or MEPS

https://doi.org/10.12671/jmt.2026.00101

(3 months, P=0.102; 6 months, P=0.898; 12 months, P=0.295). Although the osteoporotic group had numerically less favorable 3-month scores, no between-group difference reached statistical significance at any fixed time point.

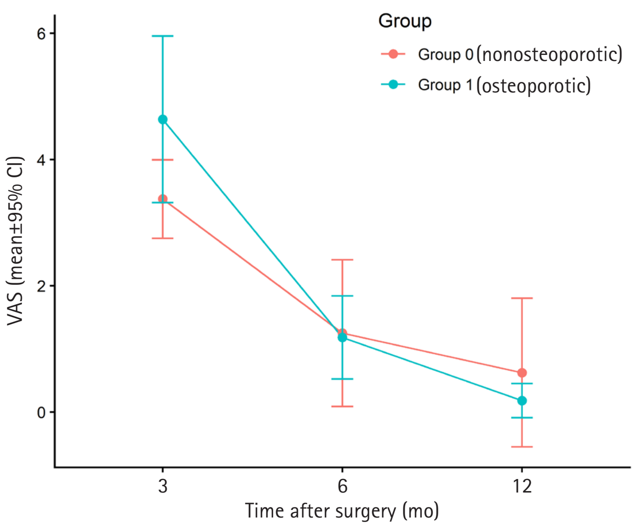

Fig. 1. Visual analog scale (VAS) scores over time (mean±95% confidence interval [CI]). Mean VAS pain scores at 3, 6, and 12 months postoperatively are shown for osteoporotic (n=11) and nonosteoporotic (n=8) groups. The points represent group means and error bars indicate 95% CI. Lower VAS scores indicate less pain.

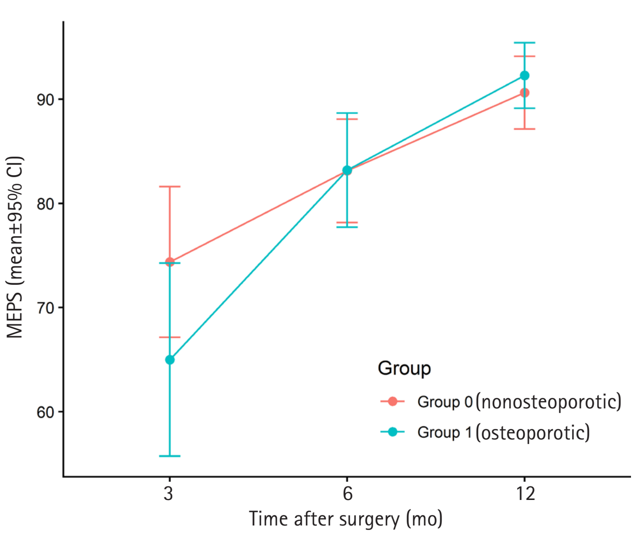

Fig. 2. Mayo Elbow Performance Score (MEPS) over time (mean±95% confidence interval [CI]). MEPS at 3, 6, and 12 months postoperatively are shown for osteoporotic (n=11) and nonosteoporotic (n=8) groups. Points represent group means and error bars indicate 95% CI. Higher MEPS values indicate better elbow function.

Therefore, these subgroup observations should not be interpreted as evidence of a different treatment effect according to osteoporosis status.

Radiographic outcomes and postoperative complications

No radiographic nonunion was recorded during the available imaging follow-up. In five patients, radiographic follow-up was limited to 6 months because union had already been confirmed and the patients remained clinically asymptomatic. In the two representative cases shown in Figs. 3-5 (one from each group), postoperative radiographs obtained at approximately 4 months (Fig. 5) demonstrated maintained alignment and progression to union without evidence of nonunion.

Complications were recorded in 2/19 patients (10.5%). One patient in the nonosteoporotic group developed postoperative stiffness with hematoma, and one patient in the osteoporotic group demonstrated screw pullout/loosening. Both were managed without documented nonunion. No other major complications were recorded.

Fig. 3. Preoperative radiographs of nonosteoporotic and osteoporotic patients with complete articular distal humerus fractures. Nonosteoporotic patient: (A) oblique view and (B) anteroposterior (AP) view. Osteoporotic patient: (C) lateral view and (D) AP view.

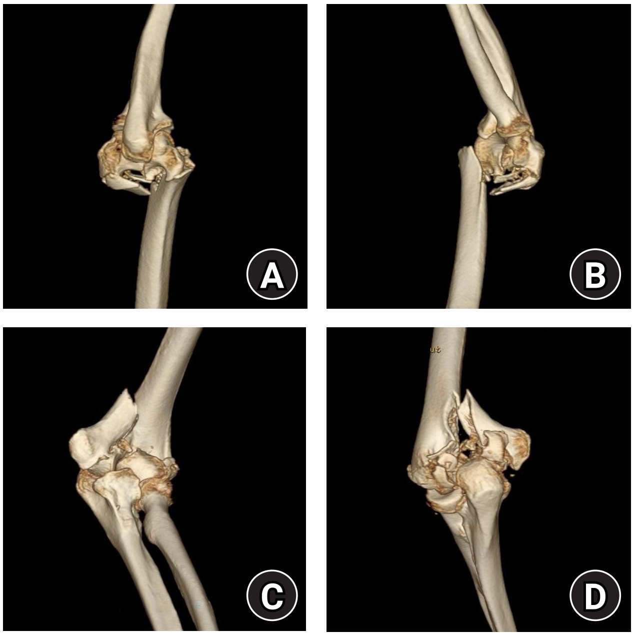

Fig. 4. Preoperative three-dimensional computed tomography reconstructions of complete articular distal humerus fractures. (A, B) Lateral view of a nonosteoporotic patient. (C) External oblique view and (D) posterior view of an osteoporotic patient, demonstrating more severe comminution and bone fragmentation.

Fig. 5. Postoperative (4-mo) radiographs demonstrating successful union in both groups. Nonosteoporotic patient: (A) anteroposterior view and (B) lateral view. Osteoporotic patient: (C) lateral view and (D) anteroposterior view.

A representative nonosteoporotic case and an osteoporotic case are presented in Figs. 3-5. In both cases, an olecranon osteotomy provided adequate joint exposure for intra-articular reduction, ulnar nerve transposition was performed to protect the ulnar nerve, and stable fixation was achieved using parallel dual-plate constructs supplemented with cannulated screw fixation. At 12 months, both representative cases demonstrated low pain (VAS, 0 and 1, respectively) and excellent elbow function (MEPS, 95 and 95, respectively).

Discussion

The management of complete articular distal humerus fractures in elderly patients remains particularly challenging, especially in the context of osteoporosis. Previous studies have emphasized that intra-articular distal humerus fractures in older adults are technically demanding because of fracture complexity, comminution, and compromised bone quality [13]. With ongoing population aging and the increasing prevalence of fragility fractures, the incidence of complex intra-articular distal humerus fractures in elderly patients is expected to continue to rise [14].

In the present study, ORIF yielded satisfactory radiographic and functional outcomes in selected patients aged ≥75 years with complete articular distal humerus fractures (AO/OTA type 13C). No radiographic nonunion was identified during the available imaging follow-up, and both groups showed progressive improvement in pain and elbow function over time. Because between-group differences at fixed postoperative time points were not statistically significant, these subgroup findings should be regarded as descriptive rather than confirmatory.

Surgical approach: olecranon osteotomy vs. triceps-sparing

The optimal surgical approach for AO/OTA type 13C distal humerus fractures remains debated. Olecranon osteotomy and posterior triceps-sparing (paratricipital) approaches are both commonly used, and comparative evidence suggests that overall functional outcomes are similar; therefore, the approach can be individualized based on fracture

https://doi.org/10.12671/jmt.2026.00101

morphology and the need for articular visualization [15,16]. Olecranon osteotomy can provide excellent exposure for accurate reduction in extensively comminuted patterns, but it introduces osteotomy-specific risks such as delayed union/nonunion, symptomatic hardware, and infection [17]. Triceps-sparing approaches preserve the extensor mechanism and avoid osteotomy-related complications, but limited exposure may compromise reduction quality in severely comminuted fractures [15,16].

Given the predominance of highly comminuted AO/OTA type 13C fractures in the present cohort, olecranon osteotomy was preferentially employed to obtain adequate articular exposure and achieve stable reconstruction. Despite its potential disadvantages, this approach resulted in reliable fracture union and favorable functional outcomes, supporting its continued role in the management of complex intra-articular distal humerus fractures when complete visualization of the articular surface is required [15,16].

The necessity of bone grafting in comminuted fractures

The role of bone grafting in the surgical management of comminuted distal humerus fractures remains controversial. Bone grafting may be considered to address metaphyseal voids or segmental defects and to augment fixation when structural support and/or biology are a concern, but the decision depends on graft source, timing, and alternative options. Autograft offers osteogenic, osteoinductive, and osteoconductive potential but entails donor-site morbidity, whereas allograft avoids donor-site morbidity but may incorporate more slowly and carries risks related to immune response and infection transmission [18]. Regardless of graft use, heterotopic ossification and postoperative elbow stiffness are recognized complications after distal humerus fracture fixation and should be minimized through careful soft-tissue handling and early rehabilitation [19].

In this series, bone grafting was not performed in any patient. Instead, surgical management focused on meticulous reduction, preservation of native bone fragments, rigid bicolumnar fixation, and restoration of overall articular congruity [10-12,20]. Despite severe comminution and osteoporotic bone quality, all fractures achieved radiographic union within 1 year, without excessive postoperative stiffness or heterotopic ossification. These findings suggest that routine bone grafting may not be mandatory in elderly patients with complex intra-articular distal humerus fractures when stable fixation and accurate reconstruction are achieved [19].

Ulnar nerve management: routine transposition

Routine anterior ulnar nerve transposition was performed in all cases to minimize the risk of postoperative ulnar neuropathy. In distal humerus fractures treated through posterior approaches, the ulnar nerve is susceptible to traction, compression, and implant-related irritation. However, comparative studies have reported that routine transposition in patients without preoperative ulnar neuropathy may not reduce—and may increase—the incidence of postoperative ulnar neuritis compared with in situ management [21,22]. In the present cohort, no clinically significant ulnar nerve complications were observed, underscoring the importance of careful ulnar nerve identification, decompression, and gentle handling regardless of the chosen strategy [19].

Limitations

This study has several limitations. First, its retrospective single-center design and the fact that all procedures were performed by a single surgeon introduce potential selection bias and limit external generalizability. In addition, the relative rarity of distal humerus fractures resulted in a small sample size (n=19), leading to limited statistical power to detect small-to-moderate effects and reducing the power of subgroup analyses; therefore, the findings should be interpreted as exploratory.

Second, patients were included over a 12-year period. Although the same surgeon maintained consistent surgical principles, exposure strategy, and bicolumnar fixation concept, temporal changes in implant availability, perioperative care, and accumulated surgeon experience may still have introduced time-related confounding.

Third, only patients treated with ORIF were included, whereas those managed nonoperatively or with other treatment strategies were excluded. Because only cases considered suitable for reconstruction were analyzed, treatment-selection bias cannot be excluded.

Fourth, although clinical outcomes (VAS and MEPS) were available through 12 months in all included patients, radiographic follow-up duration was shorter in five asymptomatic patients because imaging was discontinued after confirmed union at 6 months. Accordingly, the radiographic follow-up range should not be interpreted as incomplete 12-month clinical follow-up, although this approach may still have limited the assessment of later radiographic changes.

Fifth, although ROM was assessed clinically, measurements were not obtained under a fully standardized protocol at every visit, and other validated patient-reported outcome measures were not uniformly available.

Conclusions

ORIF can provide satisfactory clinical recovery and reliable radiographic union in selected elderly patients with severely comminuted intra-articular distal humerus fractures. In this small retrospective comparative study, postoperative outcomes at predefined time points were not significantly influenced by osteoporosis status.

However, given the limited sample size and nonrandomized design, these findings should be interpreted with caution. Further large-scale studies with standardized follow-up protocols and comparative analyses are warranted to better define the role of ORIF relative to alternative treatment strategies in this patient population.

Article Information

Author contributions

Conceptualization: TJL. Data curation: HBS, YL. Formal analysis: TJL, HBS, YL. Funding acquisition: TJL. Writing–original draft: TJL, HBS, YL. Writing–review & editing: TJL, HBS, YL. All authors read and approved the final manuscript.

Conflicts of interest

No potential conflict of interest relevant to this article was reported.

Funding

This research was supported by an Inha University Research Grant (2025).

Data availability

Contact the corresponding author for data availability.

Acknowledgments

None.

Supplementary materials

None.

References

1. Beazley JC, Baraza N, Jordan R, Modi CS. Distal humeral fractures: current concepts. Open Orthop J 2017;11:1353-63.
2. Seok HG, Park JJ, Park SG. Comparison of the complications, reoperations, and clinical outcomes between open reduction and internal fixation and total elbow arthroplasty for distal humeral fractures in the elderly: a systematic review and meta-analysis. J Clin Med 2022;11:5775.
3. Kervinen KV, Salmela MT, Lähdeoja TA. Outcomes of AO/OTA C-type fractures of the distal humerus after open reduction and internal fixation with locking plate constructs in patients at least 65 years old. BMC Musculoskelet Disord 2022;23:523.
4. Sarafrazi N, Wambogo EA, Shepherd JA. Osteoporosis or low bone mass in older adults: United States, 2017-2018. NCHS Data Brief 2021;(405):1-8.
5. Clavert P, Ducrot G, Sirveaux F, Fabre T, Mansat P. Outcomes of distal humerus fractures in patients above 65 years of age treated by plate fixation. Orthop Traumatol Surg Res 2013;99:771-7.
6. Lee KT, Lai CH, Singh S. Results of total elbow arthroplasty in the treatment of distal humerus fractures in elderly Asian patients. J Trauma 2006;61:889-92.
7. Parker P, Furness ND, Evans JP, Batten T, White WJ, Smith CD. A systematic review of the complications of contemporary total elbow arthroplasty. Shoulder Elbow 2021;13:544-51.
8. Githens M, Yao J, Sox AH, Bishop J. Open reduction and internal fixation versus total elbow arthroplasty for the treatment of geriatric distal humerus fractures: a systematic review and meta-analysis. J Orthop Trauma 2014;28:481-8.
9. Shin SJ, Sohn HS, Do NH. A clinical comparison of two different double plating methods for intraarticular distal humerus fractures. J Shoulder Elbow Surg 2010;19:2-9.
10. O'Driscoll SW. Optimizing stability in distal humeral fracture fixation. J Shoulder Elbow Surg 2005;14(1 Suppl S):186S-194S.
11. Sanchez-Sotelo J, Torchia ME, O'Driscoll SW. Complex distal

https://doi.org/10.12671/jmt.2026.00101

humeral fractures: internal fixation with a principle-based parallel-plate technique. J Bone Joint Surg Am 2007;89:961-9.
12. Lee SK, Kim KJ, Park KH, Choy WS. A comparison between orthogonal and parallel plating methods for distal humerus fractures: a prospective randomized trial. Eur J Orthop Surg Traumatol 2014;24:1123-31.
13. Stoddart MT, Panagopoulos GN, Craig RS, et al. A systematic review of the treatment of distal humerus fractures in older adults: a comparison of surgical and non-surgical options. Shoulder Elbow 2024;16:175-85.
14. Charissoux JL, Vergnenegre G, Pelissier M, Fabre T, Mansat P. Epidemiology of distal humerus fractures in the elderly. Orthop Traumatol Surg Res 2013;99:765-9.
15. Jeong HS, Yang JY, Jeon SJ, Shon HC, Oh JK, Lim EJ. Comparison of olecranon osteotomy and paratricipital approach in distal humerus intra-articular fracture: a systematic review and meta-analysis. Medicine (Baltimore) 2022;101:e30216.
16. Chen G, Liao Q, Luo W, Li K, Zhao Y, Zhong D. Triceps-sparing versus olecranon osteotomy for ORIF: analysis of 67 cases of intercondylar fractures of the distal humerus. Injury 2011;42:366-70.
17. Spierings KE, Schoolmeesters BJ, Doornberg JN, Eygendaal D, van den Bekerom MP. Complications of olecranon osteotomy in the treatment of distal humerus fracture. Clin Shoulder Elb 2022;25:163-9.
18. Egol KA, Nauth A, Lee M, Pape HC, Watson JT, Borrelli J. Bone grafting: sourcing, timing, strategies, and alternatives. J Orthop Trauma 2015;29 Suppl 12:S10-4.
19. Savvidou OD, Zampeli F, Koutsouradis P, et al. Complications of open reduction and internal fixation of distal humerus fractures. EFORT Open Rev 2018;3:558-67.
20. Self J, Viegas SF, Buford WL, Patterson RM. A comparison of double-plate fixation methods for complex distal humerus fractures. J Shoulder Elbow Surg 1995;4(1 Pt 1):10-6.
21. Chen RC, Harris DJ, Leduc S, Borrelli JJ, Tornetta P, Ricci WM. Is ulnar nerve transposition beneficial during open reduction internal fixation of distal humerus fractures? J Orthop Trauma 2010;24:391-4.
22. Ahmed AF, Parambathkandi AM, Kong WJ, et al. The role of ulnar nerve subcutaneous anterior transposition during open reduction and internal fixation of distal humerus fractures: a retrospective cohort study. Int Orthop 2020;44:2701-8.

JMT Journal of Musculoskeletal Trauma

pISSN 3058-6267 · eISSN 3058-6275
J Musculoskelet Trauma 2026;39(3):236-244
https://doi.org/10.12671/jmt.2025.00374

Clinical and radiographic outcomes after surgical treatment of supination-adduction type ankle fractures in older (≥65 years) and younger (<65 years) patients: a retrospective single-center comparative study in Korea

JungHo Lee[1], Bawoo Ko[1], Hongik Choi[1], Jun-young Lee[1,2]

[1]Department of Orthopedic Surgery, Chosun University Hospital, Gwangju, Korea
[2]Department of Orthopedic Surgery, Chosun University College of Medicine, Gwangju, Korea

Background: Supination-adduction (SAD) ankle fractures involve a vertical medial malleolar fracture and potential tibial plafond impaction, but pattern-specific evidence in older patients remains limited. We compared postoperative complications and clinical/radiographic outcomes between older and younger patients and explored complication-associated factors within the older group.
Methods: We retrospectively reviewed 51 patients who underwent surgery for SAD-type ankle fractures (2010–2020): 30 younger (<65 years) and 21 older (≥65 years). The primary outcome was a composite of surgical site infection, loss of reduction, or delayed union. Functional recovery was assessed using Olerud-Molander Ankle Score (OMAS) and American Orthopaedic Foot & Ankle Society (AOFAS) scores through 12 months. Union and posttraumatic osteoarthritis were assessed radiographically at ≥18 months. Preoperative dual-energy X-ray absorptiometry was performed in older patients for exploratory analyses.
Results: Postoperative complications were higher in the older group (38.1% vs. 10.0%, P=0.035). In older patients, diabetes mellitus was associated with complications (odds ratio [OR], 9.17; 95% confidence interval [CI], 1.15–73.24; P=0.037); smoking was not (OR, 5.50; 95% CI, 0.71–42.60; P=0.103). At 12 months, OMAS and AOFAS scores did not differ significantly. One older patient developed nonunion, and posttraumatic osteoarthritis occurred in one patient per group. Lower T-scores (mean, −2.3±0.5) correlated with greater tibial plafond impaction depth (3.1±1.2 mm; ρ=−0.46, P=0.036) and showed a borderline significant correlation with articular step-off (2.0±0.8 mm; ρ=−0.43, P=0.052).
Conclusions: Older patients had higher postoperative complication rates than younger patients, although 12-month functional and late radiographic outcomes were comparable. Diabetes was associated with complications, though the small sample warrants cautious interpretation. Findings support careful perioperative optimization and individualized fixation based on fracture morphology and bone quality in older patients, especially those with diabetes.
Level of evidence: III.

Keywords: Ankle fractures; Aged; Postoperative complications; Diabetes mellitus; Treatment outcome

Original Article

Received: December 1, 2025
Revised: July 13, 2026
Accepted: July 16, 2026

Correspondence to:
Jun-young Lee
Department of Orthopedic Surgery, Chosun University Hospital, 365 Pilmun-daero, Dong-gu, Gwangju 61453, Korea
Tel: +82-62-220-3147
Email: leejy88@chosun.ac.kr

Introduction

Background and rationale

Ankle fractures are among the most common fractures treated by orthopedic surgeons, and their incidence increases in older adults as life expectancy and activity levels rise [1-4]. Older patients often have medical comorbidities, impaired soft-tissue conditions, reduced bone quality, and diminished physiologic reserve, all of which may complicate operative treatment and recovery [4-6]. Most studies of geriatric ankle fractures, however, have analyzed heterogeneous fracture patterns, which may obscure pattern-specific challenges.

The supination-adduction (SAD) pattern described by Lauge-Hansen is characterized by a transverse or avulsion injury of the lateral malleolus followed by a vertical medial malleolar fracture [7,8]. Varus loading and axial compression may produce marginal impaction of the medial tibial plafond and an articular step-off [9]. Restoring joint congruity and resisting vertical shear—often with buttress fixation—are therefore central to treatment. In older patients, reduced bone quality may increase articular impaction and make stable fixation more difficult even after low-energy trauma.

Objectives

Fracture-pattern–specific evidence on surgically treated SAD-type ankle fractures in older patients remains limited. The primary aim of this study was to compare postoperative complications and clinical, functional, and radiographic outcomes between older and younger patients; the secondary aim was to explore clinical and radiographic factors associated with postoperative complications within the older group. We hypothesized that older patients would have a higher postoperative complication rate and slower early functional recovery but would achieve comparable late outcomes when anatomical reduction and stable fixation were obtained.

Methods

Ethics statement

This study was conducted in compliance with the principles of the Declaration of Helsinki. The protocol was reviewed and approved by the Institutional Review Board (IRB) of Chosun University Hospital (IRB No. CHOSUN 2025-09-029-002). The requirement for individual informed consent was waived by the IRB because of the retrospective design.

Study design and participants

This retrospective comparative study reviewed patients who presented to the emergency department or outpatient clinic of our institution between January 2010 and December 2020 with an ankle fracture. SAD-type fractures were identified on preoperative plain radiographs and computed tomography (CT) according to the Lauge-Hansen pattern. Seventy-three SAD-type ankle fractures were identified; four were treated nonoperatively and 69 underwent surgery. After exclusion of patients with incomplete records or insufficient follow-up (n=8), open fractures (n=4), and multiple trauma (n=6), 51 patients were included (Fig. 1).

Patients were divided into a younger group (<65 years, n=30) and an older group (≥65 years, n=21). The 65-year cutoff was selected because it is widely used in clinical studies of geriatric ankle fractures and permits comparison with prior outcome studies [3,4,10].

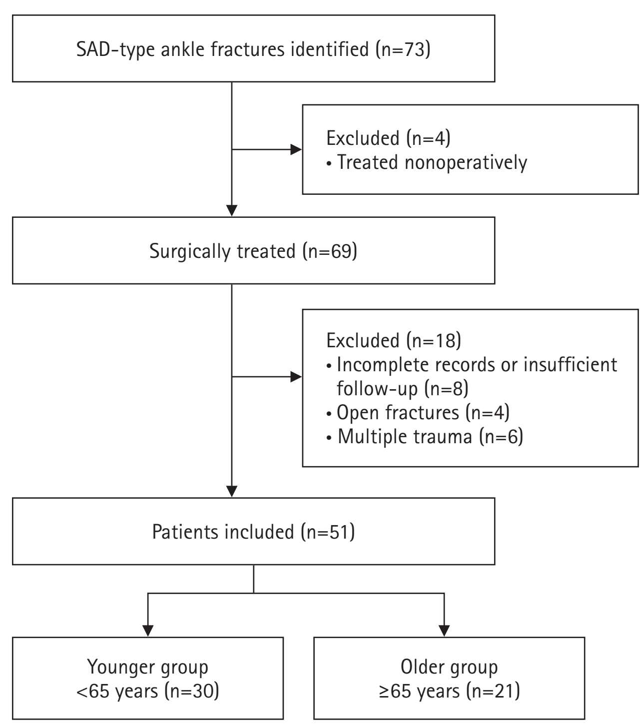

Fig. 1. Patient selection flow diagram. SAD, supination-adduction.

Clinical variables

Age, sex, body mass index, comorbidities, smoking status, trauma-energy level, fracture characteristics, and follow-up duration were collected from electronic medical records. Diabetes mellitus was defined as a documented diagnosis, current use of glucose-lowering medication, or a preoperative glycated hemoglobin level of ≥6.5%, consistent with current diagnostic criteria [11]. Hypertension was defined as a documented diagnosis or current use of antihypertensive medication.

Trauma was classified according to the documented event. High-energy trauma included motor vehicle, motorcycle, or bicycle collisions with direct impact, crush injuries, falls from a height greater than standing height, and sports injuries involving a documented high-velocity impact or direct collision. Low-energy trauma included falls from standing height, simple twisting or misstep injuries, and noncontact recreational sports injuries without high-velocity impact. Sports injuries were therefore classified individually rather than uniformly categorized as high-energy trauma.

Bone mineral density assessment

Dual-energy X-ray absorptiometry (DXA) was performed in all 21 older patients, generally during the index admission and before surgery, at the lumbar spine, femoral neck, and total hip. The lowest valid T-score among these sites was recorded as the representative value, and osteoporosis was defined as a T-score ≤–2.5 [12]. Because DXA was not systematically obtained in younger patients, between-group comparisons of T-score and osteoporosis prevalence were not performed; analyses involving T-score were restricted to the older group and were considered exploratory.

Surgical technique

All operations were performed by a single orthopedic trauma surgeon. Fixation was individualized according to fracture morphology, fragment size, comminution, bone quality, and intraoperative stability. Simple, noncomminuted lateral malleolar fractures with an adequately sized fragment were treated with cannulated screw fixation, whereas plate fixation was used when the lateral malleolar fracture was comminuted, unstable, or unsuitable for screw fixation alone. Vertical medial malleolar fractures were treated with cannulated screws, a buttress plate, or a combination; buttress plating was preferred in the presence of a vertical shear component, metaphyseal comminution, poor bone quality, or inadequate stability with screws alone.

When tibial plafond impaction was present, the impacted articular fragment was elevated under direct and fluoroscopic guidance to restore joint congruity (Fig. 2), and bone graft or a bone substitute was used for a clinically

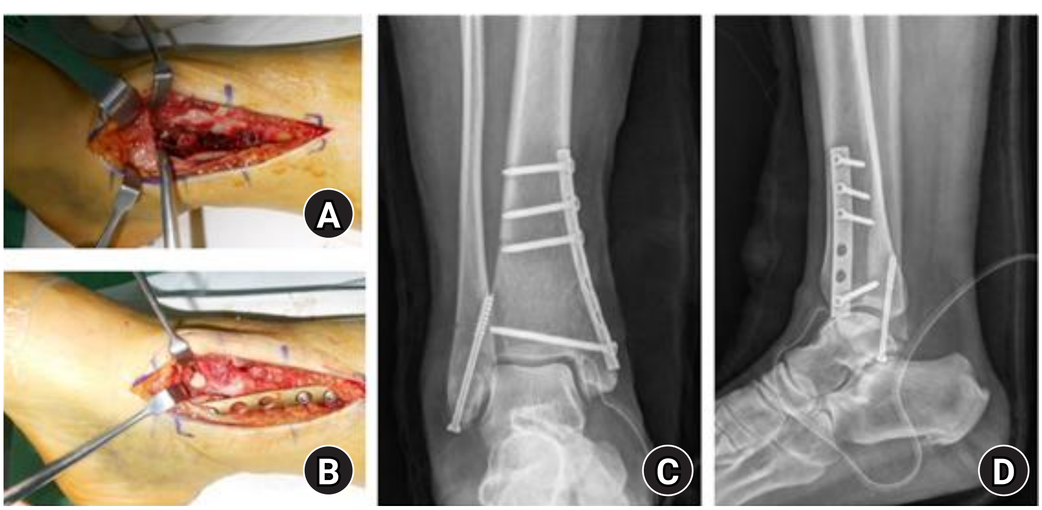

Fig. 2. Representative elderly patient with a supination–adduction-type ankle fracture in whom articular congruity was restored by elevation of the impacted articular fragment and fixation with a medial buttress plate and screws. (A) Intraoperative exposure of the impacted articular fragment of the medial tibial plafond. (B) Restoration of articular congruity after elevation and reduction of the impacted fragment, followed by fixation with a medial buttress plate and screws. (C, D) Immediate postoperative anteroposterior and lateral radiographs showing stable fixation of the medial and lateral malleoli.

https://doi.org/10.12671/jmt.2025.00374

relevant residual metaphyseal defect. Prophylactic antibiotics were administered within 30 minutes before incision and continued for 24 hours. Postoperative immobilization, range-of-motion exercises, and weight-bearing progression were individualized according to fixation stability, soft-tissue status, and bone quality.

Outcome measures

The primary outcome was a composite postoperative complication consisting of superficial incisional surgical site infection (SSI), deep incisional SSI, loss of reduction, or delayed union; each component was also evaluated separately. SSI was classified using the anatomical and clinical principles of the Centers for Disease Control and Prevention National Healthcare Safety Network definitions [13]. Superficial incisional SSI involved only skin or subcutaneous tissue with purulent drainage, a positive superficial culture, localized inflammatory findings with deliberate opening or aspiration, or a clinical diagnosis of superficial SSI. Deep incisional SSI involved the fascial or muscular layers with purulent deep drainage, a positive deep-tissue culture, spontaneous or deliberate dehiscence with compatible findings, or an abscess on examination, surgery, or imaging. Treatment method alone was not used to determine infection depth.

Loss of reduction was defined as new radiographic deterioration relative to immediate postoperative images, including coronal displacement >2 mm, talar tilt >3°, sagittal displacement >5 mm, recurrent articular displacement >2 mm, or clinically relevant implant migration or loosening with fracture displacement [14]. Delayed union was defined as persistent fracture-line visibility with incomplete cortical bridging and insufficient radiographic progression at 6 months. Fracture-related deep infection was interpreted in accordance with the international consensus definition [15]. Nonunion was defined as an ununited fracture at ≥9 months after injury without radiographic progression during the preceding 3 months [16]. Union was defined as bridging or disappearance of the fracture line in at least three of four cortices with resolution of clinically relevant pain or motion at the fracture site.

Radiographic evaluation

Preoperative CT was reconstructed using multiplanar reconstruction to obtain standardized coronal and sagittal planes. Tibial plafond impaction depth was measured as the maximum perpendicular distance between the expected intact articular contour and the deepest point of the impacted osteochondral fragment; articular step-off was the maximum vertical displacement between adjacent articular surfaces, measured on the plane of greatest displacement. Because marginal impaction is more reliably identified on CT than on plain radiographs, all measurements were performed on CT [17]. The measurement methods are illustrated in Fig. 3. Final radiographs obtained at ≥18 months were evaluated for union and posttraumatic osteoarthritis, with CT reviewed when union or articular congruity could not be reliably determined on plain films.

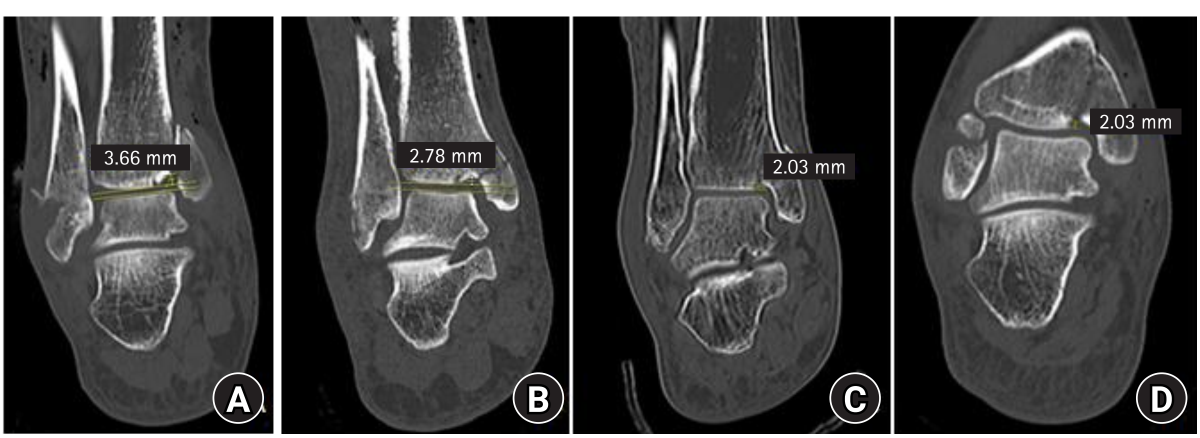

Fig. 3. Schematic illustration of radiographic measurements. (A, B) Tibial plafond impaction depth, measured as the maximum perpendicular distance from the expected intact articular contour to the deepest point of the impacted fragment. (C, D) Articular step-off, measured as the maximum vertical displacement between adjacent articular surfaces.

Functional and pain assessment

Functional outcomes were assessed using the Olerud-Molander Ankle Score (OMAS) and the American Orthopaedic Foot & Ankle Society (AOFAS) ankle-hindfoot score [18-20] at 3, 6, and 12 months postoperatively, with the 12-month assessment designated the principal functional endpoint. Because the interval beyond 12 months was used primarily for radiographic surveillance and functional scores were not systematically recollected at that stage in this retrospective cohort, functional recovery is reported through 12 months, whereas union and posttraumatic osteoarthritis were assessed on radiographs obtained at ≥18 months. A visual analog scale for pain was not consistently documented throughout the study period and was therefore not analyzed. Three-month scores are reported as descriptive measures of early recovery and interpreted with caution, as many patients were still undergoing progressive weight-bearing and rehabilitation.

Statistical analysis

Statistical analyses were performed using IBM SPSS ver. 29.0 (IBM Corp.). Continuous variables were assessed for normality with the Shapiro-Wilk test and compared using the independent-samples t-test or Mann-Whitney U test; categorical variables were compared using the chi-square or Fisher exact test. Correlations between the lowest T-score and radiographic measurements in the older group were assessed using Spearman rank correlation. Because postoperative complication is a binary outcome, associations between individual clinical variables and complications were explored using univariable logistic regression and reported as odds ratio (OR) with 95% confidence interval (CI). With only eight complication events in the older group, a multivariable model was not fitted, to avoid overfitting. A post hoc power analysis for the primary comparison of overall complication rates was performed using G*Power ver. 3.1.9.7 (Heinrich Heine University Dusseldorf). Based on a two-sided Fisher exact test, an α level of 0.05, group sizes of 30 and 21, and the observed complication rates of 10.0% and 38.1%, respectively, the achieved statistical power was approximately 57.8%. Statistical significance was set at a two-sided P<0.05.

Results

Patient characteristics

The cohort comprised 30 younger and 21 older patients. Mean age was 49.3±8.2 years (younger) and 72.4±5.7 years (older; P<0.001). The proportions of female sex, diabetes, hypertension, and smoking did not differ significantly between groups. High-energy trauma occurred in 11 younger patients (36.7%) and three older patients (14.3%; P=0.113). No open fractures were included. The mean follow-up duration was 24.5 months overall; group-specific values are presented in Table 1.

Postoperative complications

Complications occurred in three younger patients (10.0%) and eight older patients (38.1%; Fisher exact P=0.035) (Table 2). The younger group had two superficial SSIs and one deep SSI, with no loss of reduction or delayed union; the

Table 1. Baseline demographic and clinical characteristics

Variable	Younger (<65 yr) (n=30)	Older (≥65 yr) (n=21)	P-value
Age (yr)	49.3±8.2	72.4±5.7	<0.001
Female sex	18 (60.0)	14 (66.7)	0.771
Diabetes mellitus	5 (16.7)	7 (33.3)	0.196
Hypertension	9 (30.0)	8 (38.1)	0.563
Current smoking	8 (26.7)	6 (28.6)	1.000
High-energy trauma	11 (36.7)	3 (14.3)	0.113
Open fracture	0 (0.0)	0 (0.0)	NA
Follow-up (mo)	25.9±7.5	22.5±7.0	0.110

Values are presented as mean±standard deviation or number (%). Categorical variables were compared using the Fisher exact test when appropriate.
NA, not applicable.

Table 2. Postoperative complications according to age group

Complication	Younger (n=30)	Older (n=21)	P-value
Superficial incisional SSI	2 (6.7)	2 (9.5)	1.000
Deep incisional SSI	1 (3.3)	2 (9.5)	0.561
Loss of reduction	0 (0.0)	1 (4.8)	0.412
Delayed union	0 (0.0)	3 (14.3)	0.064
Any postoperative complication	3 (10.0)	8 (38.1)	0.035

Values are presented as number (%). P-values by Fisher exact test. No patient experienced more than one of the listed complications; therefore, the component counts equal the patient-level total for any postoperative complication in each group.
SSI, surgical site infection.

https://doi.org/10.12671/jmt.2025.00374

older group had two superficial SSIs, two deep SSIs, one loss of reduction, and three delayed unions. No patient experienced more than one of the listed complications; therefore, the component counts equaled the number of patients with any postoperative complication in each group.

In exploratory analyses restricted to the older group, diabetes was present in five of eight patients with complications and two of 13 without (OR, 9.17; 95% CI, 1.15–73.24; P=0.037). Smoking was present in four of eight versus two of 13 (OR, 5.50; 95% CI, 0.71–42.60; P=0.103). Hypertension, female sex, and osteoporosis were not significantly associated with complications (Table 3). The wide CIs reflect the small number of events and indicate that these estimates are exploratory.

Bone mineral density and radiographic morphology

All 21 older patients underwent preoperative DXA. The mean lowest T-score was –2.3±0.5, and 10 patients (47.6%) met the densitometric criterion for osteoporosis. The mean tibial plafond impaction depth was 3.1±1.2 mm, and the mean articular step-off was 2.0±0.8 mm. Lower T-scores were associated with greater impaction depth (Spearman ρ=–0.46, P=0.036), with a similar but nonsignificant association for articular step-off (ρ=–0.43, P=0.052) (Table 4).

Functional and radiographic outcomes

OMAS and AOFAS scores improved over time in both groups (Table 5). At 3 and 6 months, the older group had lower scores; these early time-point differences are presented descriptively and should be interpreted cautiously because many patients were still progressing through weight-bearing and rehabilitation. At 12 months, the principal functional endpoint, the between-group differences were no longer significant for OMAS (85.7±5.6 vs. 83.2±6.2; P=0.181) or AOFAS score (91.4±5.1 vs. 89.6±5.4; P=0.234).

No younger patient developed nonunion, whereas one older patient did (0% vs. 4.8%; P=0.412). Posttraumatic osteoarthritis was identified in one patient in each group (3.3% vs. 4.8%; P=1.000) (Table 6). The same representative older patient shown in Fig. 2 demonstrated solid bony union without posttraumatic osteoarthritis at 18 months postoperatively (Fig. 4).

Discussion

Summary of key findings

The principal finding was that older patients with surgically treated SAD-type ankle fractures had a higher overall postoperative complication rate than younger patients. Early functional recovery was slower in the older group, but the differences in OMAS and AOFAS scores were no longer significant by 12 months, and late nonunion and posttraumatic osteoarthritis were uncommon in both groups. These findings suggest that age and systemic vulnerability influence the early postoperative course, whereas satisfactory longer-term recovery may still be achieved when anatomical reduction and stable fixation are obtained.

Table 3. Exploratory univariable associations with postoperative complications in older patients

Variable	Complication (+) (n=8)	Complication (–) (n=13)	Odds ratio (95% CI)	P-value
Diabetes mellitus	5 (62.5)	2 (15.4)	9.17 (1.15–73.24)	0.037
Smoking	4 (50.0)	2 (15.4)	5.50 (0.71–42.60)	0.103
Hypertension	4 (50.0)	4 (30.8)	2.25 (0.37–13.87)	0.382
Female sex	6 (75.0)	8 (61.5)	1.88 (0.27–13.20)	0.528
Osteoporosis	5 (62.5)	5 (38.5)	2.67 (0.43–16.39)	0.290

Values are presented as number (%) unless otherwise indicated. Odds ratios were estimated using univariable logistic regression.
CI, confidence interval.

Table 4. Dual-energy X-ray absorptiometry and radiographic parameters in older patients

Variable	Value	Correlation with lowest T-score, ρ	P-value
Lowest T-score	–2.3±0.5	NA	NA
Osteoporosis	10 (47.6)	NA	NA
Tibial plafond impaction depth (mm)	3.1±1.2	–0.46	0.036
Articular step-off (mm)	2.0±0.8	–0.43	0.052

Values are presented as mean±standard deviation or number (%). Correlations were assessed using Spearman rank correlation.

Table 5. Functional outcomes during follow-up

Follow-up (mo)	OMAS			AOFAS		
	<65 yr	≥65 yr	P-value	<65 yr	≥65 yr	P-value
3	58.3±8.7	50.9±9.1	0.012	71.6±7.5	64.8±8.2	0.015
6	73.4±7.2	67.5±6.8	0.021	82.3±6.5	76.9±7.4	0.027
12	85.7±5.6	83.2±6.2	0.181	91.4±5.1	89.6±5.4	0.234

Values are presented as mean±standard deviation. The 12-month assessment was designated as the principal functional endpoint. The 3- and 6-month values are descriptive measures of early recovery and should be interpreted cautiously because weight-bearing progression and rehabilitation were ongoing. The visual analog scale was not consistently recorded and is not reported.
OMAS, Olerud-Molander Ankle Score; AOFAS, American Orthopaedic Foot & Ankle Society ankle-hindfoot score.

Table 6. Final radiographic outcomes at ≥18 months

Outcome	Younger (n=30)	Older (n=21)	P-value
Nonunion	0 (0.0)	1 (4.8)	0.412
Posttraumatic osteoarthritis	1 (3.3)	1 (4.8)	1.000

Values are presented as number (%). P-values by Fisher exact test.

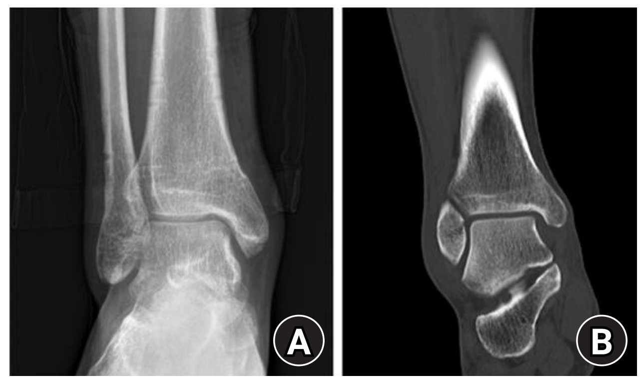

Fig. 4. Eighteen-month postoperative images of the patient shown in Fig. 2. (A) Anteroposterior radiograph and (B) coronal computed tomography image demonstrate solid bony union without posttraumatic osteoarthritis, residual marginal impaction of the medial tibial plafond, articular step-off, or other notable abnormalities.

Interpretation of complications and risk factors

The higher complication rate in older patients is consistent with studies showing that age, diabetes, soft-tissue vulnerability, and comorbidities affect outcomes after ankle fracture treatment [4,5,10,21-23]. SAD-type fractures pose additional mechanical challenges because the vertical medial malleolar component is exposed to shear and may coexist with marginal plafond impaction [9,17]. In our cohort, loss of reduction and delayed union occurred only in the older group, supporting fixation strategies that resist vertical shear and account for fragment size, comminution, and bone quality rather than a uniform screw-only technique.

Diabetes showed an exploratory, unadjusted association with complications, although the CI was wide. Diabetes may impair leukocyte function, microvascular perfusion, soft-tissue healing, and bone repair, and complicated diabetes is particularly associated with infection, nonunion, and revision after ankle fracture fixation [21-23]. Smoking was more common among older patients with complications but did not reach significance in this small cohort and should be regarded as a clinically plausible signal rather than a confirmed independent predictor.

Bone density and functional outcomes

DXA was analyzed only within the older group because younger patients were not systematically tested, which avoids an invalid age-group comparison. The exploratory association between lower T-score and greater plafond impaction or step-off suggests that reduced systemic bone density may influence fracture morphology. However, lumbar spine and proximal femoral DXA do not directly measure local subchondral bone quality at the ankle; degenerative change at the spine, site-specific variation, and use of the lowest T-score may further limit precision. The absence of a clear association between T-score and complications therefore does not exclude a role for local bone quality in fixation stability.

The comparable 12-month functional outcomes and the low frequency of late nonunion or posttraumatic osteoarthritis are clinically relevant. Posttraumatic osteoarthritis after SAD-type ankle fracture is closely related to the quality of reduction and articular congruity, and plafond malreduction or residual impaction accelerates arthrosis [24-27]. The low rate observed here is consistent with the emphasis on anatomical restoration and elevation of impacted ar-

https://doi.org/10.12671/jmt.2025.00374

ticular fragments. The lower scores in the older group at 3 and 6 months are descriptive measures of early recovery and may reflect delayed weight-bearing, reduced muscle strength, comorbidities, or slower rehabilitation. Because the 12-month assessment was the principal functional endpoint, the convergence of scores by that time indicates that early differences should not be interpreted as inevitable long-term disability [28].

Clinical implications

These results have practical implications. Older patients with an SAD-type fracture, particularly those with diabetes or compromised bone quality, require careful soft-tissue evaluation, perioperative medical optimization, anatomical elevation of impacted articular fragments, and fixation capable of resisting vertical shear. Buttress plating or combined fixation may be preferable when screw fixation alone is inadequate, although the construct should remain individualized to fracture morphology and intraoperative stability.

Limitations

This study has several limitations. Its retrospective design introduces selection bias and information bias, and rehabilitation adherence and activity level could not be fully controlled. The sample size and number of events were small, and the achieved post hoc power for the primary comparison was approximately 57.8%, indicating limited statistical power; only eight complication events in the older group also precluded reliable multivariable modeling. DXA was obtained systematically only in the older group, so age-group comparisons of bone density were not possible, and spine or proximal femoral T-scores may not represent local ankle bone quality. Functional assessment was standardized only through 12 months, and a validated patient-reported pain outcome measure (e.g., visual analog scale) was not consistently available in this retrospective cohort; the ≥18-month interval was used for radiographic rather than functional evaluation. Finally, the study was performed at a single institution by one surgeon, which improves technical consistency but may limit generalizability. Larger prospective studies with standardized final functional follow-up and local bone-quality measurements are warranted.

Conclusions

Older patients with surgically treated SAD-type ankle fractures had a higher postoperative complication rate than younger patients, although 12-month functional outcomes and late radiographic outcomes were broadly comparable. In the exploratory within-group analysis, diabetes mellitus was associated with postoperative complications; however, the wide CI reflects the limited sample and warrants cautious interpretation. This finding is consistent with the recognized adverse effects of diabetes on soft-tissue and bone healing. Older patients with diabetes may therefore represent a higher-risk subgroup warranting preoperative glycemic optimization, vigilant soft-tissue management, anatomical restoration of the articular surface, and fixation designed to resist vertical shear while accommodating comminution and bone quality. The role of smoking remains uncertain and warrants further study.

Article Information

Author contributions

Conceptualization: JHL, JL. Data curation: BK, HC. Formal analysis: HC. Methodology: JHL, BK. Writing-original draft: JHL, BK. Writing-review & editing: JHL, BK, HC, JL. All authors read and approved the final manuscript.

Conflicts of interest

No potential conflict of interest relevant to this article was reported.

Funding

This study was supported by the Chosun University Hospital Research Fund (2024).

Data availability

Contact the corresponding author for data availability.

Acknowledgments

None.

Supplementary materials

None.

References

1. Court-Brown CM, Caesar B. Epidemiology of adult fractures: a review. Injury 2006;37:691-7.
2. Kannus P, Palvanen M, Niemi S, Parkkari J, Jarvinen M. Increasing number and incidence of low-trauma ankle fractures in elderly people: Finnish statistics during 1970-2000 and projections for the future. Bone 2002;31:430-3.
3. Koval KJ, Lurie J, Zhou W, et al. Ankle fractures in the elderly: what you get depends on where you live and who you see. J Orthop Trauma 2005;19:635-9.
4. Koval KJ, Zhou W, Sparks MJ, et al. Complications after ankle fracture in elderly patients. Foot Ankle Int 2007;28:1249-55.
5. SooHoo NF, Krenek L, Eagan MJ, et al. Complication rates following open reduction and internal fixation of ankle fractures. J Bone Joint Surg Am 2009;91:1042-9.
6. Wukich DK, Kline AJ. The management of ankle fractures in patients with diabetes. J Bone Joint Surg Am 2008;90:1570-8.
7. Lauge-Hansen N. Fractures of the ankle. II. Combined experimental-surgical and experimental-roentgenologic investigations. Arch Surg (1920) 1950;60:957-85.
8. Ebraheim NA, Mekhail AO, Haman SP. External rotation-lateral view of the ankle in the assessment of the posterior malleolus. Foot Ankle Int 1999;20:379-83.
9. McConnell T, Tornetta P. Marginal plafond impaction in association with supination-adduction ankle fractures: a report of eight cases. J Orthop Trauma 2001;15:447-9.
10. Gauthé R, Desseaux A, Rony L, Tarissi N, Dujardin F. Ankle fractures in the elderly: treatment and results in 477 patients. Orthop Traumatol Surg Res 2016;102(4 Suppl):S241-4.
11. American Diabetes Association Professional Practice Committee for Diabetes. 2. Diagnosis and classification of diabetes: standards of care in diabetes—2026. Diabetes Care 2026;49(Suppl 1):S27-49.
12. International Society for Clinical Densitometry (ISCD). Official positions 2023 [Internet]. ISCD; 2023 [cited 2026 Jun 16]. Available from: https://iscd.org/official-positions-2023/
13. Centers for Disease Control and Prevention (CDC). National Healthcare Safety Network patient safety component manual: surgical site infection event [Internet]. CDC; 2026 [cited 2026 Jun 16]. Available from: https://www.cdc.gov/nhsn/pdfs/pscmanual/9pscssicurrent.pdf
14. Gitajn IL, Natoli RM, Spitler CA, et al. Radiographic assessment of ankle fracture displacement: a validation study. Foot Ankle Int 2022;43:1269-76.
15. Metsemakers WJ, Morgenstern M, McNally MA, et al. Fracture-related infection: a consensus on definition from an international expert group. Injury 2018;49:505-10.
16. Hak DJ, Fitzpatrick D, Bishop JA, et al. Delayed union and nonunions: epidemiology, clinical issues, and financial aspects. Injury 2014;45 Suppl 2:S3-7.
17. Alluri RK, Hill JR, Donohoe S, et al. Radiographic detection of marginal impaction in supination-adduction ankle fractures. Foot Ankle Int 2017;38:1005-10.
18. Olerud C, Molander H. A scoring scale for symptom evaluation after ankle fracture. Arch Orthop Trauma Surg (1978) 1984;103:190-4.
19. Kitaoka HB, Alexander IJ, Adelaar RS, et al. Clinical rating systems for the ankle-hindfoot, midfoot, hallux, and lesser toes. Foot Ankle Int 1994;15:349-53.
20. McKeown R, Parsons H, Ellard DR, Kearney RS. An evaluation of the measurement properties of the Olerud Molander Ankle Score in adults with an ankle fracture. Physiotherapy 2021;112:1-8.
21. Wukich DK, Joseph A, Ryan M, Ramirez C, Irrgang JJ. Outcomes of ankle fractures in patients with uncomplicated versus complicated diabetes. Foot Ankle Int 2011;32:120-30.
22. Wukich DK, Lowery NJ, McMillen RL, Frykberg RG. Postoperative infection rates in foot and ankle surgery: a comparison of patients with and without diabetes mellitus. J Bone Joint Surg Am 2010;92:287-95.
23. Jones KB, Maiers-Yelden KA, Marsh JL, et al. Ankle fractures in patients with diabetes mellitus. J Bone Joint Surg Br 2005;87:489-95.
24. Stufkens SA, van den Bekerom MP, Kerkhoffs GM, Hintermann B, van Dijk CN. Long-term outcome after 1822 operatively treated ankle fractures: a systematic review of the literature. Injury 2011;42:119-27.
25. Horisberger M, Valderrabano V, Hintermann B. Posttraumatic ankle osteoarthritis after ankle-related fractures. J Orthop Trauma 2009;23:60-7.
26. Stufkens SA, Knupp M, Horisberger M, Lampert C, Hintermann B. Cartilage lesions and the development of osteoarthritis after internal fixation of ankle fractures: a prospective study. J Bone Joint Surg Am 2010;92:279-86.
27. Githens MF, DeBaun MR, Jacobsen KA, et al. Plafond malreduction and talar dome impaction accelerates arthrosis after supination-adduction ankle fracture. Foot Ankle Int 2021;42:1245-53.
28. Egol KA, Tejwani NC, Walsh MG, Capla EL, Koval KJ. Predictors of short-term functional outcome following ankle fracture surgery. J Bone Joint Surg Am 2006;88:974-9.

 https://doi.org/10.12671/jmt.2025.00374

JMT Journal of Musculoskeletal Trauma

pISSN 3058-6267 · eISSN 3058-6275
J Musculoskelet Trauma 2026;39(3):245-251
https://doi.org/10.12671/jmt.2026.00059

Successful reconstruction and functional recovery of a pediatric medial malleolus defect in an 8-year-old girl using autologous iliac crest bone grafting in Korea: a case report

Sung Yoon Jung[1], Dong-hee Kim[2], Sang Hyun Lee[3], Ki-Hun Kim[3]

[1]Department of Orthopedic Surgery, Dong-A University Hospital, Dong-A University School of Medicine, Busan, Korea
[2]Department of Orthopedic Surgery, Samsung Changwon Hospital, Sungkyunkwan University School of Medicine, Changwon, Korea
[3]Department of Orthopedic Surgery, Pusan National University Hospital, Pusan National University School of Medicine, Busan, Korea

An 8-year-old girl presented after a traffic accident with a severe crush and degloving injury of the medial right ankle and foot, a distal tibiofibular fracture, and medial midfoot bone defects. After staged irrigation and debridement with temporary external fixation, definitive reconstruction was performed on August 6, 2016. The medial malleolar defect (2.5×2.0 cm) was reconstructed using a contoured autologous iliac crest bone graft secured with internal fixation, and medial stability was augmented using harvested gluteal fascia as a deltoid ligament substitute fixed with suture anchors. A bone-cement spacer was placed adjacent to the injured physis to mitigate physeal bridging, and the extensive soft-tissue defect was covered with a free anterolateral thigh flap and skin graft. During follow-up, progressive varus deformity and contracture were managed with corrective osteotomy and plating, Achilles tendon lengthening, Z-plasty, and Ilizarov fixation. At the final follow-up (March 6, 2025), the limb-length discrepancy was 5 mm, active ankle dorsiflexion was 0° (passive dorsiflexion 5°), and the patient was pain-free with full participation in daily activities, including hiking and dancing. This case emphasizes the value of an integrated staged strategy that combines bony reconstruction, medial stabilization, physeal management, and durable soft-tissue coverage during skeletal growth.
Level of evidence: V.

Keywords: Growth plate; Salter-Harris fractures; Bone transplantation; Free tissue flaps; Tibia

Introduction

Salter-Harris type VI physeal injuries represent rare lesions characterized by loss of a portion of the physis and adjacent osteochondral/perichondrial structures, frequently associated with high-energy trauma and extensive soft-tissue injury [1,2]. In the distal tibia, traumatic loss of the medial malleolus is particularly consequential in skeletally immature patients because it simultaneously threatens physeal integrity and ankle stability, including potential growth disturbance from physeal bar formation and medial instability due to deltoid ligament deficiency [1-3]. Management is therefore challenging and must balance limb salvage, infection control, durable soft-tissue coverage, structural reconstruction, and long-term growth-related alignment preservation [3]. We report a pediatric case of traumatic medial malleolar loss managed

Case Report

Received: January 15, 2026
Revised: February 13, 2026
Accepted: March 4, 2026

Correspondence to:
Sang Hyun Lee
Department of Orthopedic Surgery, Pusan National University Hospital, Pusan National University School of Medicine, 179 Gudeok-ro, Seo-gu, Busan 49241, Korea
Tel: +82-51-240-7248
Email: handsurgeon@pusan.ac.kr

with staged debridement, autologous iliac crest bone graft reconstruction with medial stabilization, physeal management using a bone-cement spacer, free anterolateral thigh (ALT) flap coverage, and subsequent deformity correction, resulting in long-term functional recovery through growth.

Case report

Ethics statement

This study was approved by the Institutional Review Board (IRB) of Pusan National University Hospital (IRB No. 2601-031-159), and written informed consent was obtained from the patient's legal guardian for publication of this report, including all clinical images.

Patient information

An 8-year-old girl presented on June 14, 2016 after a traffic accident with a severe crush/degloving injury involving the medial aspect of the right ankle and foot. The family's main concerns were limb salvage and the risk of growth-related deformity and long-term functional limitation. She had no relevant past medical history.

Clinical findings and diagnostic assessment

At presentation, extensive soft-tissue loss of the medial ankle/foot was noted, consistent with a high-energy crush/degloving mechanism (Fig. 1). The wound severity raised concerns for soft-tissue viability, contamination, and subsequent infection risk, and suggested the need for a staged approach with temporary stabilization followed by definitive reconstruction.

Initial plain radiographs demonstrated a distal tibiofibular fracture in a skeletally immature patient, with associated medial-sided midfoot injuries (first metatarsal, medial cuneiform, and medial navicular bone defects) (Fig. 1). During staged management, traumatic loss of the distal tibial medial malleolus was identified, consistent with a Salter-Harris type VI injury pattern and raising concern for physeal bar formation and medial ankle instability due to deltoid ligament deficiency [2,3]. The medial malleolar bony defect was measured intraoperatively as 2.5×2.0 cm to guide graft contouring. Given the severity of the soft-tissue injury, a staged strategy was adopted [1,4].

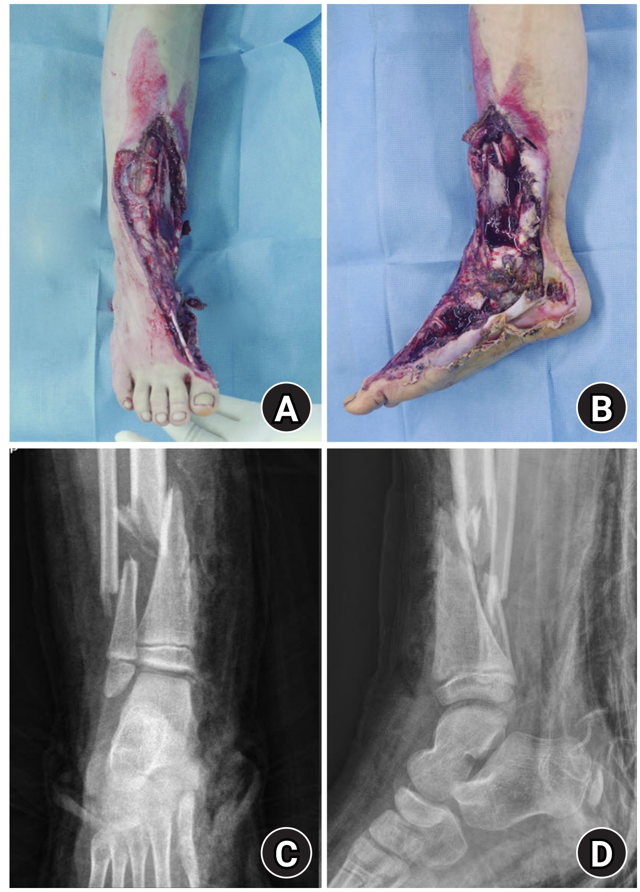

Fig. 1. Initial injury on June 14, 2016. (A) Anteroposterior gross photograph obtained at presentation showing a severe crush and degloving injury involving the medial aspect of the right ankle and foot. (B) Lateral gross photograph obtained at presentation demonstrating extensive soft-tissue loss and degloving injury of the medial right ankle and foot. (C) Anteroposterior radiograph obtained at presentation showing an associated distal tibiofibular fracture in a skeletally immature patient. (D) Lateral radiograph obtained at presentation demonstrating the distal tibiofibular fracture.

Therapeutic intervention

Stage 1 (damage control; June 14, 2016)

The patient underwent irrigation and debridement with temporary stabilization using an external fixator (Fig. 2). Serial irrigation and debridement procedures (marginal debridement) were performed as needed until the wound condition allowed definitive reconstruction.

Stage 2 (definitive reconstruction; August 6, 2016)

The medial malleolar defect (2.5×2.0 cm) was reconstructed using an autologous iliac crest bone graft harvested and

https://doi.org/10.12671/jmt.2026.00059

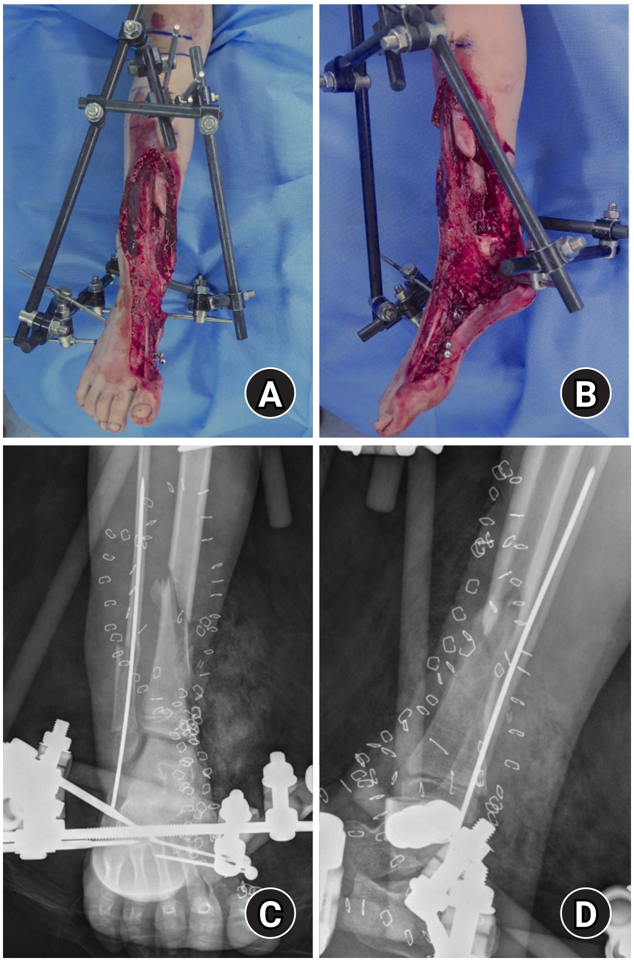

Fig. 2. Postdamage control stabilization with external fixation. (A) Anteroposterior gross photograph obtained after initial irrigation and debridement, showing temporary stabilization with an external fixator. (B) Lateral gross photograph obtained after initial irrigation and debridement, demonstrating temporary stabilization with an external fixator. (C) Anteroposterior radiograph obtained after initial irrigation and debridement, showing temporary stabilization with an external fixator. (D) Lateral radiograph obtained after initial irrigation and debridement, demonstrating temporary stabilization with an external fixator.

contoured to match the defect (Fig. 3) [4,5]. The graft was secured with internal fixation, and postoperative clinical appearance and radiographs confirmed reconstruction and stabilization (Fig. 4). To restore medial ankle stability, harvested gluteal fascia was used as a deltoid ligament substitute and fixed using suture anchors [1]. To mitigate physeal bridging in the residual void adjacent to the injured physis, a bone-cement spacer was placed [4,5]. The extensive soft-tissue defect was covered using ALT flap and

Fig. 3. Autologous iliac crest bone graft. Intraoperative photograph of the harvested autologous iliac crest bone graft prepared for medial malleolus reconstruction (defect size, 2.5×2.0 cm).

skin graft, achieving stable coverage (Fig. 5) [6,7].

Stage 3 (deformity correction; January 9, 2017)

Progressive varus deformity during follow-up was treated with corrective osteotomy and plate fixation (Fig. 6).

Stage 4 (alignment and contracture management; May 29, 2017)

The patient was observed for more than 6 months after plate fixation, and bone union was achieved for the remaining fracture sites. However, varus deformity gradually occurred (lateral distal tibial angle, 111.5°; tibiotalar tilt, 0.4°). As the patient was relatively young and had substantial remaining growth, early correction was considered advantageous and was therefore performed. Residual deformity tendency and contracture were managed with additional procedures including Achilles tendon lengthening and Z-plasty for tendon/skin contracture release. The bone-cement spacer was removed during this phase. Alignment correction/overcorrection and continued alignment management were supported with an Ilizarov external fixator (Fig. 7). After applying the Ilizarov external fixator for 3 months, radiologic indices were corrected (lateral distal tibial angle, 97.6°; tibiotalar tilt, 0.3°).

Follow-up and outcomes

At the final follow-up on March 6, 2025, clinical photographs and radiographs demonstrated healed soft tissue, maintained alignment, and functional recovery without

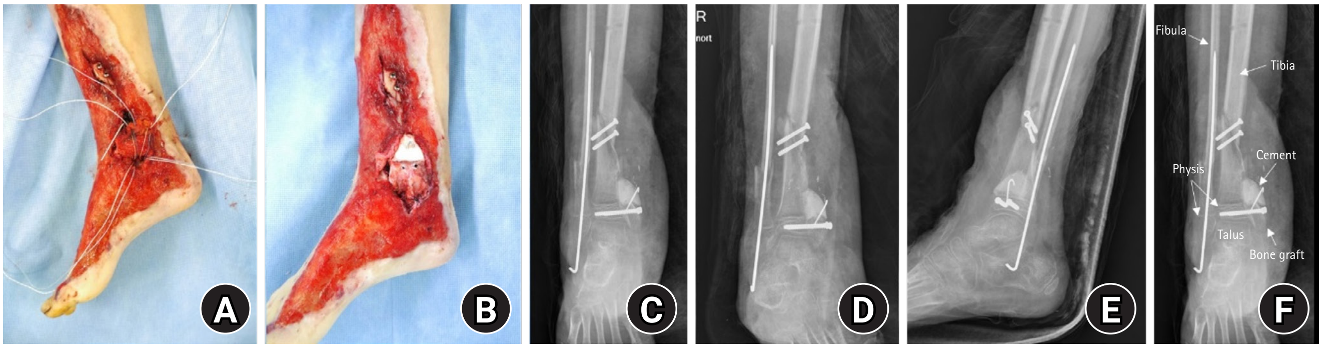

Fig. 4. Postmedial malleolus reconstruction. (A) Medial clinical photograph obtained after reconstruction of the medial malleolus using an autologous iliac crest bone graft with internal fixation. (B) Medial clinical photograph obtained after reconstruction, showing restoration of the medial malleolar contour and soft-tissue coverage. (C) Anteroposterior postoperative radiograph demonstrating reconstruction of the medial malleolus with internal fixation. (D) Mortise postoperative radiograph demonstrating reconstruction of the medial malleolus with internal fixation. (E) Lateral postoperative radiograph demonstrating reconstruction of the medial malleolus with internal fixation. (F) Anteroposterior radiograph, showing the reconstructed medial malleolus and surrounding anatomical structures.

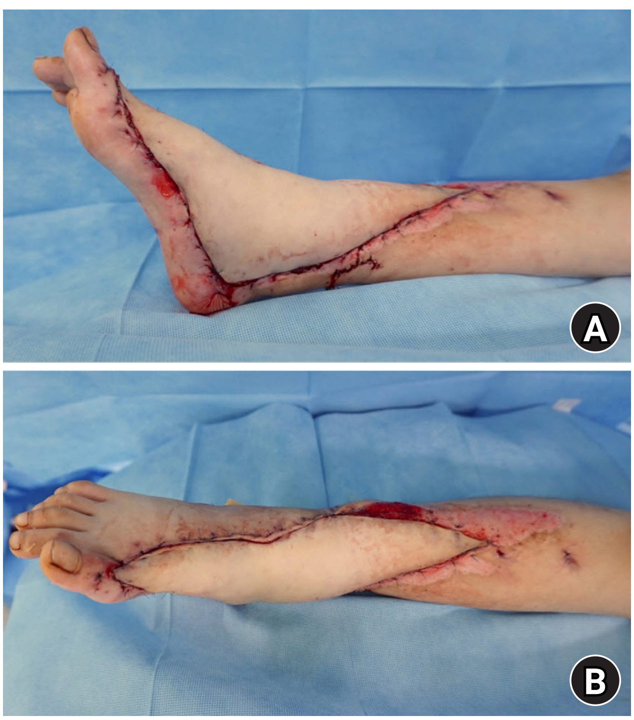

Fig. 5. Soft-tissue coverage with a free anterolateral thigh flap. (A) Lateral gross photograph obtained after coverage of the medial ankle and foot defect using a free anterolateral thigh flap. (B) Anteroposterior gross photograph obtained after coverage of the medial ankle and foot defect using a free anterolateral thigh flap.

recurrent deformity (Fig. 8). Limb-length discrepancy was 5 mm. Active ankle dorsiflexion was 0° with passive dorsiflexion of 5°. The patient reported no pain and returned to unrestricted activities of daily living, including hiking and dancing. Complications during the treatment course were limited to superficial skin/soft-tissue problems, without reported deep infection (Table 1).

Discussion

Salter-Harris type VI physeal injuries are rare and usually occur after high-energy trauma with substantial soft-tissue compromise. In the distal tibia, loss of the medial malleolus is particularly problematic because it combines a risk of physeal bar formation with subsequent angular deformity, limb-length discrepancy and loss of the medial buttress with potential deltoid ligament insufficiency and chronic instability [1-3].

In adults with extensive medial malleolar loss or non-reconstructable tibiotalar articular damage, tibiotalar arthrodesis is often selected as a definitive solution. In children, however, ankle fusion sacrifices a growing joint and may be followed by progressive varus/valgus deformity, limb-length discrepancy, and adjacent-joint overload as growth continues. Therefore, we prioritized a joint-preserving strategy aimed at restoring the medial malleolar buttress and medial stability while actively managing the injured physis [2,3].

A staged pathway (serial debridement and temporary external fixation followed by definitive reconstruction) allowed infection control and optimization of the wound bed before structural reconstruction. After initial temporary fixation with fibular pinning, fibular length was largely maintained.

https://doi.org/10.12671/jmt.2026.00059

Fig. 6. Corrective osteotomy for progressive varus deformity. (A) Preoperative anteroposterior radiograph obtained during follow-up, showing progressive varus deformity of the ankle. (B) Preoperative lateral radiograph obtained during follow-up. (C) Preoperative mortise radiograph obtained during follow-up. (D) Postoperative anteroposterior radiograph obtained after corrective osteotomy and plate fixation. (E) Postoperative lateral radiograph obtained after corrective osteotomy and plate fixation. (F) Postoperative mortise radiograph obtained after corrective osteotomy and plate fixation.

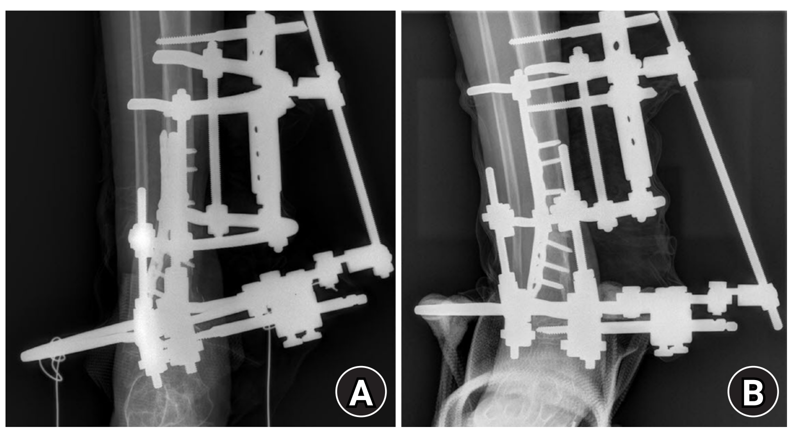

Fig. 7. Ilizarov fixation for correction/overcorrection. (A) Anteroposterior radiograph obtained after application of an Ilizarov external fixator for deformity correction, intentional overcorrection, and alignment management. (B) Lateral radiograph obtained after application of an Ilizarov external fixator for deformity correction, intentional overcorrection, and alignment management.

However, by the time of definitive reconstruction, the fibula had begun to unite with surrounding soft-tissue contracture involving the syndesmosis, precluding anatomic reduction to a neutral position. The reconstruction was therefore completed with some residual varus, followed by flap coverage. The medial malleolar defect was reconstructed with a contoured autologous iliac crest graft and rigid fixation, consistent with prior pediatric reports using iliac crest-derived graft to reconstitute the distal medial tibial epiphysis. Medial stability was augmented by reconstructing the deltoid complex using autologous fascia and suture anchors [1,6].

Because type VI injuries involve loss of the perichondral ring and are prone to partial growth arrest, physeal management is a key parallel objective. Interpositional techniques (classically fat interposition after physeal bridge resection or anticipatory procedures) have been advocated to prevent or delay physeal bridging; in the present case, a temporary bone-cement spacer was used as a barrier adjacent to the injured physis during the reconstructive phase and was removed once alignment management was undertaken [1,4,5]. Compared to fat interposition, cement spacers have the advantage of space-occupying properties, allowing them to conform to their original shape during flap wound implantation. They also offer the advantage of

Fig. 8. Final follow-up on March 6, 2025. (A) Orthoroentgenogram radiograph obtained at the final follow-up, demonstrating maintained overall alignment. (B) Anteroposterior radiograph of the right ankle obtained at the final follow-up, showing osseous healing and maintained alignment. (C) Lateral radiograph of the right ankle obtained at the final follow-up. (D) Anteroposterior clinical photograph obtained at the final follow-up, demonstrating healed soft tissue and maintained alignment. (E) Lateral clinical photograph obtained at the final follow-up, demonstrating healed soft tissue and functional recovery.

Table 1. Timeline of staged reconstruction and follow-up

Date	Event
2016-06-14	Injury. Emergency I&D, temporary stabilization with external fixation, and fibular Rush pinning as indicated.
2016-06 to 2016-08	Multiple staged I&D procedures (marginal debridement) and wound management.
2016-08-06	Definitive reconstruction: medial malleolus reconstruction with a defect-matched autologous iliac crest bone graft (2.5×2.0 cm) and cannulated screw fixation; gluteal fascia used as a deltoid ligament substitute and secured with suture anchors; bone-cement spacer placed for physeal management; free ALT flap with skin graft for soft-tissue coverage.
2017-01-09	Corrective osteotomy and plate fixation for progressive varus deformity.
2017-05-29	Achilles tendon lengthening and Z-plasty for tendon/skin contracture; Ilizarov external fixation for correction/overcorrection; cement spacer removal as indicated.
2025-03-06	Final follow-up: limb-length discrepancy 5 mm; ankle dorsiflexion 0° active and 5° passive; pain-free; full activities of daily living including hiking and dancing.

I&D, irrigation and debridement; ALT, anterolateral thigh.

weight bearing. In principle, they are not removed unless there are specific concerns. However, in this case, the cement spacer itself could induce soft-tissue tethering during the correction of varus deformity, so it was removed and gradually corrected.

Durable soft-tissue coverage is equally important for limb salvage in these injuries. A free ALT flap provides reliable coverage for pediatric foot and ankle defects and was instrumental in maintaining a stable envelope that permitted subsequent osteotomy and gradual correction during growth [7,8].

This case also highlights the need for prolonged surveillance through skeletal maturity: even after successful initial reconstruction, progressive deformity and contracture can emerge as growth proceeds, requiring timely osteotomy, soft-tissue procedures, and, when necessary, circular external fixation to protect alignment and function [2,3].

Limitations include the inherent constraints of a single case, the lack of standardized patient-reported outcome measures, and the absence of a comparator strategy. In addition, computed tomography was not performed due to concerns regarding radiation exposure, and magnetic resonance imaging was not performed due to artifacts from metallic implants. The authors postulated that differ-

 https://doi.org/10.12671/jmt.2026.00059

ential growth between the flap-covered and native tissues contributed to the observed deformity. Accordingly, early correction was performed to prevent progression of residual deformity. This may be attributed to several factors, including residual varus alignment after plate fixation, incomplete accommodation of longitudinal growth by the flap-covered soft tissue, and persistent soft-tissue tethering, including involvement of the syndesmosis.

Nevertheless, the long-term follow-up to 9 years after injury demonstrates that an integrated, joint-preserving staged strategy can achieve durable function while minimizing growth-related sequelae in pediatric medial malleolar loss.

Article Information

Author contributions

Conceptualization: SYJ, SHL. Methodology: SYJ, DK, KHK. Supervision: SHL. Visualization: KHK, SHL. Writing–original draft: SYJ. Writing–review & editing: SYJ, DK, SHL, KHK. All authors read and approved the final manuscript.

Conflicts of interest

No potential conflict of interest relevant to this article was reported.

Funding

This work was supported by a clinical research grant from Pusan National University Hospital in 2025.

Data availability

Not applicable.

Acknowledgments

This case report was presented in the Case Discussion section of the 2026 Annual Congress of the Korean Orthopaedic Trauma Association (KOTA).

Supplementary materials

None.

References

1. Abbo O, Accadbled F, Laffosse JM, De Gauzy JS. Reconstruction and anticipatory Langenskiold procedure in traumatic defect of tibial medial malleolus with type 6 physeal fracture. J Pediatr Orthop B 2012;21:434-8.
2. Havranek P, Pesl T. Salter (Rang) type 6 physeal injury. Eur J Pediatr Surg 2010;20:174-7.
3. Singh V, Garg V, Parikh SN. Management of physeal fractures: a review article. Indian J Orthop 2021;55:525-38.
4. Foster BK, John B, Hasler C. Free fat interpositional graft in acute physeal injuries: the anticipatory Langenskiold procedure. J Pediatr Orthop 2000;20:282-5.
5. Williamson RV, Staheli LT. Partial physeal growth arrest: treatment by bridge resection and fat interposition. J Pediatr Orthop 1990;10:769-76.
6. Zhu C, Shi B, Rai S, Zhong H, Tang X. Case report: reconstruction of distal medial tibial epiphysis using iliac crest apophyseal autograft. Front Pediatr 2022;10:950211.
7. Acar MA, Gulec A, Aydin BK, Erkoçak OF, Yilmaz G, Senaran H. Reconstruction of foot and ankle defects with a free anterolateral thigh flap in pediatric patients. J Reconstr Microsurg 2015;31:225-32.
8. Hu R, Ren YJ, Yan L, et al. A free anterolateral thigh flap and iliotibial band for reconstruction of soft tissue defects at children's feet and ankles. Injury 2015;46:2019-23.

JMT Journal of Musculoskeletal Trauma

pISSN 3058-6267 · eISSN 3058-6275
J Musculoskelet Trauma 2026;39(3):252-261
https://doi.org/10.12671/jmt.2026.00136

Fixation with two headless compression screws and a distal-radius bone graft for proximal scaphoid nonunion with dorsal intercalated segment instability deformity: a report of three cases

Seonjeong Lee, Won Sun Lee, Jae Kwang Kim

Department of Orthopedic Surgery, Asan Medical Center, University of Ulsan College of Medicine, Seoul, Korea

Proximal scaphoid nonunion is difficult to treat because the proximal fragment is small and biologically compromised. Secure fixation can be especially challenging when dorsal intercalated segment instability (DISI) is present and requires correction. We report three male patients with proximal scaphoid nonunion and DISI deformity who underwent volar fixation with two 2.4-mm headless compression screws and cancellous bone graft harvested from the distal radius at the Lister tubercle. Preoperative computed tomography confirmed a proximal nonunion line and proximal fragment dimensions considered sufficient for dual-screw fixation, and magnetic resonance imaging showed no definite avascular necrosis. Early postoperative computed tomography showed maintained fixation and alignment in all three patients. Although CT-confirmed union at final follow-up was not uniformly available, radiographic union defined on plain radiographs was achieved in all cases without loss of alignment or carpal collapse. Carpal alignment improved in two patients, but DISI persisted in one. One patient underwent secondary removal of a preexisting loose body and one screw. This small case series suggests that dual-screw fixation with cancellous grafting may be technically feasible in selected proximal scaphoid nonunions with concomitant DISI.

Level of evidence: V.

Keywords: Ununited fractures; Scaphoid bone; Bone screws; Bone transplantation; Case reports

Case Report

Received: March 27, 2026
Revised: April 30, 2026
Accepted: May 11, 2026

Correspondence to:
Jae Kwang Kim
Department of Orthopedic Surgery, Asan Medical Center, University of Ulsan College of Medicine, 88 Olympic-ro 43-gil, Songpa-gu, Seoul 05505, Korea
Tel: +82-2-3010-3523
Email: orth4535@gmail.com

Introduction

Background

Scaphoid nonunion remains a challenging problem in wrist surgery, particularly when the nonunion involves the proximal pole. The proximal fragment is often small and biologically compromised, making stable fixation and reliable union difficult to achieve [1]. In addition, proximal scaphoid nonunion may be accompanied by carpal malalignment, including dorsal intercalated segment instability (DISI), which further complicates treatment [2,3].

Headless compression screw fixation is widely used for scaphoid fractures and nonunions [4-6]. However, in proximal nonunion, a single-screw construct may provide insufficient rotational control because of the limited size of the proximal fragment and the multidirectional loading environment of the scaphoid [7]. Biomechanical evidence suggests that a dual-screw construct can improve qualitative rotational control compared with a single screw, although overall stiffness and load to failure may be similar [8]. Garcia et al. [9] reported excellent union in a heterogeneous series of scaphoid nonunions treated with two headless compression screws and bone grafting; however, the majority of cases involved waist or distal third, and the presence of concomitant DISI in those subgroups was not specifically described.

Objectives

The purpose of this report is to describe three proximal scaphoid nonunions with DISI deformity treated using a uniform strategy of dorsal cancellous bone graft harvest from the distal radius at the Lister tubercle and volar fixation with two 2.4-mm headless compression screws. We focused on feasibility, radiographic alignment, functional outcomes, and complications of this technique in carefully selected cases.

Case reports

Ethics statement

This retrospective case series was approved by the Institutional Review Board (IRB) of the Medical Research Institute of Asan Medical Center (IRB No. S2025-1785-0001) and was conducted in accordance with the principles of the Declaration of Helsinki. Because the study used anonymized patient data and posed minimal risk to the participants, the requirement for informed consent was waived by the IRB.

Case definition

This retrospective report describes three male patients with symptomatic proximal scaphoid nonunion and DISI deformity who were treated by a single senior surgeon between March 2023 and March 2025 using the same technique of dorsal distal-radius cancellous bone grafting and volar dual 2.4-mm headless compression screw fixation. Proximal nonunion was defined when the fracture or nonunion line was located proximal to the dorsal apex of the scaphoid on computed tomography (CT) [10]. DISI deformity was defined as a radiolunate (RL) angle of 15° or greater on lateral radiographs [11]. No patient showed advanced degenerative arthritic change at presentation. Preoperative magnetic resonance imaging (MRI) was available in all patients and did not show definite proximal-pole avascular necrosis (AVN). Demographic and radiographic characteristics of the three cases are summarized in Table 1.

Preoperative imaging assessment and surgical eligibility

Preoperative CT was used to assess nonunion location, displacement, proximal fragment morphology, and the feasibility of dual distal-to-proximal screw fixation. Proximal fragment width and depth were measured on reconstructed coronal and sagittal CT images using the cut in each plane on which the proximal fragment appeared longest (Fig. 1). Because two 2.4-mm screws occupy a combined diameter of 4.8 mm and the DePuy Synthes 2.4-mm short-thread screw has a 4-mm leading threaded portion, fragment width greater than 4.8 mm and fragment depth greater than 4 mm were used as supportive thresholds when considering this technique. Depth was defined as the distance from the nonunion line to the proximal

Table 1. Demographic and radiographic characteristics of the three cases

Case	Age/sex	Side/dominance	Smoking	Injury-to-surgery interval	MRI/AVN assessment	Proximal fragment size (coronal width/depth, mm)	Proximal fragment size (sagittal width/depth, mm)	Preop SL/RL (°)	Immediate postop SL/RL (°)	Final F/U SL/RL (°)
1	23/male	Left/non-dominant	Current smoker (2 pack-years)	8 mo	Nonenhanced MRI; no AVN	5.6/5.9	8.2/5.37	73.6/20.4	74.6/23.7	73.4/24.0
2	45/male	Right/dominant	Non-smoker	approximately 10 yr	Gd-enhanced MRI; no AVN	6.49/6.18	11.23/6.01	59.3/15.3	62.2/9.7	60.3/12.4
3	41/male	Left/non-dominant	Ex-smoker	10-20 yr	Nonenhanced MRI; no AVN	7.06/9.12	16.53/7.55	59.4/18.5	53.9/15.2	60.7/12.7

MRI, magnetic resonance imaging; AVN, avascular necrosis; SL, scapholunate; RL, radiolunate; Preop, preoperative; postop, postoperative; F/U, follow-up; Gd, gadolinium.
Enhanced MRI indicates whether gadolinium-enhanced MRI was obtained.

subchondral boundary in the intended distal-to-proximal screw direction. However, because the proximal pole has a dome-shaped three-dimensional morphology and usable bone stock varies according to the exact screw trajectory and the bone bridge required between the two screws, these measurements were not considered absolute criteria. Final suitability for dual-screw fixation was determined qualitatively by integrating the measurements with overall fragment morphology, the proximal extent of the fracture line, possible screw trajectories, and proximity to the articular surfaces.

Radiographic union and clinical outcome assessment

Radiographic union at the latest follow-up was assessed on plain radiographs by the treating surgeon. CT-confirmed union was not uniformly available at final follow-up; rather, union was defined as bridging callus across at least three cortices on posteroanterior, lateral, and/or oblique views, similar to the radiographic definition used by Rodriguez-Fontan et al. [12]. Time to union was defined as the first postoperative visit at which radiographic bridging across at least three cortices was observed. Postoperative radiographs were routinely obtained at approximately 2 weeks, 6 weeks, 12 weeks, 6 months, 12 months, and 24 months, and CT was additionally obtained at approximately 6 weeks. In all three cases, union was first observed on radiographs obtained approximately 12 weeks after surgery (Table 2). Early postoperative CT was used to confirm screw position and alignment. Functional outcomes were retrospectively extracted from clinical records and included wrist volar flexion and dorsiflexion, grip strength, visual analog scale (VAS) pain score, Disabilities of the Arm, Shoulder and Hand (DASH) score, and patient satisfaction.

Surgical technique and postoperative protocol

In all cases, the procedure followed a two-incision strategy conceptually similar to the cancellous-grafting technique that was previously described [13], but joystick Kirschner (K)-wire manipulation of the fragments was not used. Through a volar approach, the nonunion site was

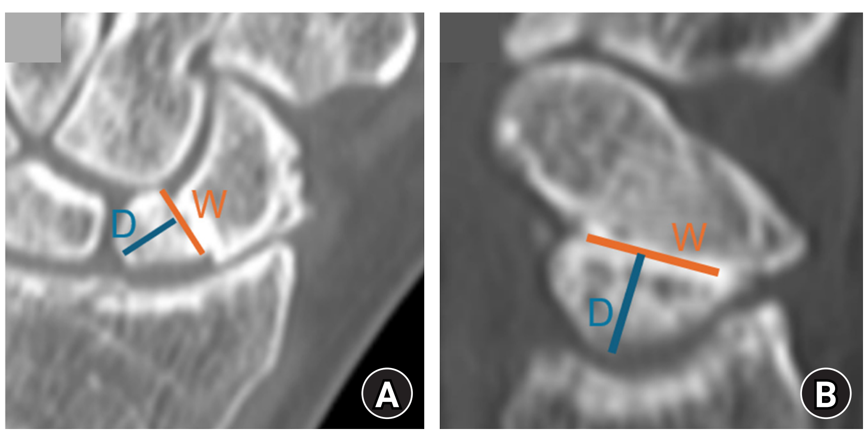

Fig. 1. Computed tomography-based assessment of proximal fragment dimensions. (A) Width (W) and depth (D) measured on the reconstructed coronal image using the section in which the proximal fragment appeared longest. (B) Width (W) and depth (D) measured similarly on the reconstructed sagittal image using the section in which the proximal fragment appeared longest. Depth was defined as the distance from the nonunion line to the proximal subchondral boundary in the intended distal-to-proximal screw direction.

Table 2. Final outcomes of the three cases

Case	Latest F/U (mo)	Time to union (wk)	Final ROM VF/DF (°)	Final grip strength kg (% contra)	Final VAS	Final DASH	Patient satisfaction	Complication
1	11	12	70/60	34.5 (82)	0	9.09	Very satisfied	None
2	7	12	70/50	30.0 (85)	1	13.63	Very satisfied	None
3	23	12	70/60	36.9 (94)	0	9.17	Very satisfied	Secondary removal of a preexisting loose body and one screw at 20 mo

F/U, follow-up; VF, volar flexion; DF, dorsiflexion; contra, contralateral side; VAS, visual analog scale; DASH, Disabilities of the Arm, Shoulder and Hand.

https://doi.org/10.12671/jmt.2026.00136

exposed, interposed fibrous tissue and sclerotic bone were excised, and the nonunion surfaces were prepared until viable cancellous bone was encountered. Scaphoid reduction and carpal alignment were confirmed under fluoroscopic guidance, but the degree of DISI correction varied (Table 1). Guidewires for the planned screws and an additional temporary derotational K-wire were then inserted from the distal scaphoid toward the proximal pole to maintain the reduced position. Through a separate limited dorsal approach centered just proximal to the Lister tubercle, cancellous bone graft was harvested with identification and protection of the extensor pollicis longus tendon. This dorsal harvest was preferred because cancellous bone could be obtained readily through a small dorsal cortical window.

A portion of the cancellous graft was first packed into the dorsal and deep aspect of the prepared cavity while preserving the planned screw paths. Fixation was then performed with two 2.4-mm cannulated short-thread headless compression screws with a 4-mm leading threaded portion (DePuy Synthes). Each 2.4-mm screw was inserted over its guidewire so that the leading thread crossed the nonunion site and engaged the proximal fragment. After definitive fixation, the guidewires and temporary derotational K-wire were removed, and the remaining volar defect was packed with cancellous bone graft. Reduction, the degree of DISI correction, screw position, and absence of radiocarpal or midcarpal joint violation were checked on anteroposterior, lateral, oblique, and scaphoid-view fluoroscopy. Postoperatively, the wrist was immobilized in a thumb-spica cast for 2 months, followed by range-of-motion exercises.

Case 1

Patient information and clinical findings

A 23-year-old male patient presented with persistent pain in the left wrist, which was his non-dominant side, after a fall approximately 8 months earlier. He had initially been told that plain radiographs were unremarkable, but his symptoms persisted despite conservative treatment. At presentation, he reported pain during exercise and wrist hyperextension, with difficulty loading the hand. He had a 2 pack-year smoking history and no diabetes.

Diagnostic assessment

Plain radiographs demonstrated scaphoid nonunion with carpal malalignment, and CT confirmed proximal scaphoid nonunion with DISI deformity. Preoperative SL and RL angles were 73.6° and 20.4°, respectively. Preoperative nonenhanced MRI did not show definite AVN.

Therapeutic intervention

He underwent nonunion debridement, dorsal cancellous bone graft harvest from the Lister tubercle, and volar fixation using two 2.4-mm headless compression screws. The wrist was immobilized in a thumb-spica cast for 2 months, followed by range-of-motion exercises.

Follow-up and outcomes

Postoperative CT obtained 7 weeks after surgery demonstrated maintained screw position. Immediate postoperative scapholunate (SL) and RL angles were 74.6° and 23.7°, and final SL and RL angles were 73.4° and 24.0°, indicating persistent DISI despite union. At 11 months after surgery, plain radiographs demonstrated union without loss of alignment or hardware failure (Fig. 2). Final wrist volar flexion/dorsiflexion was 70°/60°, grip strength was 34.5 kg (82% of the contralateral side), VAS pain score was 0, DASH score was 9.09, and the patient was very satisfied (Table 2).

Case 2

Patient information and clinical findings

A 45-year-old male patient presented with chronic pain in the right wrist, which was his dominant side, after a remote wrist injury approximately 10 years earlier. His symptoms were most bothersome during wrist flexion and daily activities. He was a non-smoker and had no diabetes.

Diagnostic assessment

Plain radiographs demonstrated scaphoid nonunion with carpal malalignment, and CT confirmed proximal scaphoid nonunion with DISI deformity. Preoperative SL and RL angles were 59.3° and 15.3°, respectively. Preoperative gadolinium-enhanced MRI showed no evidence of AVN.

Therapeutic intervention

He underwent the same operative procedure, including dorsal cancellous bone graft harvest from the distal radius at the Lister tubercle and volar fixation with two 2.4-mm headless compression screws. The wrist was immobilized

Fig. 2. Imaging course of case 1. (A) Initial posteroanterior radiograph showing proximal scaphoid nonunion; the arrowhead indicates the fracture line. (B) Initial lateral radiograph demonstrating DISI deformity; the yellow lines indicate a radiolunate angle of 20.4°. (C, D) Intraoperative fluoroscopic images showing guidewire placement followed by dual 2.4-mm short-thread headless compression screw fixation through a volar approach. (E, F) Follow-up computed tomography obtained 7 weeks after surgery. Coronal and sagittal reconstructed images aligned with the scaphoid axis demonstrate satisfactory intraosseous positioning of the two 2.4-mm screws and adequate purchase of the proximal fragment. (G, H) Radiographs obtained 11 months after surgery show union without loss of alignment or hardware failure; the arrowhead in (G) indicates bridging callus at the nonunion site.

in a thumb-spica cast for 2 months, after which range-of-motion exercises were initiated.

Follow-up and outcomes

Postoperative CT obtained 7 weeks after surgery demonstrated maintained fixation and alignment. Immediate postoperative SL and RL angles were 62.2° and 9.7°, and final SL and RL angles were 60.3° and 12.4°. At 7 months after surgery, follow-up radiographs showed union without loss of alignment or hardware failure (Fig. 3). Final wrist volar flexion/dorsiflexion was 70°/50°, grip strength was 30.0 kg (85% of the contralateral side), VAS pain score was 1, DASH score was 13.63, and the patient was very satisfied (Table 2).

Case 3

Patient information and clinical findings

A 41-year-old male patient presented with chronic pain in the left wrist, which was his non-dominant side. He had a remote history of wrist injury 10 to 20 years earlier and had reportedly been told at that time that no fracture was present. Persistent symptoms remained, and the pain worsened after a traffic accident while he was gripping the steering wheel. He was an ex-smoker and had no diabetes.

Diagnostic assessment

Plain radiographs demonstrated scaphoid nonunion with carpal malalignment, and CT confirmed proximal scaphoid nonunion with DISI deformity. Preoperative SL and RL angles were 59.4° and 18.5°, respectively. Preoperative nonenhanced MRI did not show definite AVN. On retrospective review, a small loose body adjacent to the scaphoid was identifiable on both preoperative radiographs and CT (Fig. 4B).

Therapeutic intervention

He also underwent the same operative procedure, including dorsal cancellous bone graft harvest from the distal radius at the Lister tubercle and volar fixation with two 2.4-

https://doi.org/10.12671/jmt.2026.00136

Fig. 3. Imaging course of case 2. (A) Initial posteroanterior radiograph showing proximal scaphoid nonunion; the arrowhead indicates the fracture line. (B) Initial lateral radiograph demonstrating DISI deformity; the yellow lines indicate a radiolunate angle of 15.3°. (C, D) Intraoperative fluoroscopic images showing guidewire placement followed by dual 2.4-mm short-thread headless compression screw fixation through a volar approach. (E, F) Follow-up computed tomography obtained 7 weeks after surgery. Coronal and sagittal reconstructed images aligned with the scaphoid axis demonstrate satisfactory intraosseous positioning of the two 2.4-mm screws and adequate purchase of the proximal fragment. (G, H) Radiographs obtained 7 months after surgery show union without loss of alignment or hardware failure; the arrowhead in (G) indicates bridging callus at the nonunion site.

mm headless compression screws. The wrist was immobilized in a thumb-spica cast for 2 months, after which range-of-motion exercises were initiated.

Follow-up and outcomes

Postoperative CT obtained 6 weeks after the index procedure demonstrated maintained screw position and alignment without definite joint penetration. Immediate postoperative SL and RL angles were 53.9° and 15.2°, and final SL and RL angles were 60.7° and 12.7°. During follow-up, persistent pain on wrist extension developed. Because the loose body had been present preoperatively and remained visible on follow-up imaging, and because irritation from one slightly long screw could not be excluded, secondary surgery was performed approximately 20 months after the index procedure. The loose body and one headless compression screw were removed; the exact pathological origin of the loose body was not confirmed. At 23 months after the index procedure, final follow-up radiographs demonstrated maintained union and alignment without fixation failure (Fig. 4). Final wrist volar flexion/dorsiflexion was 70°/60°, grip strength was 36.9 kg (94% of the contralateral side), VAS pain score was 0, DASH score was 9.17, and the patient was very satisfied (Table 2).

Discussion

This report describes three selected cases of proximal scaphoid nonunion with DISI deformity, without definite preoperative AVN, treated using dorsal distal-radius cancellous bone grafting and volar fixation with two 2.4-mm short-thread headless compression screws. The main observation is not that this technique reliably corrects DISI or is superior to single-screw fixation, but rather that dual-screw fixation was technically feasible in carefully selected proximal nonunions when preoperative CT suggested sufficient proximal fragment size and morphology, including enough depth for the 4-mm leading thread to cross the

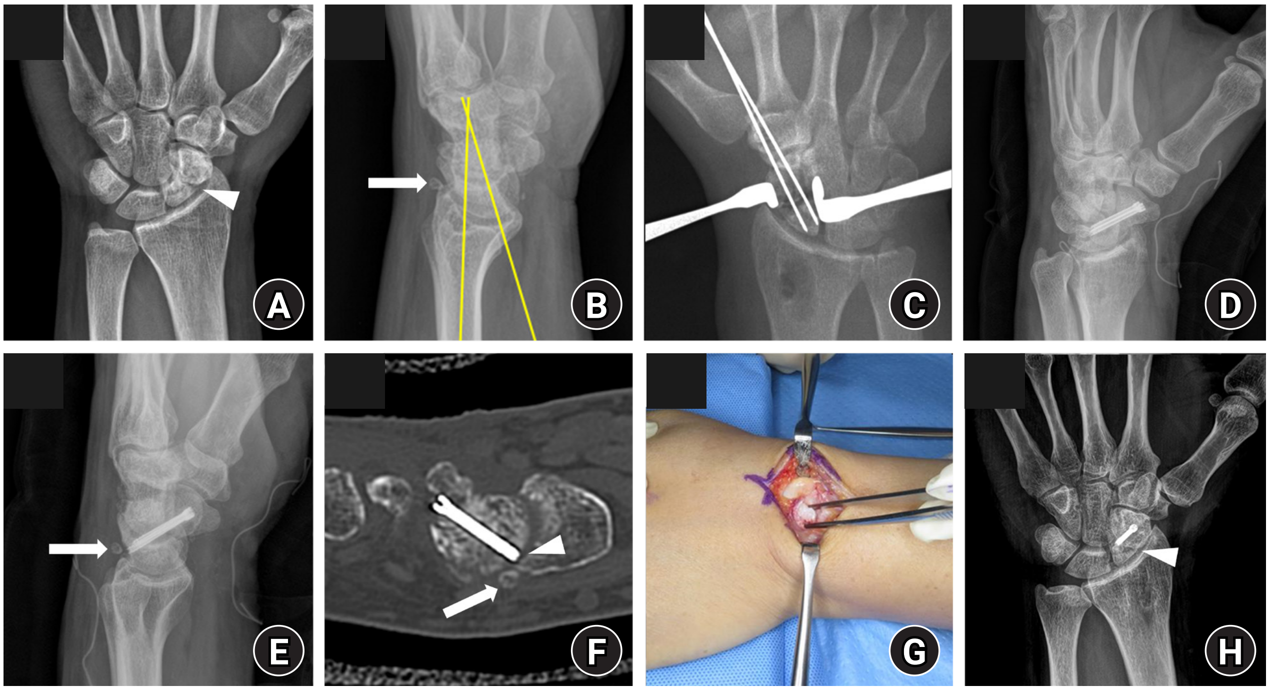

Fig. 4. Imaging course of case 3. (A) Initial posteroanterior radiograph showing proximal scaphoid nonunion; the arrowhead indicates the fracture line. (B) Initial lateral radiograph demonstrating DISI deformity; the yellow lines indicate a radiolunate angle of 18.5°, and the arrow indicates a loose body at the dorsal aspect of the scaphoid. (C, D) Intraoperative fluoroscopic images showing guidewire placement followed by dual 2.4-mm short-thread headless compression screw fixation through a volar approach. (E) Follow-up lateral radiograph obtained before secondary surgery showing the loose body near the dorsal aspect of the scaphoid (arrow). (F) Follow-up computed tomography obtained 6 weeks after the index procedure demonstrates satisfactory intraosseous screw positioning without definite joint penetration; the arrow indicates the loose body, and the arrowhead indicates the tip of a slightly long screw. (G) Intraoperative image obtained during secondary surgery showing removal of the loose body. (H) Final follow-up radiograph after secondary surgery demonstrates maintained union and alignment without fixation failure; the arrowhead indicates bridging callus at the nonunion site.

nonunion site and enough width to accommodate two safe screw trajectories. Radiographic union was observed in all three patients, and final patient-centered outcomes were favorable; however, carpal alignment correction was not uniform and one patient required secondary surgery.

The potential advantage of two screws is improved rotational control of the proximal fragment. This concept is supported by biomechanical data showing that a dual-screw construct may better maintain rotational stability than a single-screw construct, although stiffness and load-to-failure values may not differ significantly. Compared with Garcia et al. [9], the present report is more homogeneous in both pathology and technique. Garcia et al. [9] treated a heterogeneous group of scaphoid nonunions, only a minority of which involved the proximal third; among those proximal-third cases, most were approached dorsally, and most grafts in the overall series were harvested from the iliac crest. In contrast, all three patients in the present report had proximal scaphoid nonunion with DISI deformity and were managed with the same strategy: local cancellous graft harvested from the distal radius and distal-to-proximal dual short-thread screw fixation through a volar approach. This may represent the main technical distinction and clinical relevance of the present report.

A central concern is whether two 2.4-mm screws can be safely accommodated in a small proximal fragment and whether distal-to-proximal compression can be achieved when the nonunion line is very proximal. In our series, the proximal fragment measured 5.60 to 7.06 mm in width and 5.90 to 9.12 mm in depth on coronal CT, and 8.20 to 16.53 mm in width and 5.37 to 7.55 mm in depth on sagittal CT (Table 1). These measurements were obtained on the reconstructed CT cut in each plane on which the fragment appeared largest (Fig. 1). We used 2.4-mm short-thread screws and

 https://doi.org/10.12671/jmt.2026.00136

limited this technique to cases in which CT suggested that the 4-mm leading thread could cross the nonunion and engage the proximal fragment. However, because the proximal fragment is approximately dome-shaped, maximum-cut measurements do not guarantee that two screws will be securely engaged along their entire trajectories. Thus, the decision to use dual 2.4-mm screws was made qualitatively by integrating the measurements with fragment morphology, the proximal extent of the fracture line, possible parallel screw trajectories, the anticipated bone bridge between screws, and the distance from the articular surfaces. These criteria support the technical feasibility of compression in the present selected cases, but the safety margin remains narrow. Two 2.4-mm screws occupy substantial volume and require an adequate bone bridge between trajectories; therefore, this technique should not be generalized to all proximal pole nonunions. Smaller-diameter screws, alternative trajectories, single-screw fixation, vascularized grafting, or salvage procedures may be more appropriate when CT shows severe fragmentation, limited bone stock, insufficient proximal fragment depth for the leading thread to cross the nonunion site, or unsafe proximity to the articular surfaces.

The alignment data also requires cautious interpretation. Final RL angle decreased below the DISI threshold in case 2 and case 3, whereas DISI persisted in case 1 despite radiographic union and favorable symptoms. Therefore, the present cases do not prove that dual-screw fixation reliably corrects DISI. Rather, they suggest that volar reduction and dual-screw fixation may maintain acceptable alignment in selected cases, while complete correction is not guaranteed.

Bone graft selection was based on the expected defect morphology. Three-dimensional CT studies have shown that the defect pattern in scaphoid nonunion varies by location: waist or distal nonunion tends to create a larger volar-based wedge-shaped defect, whereas proximal nonunion more often leaves a flatter crescent-shaped defect localized around the fracture site [14]. This distinction helps explain why structural corticocancellous wedge grafting is intuitive in unstable waist nonunion with humpback collapse [15-17], yet may be less necessary in selected proximal nonunions. In the present cases, DISI correction was not obtained by wedge-graft mechanics, but rather by fluoroscopic reduction and maintenance with the screw construct; the cancellous graft was used primarily to fill the residual crescent-type cavity. Accordingly, cancellous graft was used as a biological filler rather than as a structural wedge, with part of the graft placed dorsally before screw insertion and the remaining volar defect packed after fixation. This rationale is supported by Cohen et al. [18], who reported successful treatment of scaphoid waist nonunion with humpback deformity without structural graft when stable screw fixation was obtained, and by Kim et al. [13], who found that cancellous grafting provided earlier union and similar deformity restoration and wrist function compared with corticocancellous grafting in unstable scaphoid nonunion treated with headless compression screw fixation. The dorsal Lister tubercle harvest was also practical in this setting because cancellous bone can be obtained easily through a small dorsal cortical window without disrupting the volar cortex or crowding the primary volar exposure used for reduction and screw placement.

The secondary procedure in case 3 deserves specific discussion. A small loose body adjacent to the scaphoid was retrospectively identifiable on both preoperative radiographs and CT, indicating that it was not necessarily caused by the dual-screw fixation procedure. CT obtained 6 weeks after the index procedure, before secondary surgery, showed maintained screw position without definite joint penetration. During follow-up, the patient developed persistent pain on wrist extension. Because the exact pain generator was uncertain and could have been related either to the preexisting loose body or to irritation from one slightly long screw, both the loose body and one screw were removed approximately 20 months after the index procedure. The loose body was not pathologically characterized. This case therefore should not be interpreted as definitive evidence of iatrogenic proximal fragment blowout or screw loosening inherent to dual-screw fixation. Nevertheless, it highlights the limited technical margin of this procedure and the importance of meticulous screw length selection, postoperative imaging review, and careful follow-up when extension pain persists.

The chronicity of nonunion varied widely among the three patients, from 8 months to 10–20 years. This heterogeneity may influence biology, deformity stiffness, cartilage status, and functional recovery, and it limits interpretation of the outcomes. Preoperative MRI was performed in all patients and did not show definite proximal-pole AVN. Therefore, our series does not address proximal nonunion with established AVN, in which vascularized grafting may be more strongly considered. Nevertheless, only one patient underwent gadolinium-enhanced MRI and intraoperative punctate bleeding was not systematically documented, so vascularity assessment remained limited.

This report has several limitations. It includes only three patients and represents a retrospective single-surgeon experience without a control group. The cases were selected based on fragment size, fragment depth, qualitative assessment of fragment morphology, and feasibility of two distal-to-proximal screw trajectories, which limits generalizability. Moreover, the fragment dimensions were measured on the CT cut in each plane in which the fragment appeared largest; therefore, these values may overestimate usable bone stock in the approximately dome-shaped proximal fragment and cannot guarantee secure purchase of both screws. Union was assessed on plain radiographs at final follow-up rather than uniformly confirmed by CT, which is a significant limitation in scaphoid nonunion research. Radioulnar deviation, preoperative VAS pain scores, and formal return-to-work or return-to-sport timing were not consistently available. Because all cases used 2.4-mm short-thread screws, this report cannot compare short-thread and long-thread designs or smaller screw options.

In conclusion, this small retrospective series suggests that volar dual 2.4-mm short-thread headless compression screw fixation combined with staged dorsal-to-volar distal-radius cancellous bone grafting is technically feasible for selected proximal scaphoid nonunions with concomitant DISI deformity when preoperative CT assessment suggests sufficient proximal fragment size, depth, and morphology for two safe distal-to-proximal screw trajectories. Although CT-confirmed union at final follow-up was not uniformly available, radiographic union defined on plain radiographs and favorable short-term functional outcomes were observed in all three patients. The DISI correction was not uniform and one patient required secondary surgery. Larger studies with standardized CT-based union assessment, functional outcome measures, and longer follow-up are needed to validate this technique.

Article Information

Author contributions

Conceptualization: JKK. Data curation: SL, WSL. Formal analysis: SL, WSL. Investigation: SL, WSL. Methodology: JKK. Project administration: JKK. Visualization: SL, WSL. Writing–original draft: SL. Writing–review & editing: SL, WSL, JKK. All authors read and approved the final manuscript.

Conflicts of interest

No potential conflict of interest relevant to this article was reported.

Funding

None.

Data availability

Not applicable.

Acknowledgments

This case report was presented in the Case Discussion section of the 2026 Annual Congress of the Korean Orthopaedic Trauma Association (KOTA).

Supplementary materials

None.

References

1. Large TM, Adams MR, Loeffler BJ, Gardner MJ. Posttraumatic avascular necrosis after proximal femur, proximal humerus, talar neck, and scaphoid fractures. J Am Acad Orthop Surg 2019;27:794-805.
2. de Roo MG, Dobbe JG, van der Horst CM, Streekstra GJ, Strackee SD. Carpal kinematic changes after scaphoid nonunion: an in vivo study with four-dimensional CT imaging. J Hand Surg Eur Vol 2019;44:1056-64.
3. Alanen M, Aspinen S, Höglund T, Sippo R, Waris E. Computer-aided three-dimensional analysis of carpal alignment in scaphoid nonunion advanced collapse wrists: a comparative study with scapholunate advanced collapse and healthy wrists. BMC Musculoskelet Disord 2025;26:423.
4. Newport ML, Williams CD, Bradley WD. Mechanical strength of scaphoid fixation. J Hand Surg Br 1996;21:99-102.
5. Trumble TE, Clarke T, Kreder HJ. Non-union of the scaphoid: treatment with cannulated screws compared with treatment with Herbert screws. J Bone Joint Surg Am 1996;78:1829-37.
6. Manske PR, McCarthy JA, Strecker WB. Use of the Her-

 https://doi.org/10.12671/jmt.2026.00136

bert bone screw for scaphoid nonunions. Orthopedics 1988;11:1653-61.
7. Kobayashi M, Berger RA, Nagy L, et al. Normal kinematics of carpal bones: a three-dimensional analysis of carpal bone motion relative to the radius. J Biomech 1997;30:787-93.
8. Nicholson LT, Sochol KM, Azad A, Alluri RK, Hill JR, Ghiassi A. Single versus dual headless compression screw fixation of scaphoid nonunions: a biomechanical comparison. Hand (N Y) 2022;17:1122-7.
9. Garcia RM, Leversedge FJ, Aldridge JM, Richard MJ, Ruch DS. Scaphoid nonunions treated with 2 headless compression screws and bone grafting. J Hand Surg Am 2014;39:1301-7.
10. Moritomo H, Viegas SF, Elder KW, et al. Scaphoid nonunions: a 3-dimensional analysis of patterns of deformity. J Hand Surg Am 2000;25:520-8.
11. Braun NS, Berger RA, Wolfe SW. Defining DISI and VISI. J Hand Surg Eur Vol 2021;46:566-8.
12. Rodriguez-Fontan F, Tucker NJ, Pflug EM, Leversedge FJ, Catalano LW, Lauder A. Proximal hamate reconstruction of proximal pole scaphoid nonunion: a case series and analysis of clinical outcomes. Hand (N Y) 2024;19:967-77.
13. Kim JK, Yoon JO, Baek H. Corticocancellous bone graft vs cancellous bone graft for the management of unstable scaphoid nonunion. Orthop Traumatol Surg Res 2018;104:115-20.
14. Oka K, Murase T, Moritomo H, Goto A, Sugamoto K, Yoshikawa H. Patterns of bone defect in scaphoid nonunion: a 3-dimensional and quantitative analysis. J Hand Surg Am 2005;30:359-65.
15. Tomaino MM, King J, Pizillo M. Correction of lunate malalignment when bone grafting scaphoid nonunion with humpback deformity: rationale and results of a technique revisited. J Hand Surg Am 2000;25:322-9.
16. Bindra R, Bednar M, Light T. Volar wedge grafting for scaphoid nonunion with collapse. J Hand Surg Am 2008;33:974-9.
17. Fernandez DL. A technique for anterior wedge-shaped grafts for scaphoid nonunions with carpal instability. J Hand Surg Am 1984;9:733-7.
18. Cohen MS, Jupiter JB, Fallahi K, Shukla SK. Scaphoid waist nonunion with humpback deformity treated without structural bone graft. J Hand Surg Am 2013;38:701-5.

JMT Journal of Musculoskeletal Trauma

pISSN 3058-6267 · eISSN 3058-6275
J Musculoskelet Trauma 2026;39(3):262-268
https://doi.org/10.12671/jmt.2026.00164

Open distal radius fracture with ulnar neurovascular injury treated with dorsal spanning plate fixation and vein interposition grafting: a case report

Kyeong-Eon Kim[1], Ho-Yong Lee[2], Shin-Woo Lee[1], Ji-Sup Kim[1]

[1]Department of Orthopedic Surgery, Ewha Womans University Seoul Hospital, Ewha Womans University College of Medicine, Seoul, Korea
[2]Department of Orthopedic Surgery, Ewha Womans University Mokdong Hospital, Ewha Womans University College of Medicine, Seoul, Korea

Open comminuted intra-articular distal radius fractures with associated ulnar neurovascular injury are rare; furthermore, these injuries are challenging because skeletal stabilization, arterial reconstruction, nerve assessment, and soft-tissue coverage must be coordinated. We report the case of an 80-year-old female patient who presented after a fall from stairway with a severe open distal radius fracture and a volar-ulnar distal forearm wound. She reported numbness and tingling in the ring and small fingers, with a cold sensation and delayed capillary refill. Imaging showed a severely comminuted intra-articular distal radius fracture (AO/OTA type 23-C3). Emergency surgery was performed within 6 hours. First, a dorsal spanning plate was applied, and the small volar lunate facet fragment was fixed with a volar lunate facet plate. After debridement of the injured ulnar artery, a segmental defect remained and was reconstructed using a reversed basilic vein interposition graft harvested from the ipsilateral proximal forearm. The contused but continuous ulnar nerve was treated with neurolysis. The soft-tissue defect was managed with an acellular dermal matrix and negative-pressure wound therapy, followed by staged full-thickness skin grafting 1 week later. At 1 year postoperatively, bony union was achieved, and the functional outcomes were satisfactory.
Level of evidence: V.

Keywords: Radius fractures; Ulnar artery; Ulnar nerve; Bone plates; Case reports

Case Report

Received: April 7, 2026
Revised: May 1, 2026
Accepted: May 11, 2026

Correspondence to:
Ji-Sup Kim
Department of Orthopedic Surgery, Ewha Womans University Seoul Hospital, Ewha Womans University College of Medicine, 260 Gonghang-daero, Gangseo-gu, Seoul 07804, Korea
Tel: +82-2-6956-1656
Email: kkimjsno1@naver.com

Introduction

Distal radius fractures are among the most common fractures encountered in orthopedic practice. However, vascular injury associated with distal radius fracture is uncommon, and combined injury of the ulnar artery and ulnar nerve is particularly rare [1-3]. Reported vascular complications include not only acute arterial laceration or thrombosis, but also delayed pseudoaneurysm formation after distal radius and ulna fractures [1]. Wang et al. [1] described a delayed ulnar artery pseudoaneurysm after distal radius and ulna fracture, highlighting that vascular injury may present in a delayed fashion even when the hand initially appears perfused. De Witte et al. [2] reported six cases of acute vascular injury associated with distal radius fracture and noted that these injuries were more likely to occur in open fractures, high-energy injuries, or fractures with an associated ulnar lesion. In their series, most single-artery injuries at the wrist were not associated with ischemia, but arterial reconstruction was considered necessary in the unusual patient with a dysvascular hand [2]. Sahin et al. [3] also emphasized that the ulnar neurovascular bundle may be vulnerable in severely displaced comminuted distal radius fractures.

Severe intra-articular distal radius fractures with marked metaphyseal comminution remain difficult to treat, although similar fracture patterns may also occur after a fall from standing height in elderly patients [4]. Restoration and maintenance of radial length and alignment are essential in these fractures [4,5]. Small volar lunate facet fragments may require fragment-specific fixation because inadequate stabilization of this fragment can lead to persistent instability or secondary displacement [6]. In highly comminuted intra-articular distal radius fractures, a dorsal spanning plate may provide indirect reduction through distraction and ligamentotaxis, functioning as an internal bridge construct [5]. Management becomes even more challenging when vascular compromise and soft-tissue loss are also present, because skeletal stabilization, revascularization, nerve evaluation, and soft-tissue coverage must be addressed in a coordinated manner [7]. We report a rare case of an open comminuted intra-articular distal radius fracture with combined ulnar artery and ulnar nerve injury in an elderly patient, treated with dorsal spanning plate fixation, fixation of a small volar lunate facet fragment with a volar lunate facet plate, basilic vein interposition grafting, neurolysis, and staged soft-tissue reconstruction.

Case report

Ethics statement

This study was reviewed by the Institutional Review Board (IRB) of Ewha Womans University Seoul Hospital (IRB No. 2026-05-041-001). Written informed consent for publication of clinical details and accompanying images was obtained from the patient.

Patient information and clinical findings

An 80-year-old female patient with a medical history of hypertension and chronic kidney disease presented to our emergency department after a fall from stairway, during which she landed with her outstretched right hand striking the ground. Physical examination revealed gross deformity of the wrist with the fragment protruding through an approximately 8 cm open wound over the volar-ulnar aspect of the distal forearm, with minimal contamination (Fig. 1). The patient reported numbness and tingling in the ring and small fingers. The hand was cool to touch, with capillary refill delayed to approximately 4 seconds. The radial pulse was palpable, whereas the ulnar pulse was nonpalpable distal to the injury site. Persistent clinical hypoperfusion prompted operative exploration and vascular reconstruction.

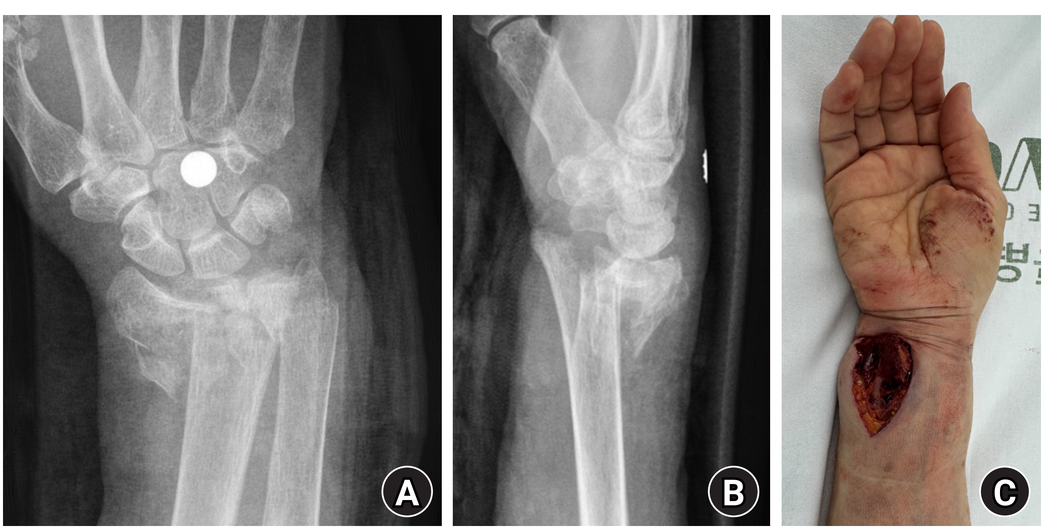

Fig. 1. Initial images of an 80-year-old female patient with a severe open distal radius fracture after a fall from stairway. (A) Posteroanterior radiograph showing a markedly displaced comminuted intra-articular distal radius fracture. (B) Lateral radiograph showing severe dorsal displacement and metaphyseal comminution. (C) Clinical photograph demonstrating a volar-ulnar open wound at the distal forearm.

https://doi.org/10.12671/jmt.2026.00164

Diagnostic assessment

Radiographs and computed tomography demonstrated a severely comminuted intra-articular distal radius fracture, classified as AO/OTA type 23-C3 (Fig. 1). After operative exploration confirmed an ulnar arterial injury requiring reconstruction, the open fracture was classified as Gustilo-Anderson type IIIC. Given the open injury and signs of impaired distal perfusion, preoperative angiography was deferred because urgent exploration, skeletal stabilization, and revascularization were prioritized. Emergency surgery was initiated within 6 hours after injury, and flow through the reconstructed ulnar artery was restored approximately 8 hours after injury.

Therapeutic intervention

On arrival at the emergency department, intravenous cefazolin and gentamicin were administered immediately and continued for 72 hours, and a tetanus toxoid booster was given after confirmation of prior immunization history. Following thorough irrigation with 9 L of normal saline using pulsed lavage and meticulous debridement of devitalized and contaminated soft tissue, a segmental defect of the ulnar artery remained and required reconstruction (Fig. 2). Because of the marked metaphyseal and intra-articular comminution with residual instability, a combined fixation strategy was chosen. Although revascularization was a priority, skeletal stabilization was performed first to provide a stable framework for the subsequent microvascular anastomosis and to allow accurate measurement of the required vein graft length. A dorsal spanning plate was applied first to restore length and provide provisional stability to the severely comminuted fracture, with particular attention to restoration of coronal alignment. As a bridge construct, the dorsal spanning plate allowed indirect reduction through longitudinal distraction and ligamentotaxis. Distal fixation over both the second and third metacarpals was assessed intraoperatively, and fixation to the second metacarpal was ultimately selected because it provided more satisfactory coronal alignment. After overall length and alignment had been re-established, the small volar lunate facet fragment was reduced through a volar approach and fixed using a volar lunate facet plate (Fig. 3) [6].

The ulnar artery was explored through the volar-ulnar wound, and the injured segment was debrided back to healthy proximal and distal ends with intact intima. Because of the open wound, gross deformity, and clinical signs of impaired distal perfusion at presentation, a formal preoperative Allen test could not be reliably performed. After debridement to healthy intima, an approximately 2-cm segmental defect remained, precluding tension-free primary repair. Because clinical evidence of distal hypoperfusion persisted after skeletal realignment, we elected to reconstruct the ulnar artery using a reversed basilic vein interposition graft. A segment of the ipsilateral basilic vein was harvested from the proximal forearm, just distal to the

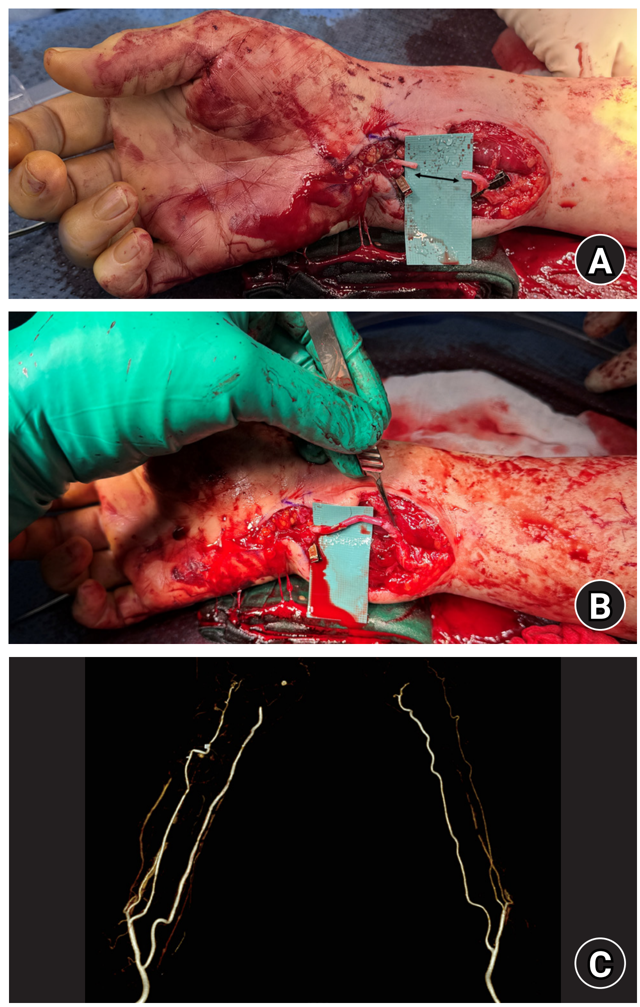

Fig. 2. Intraoperative photographs showing ulnar artery reconstruction for a segmental defect. (A) After debridement, an approximately 2-cm segmental defect remained in the ulnar artery. (B) The defect was reconstructed with a reversed interposition vein graft harvested from the ipsilateral basilic vein. (C) Postoperative three-dimensional computed tomography angiography confirming patency of the reconstructed ulnar artery.

https://doi.org/10.12671/jmt.2026.00164

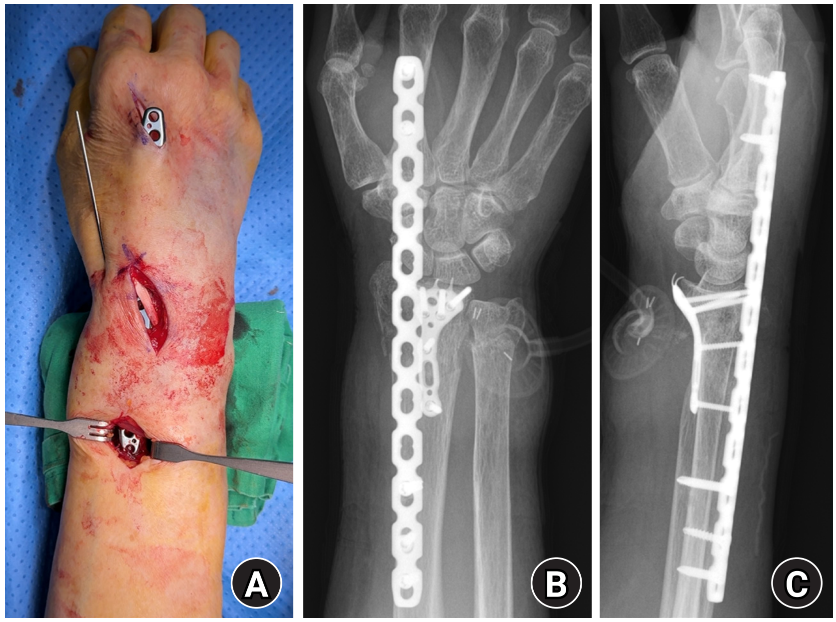

Fig. 3. Dorsal spanning plate and volar locking plate fixation. (A) Intraoperative photograph showing the dorsal spanning plate passed beneath the extensor tendons. (B, C) Immediate postoperative posteroanterior and lateral radiographs demonstrating combined dorsal spanning plate and volar plate fixation; the dorsal spanning plate was used to restore length and alignment, and the volar plate was used to restore the articular surface.

elbow crease, reversed, and interposed between the arterial ends. End-to-end anastomoses were performed under ×2.5 loupe visualization using interrupted nylon sutures. After completion of the reconstruction, distal perfusion was restored. Exploration of the ulnar nerve revealed contusion without loss of continuity; the nerve was found to be entrapped by hematoma at the level of injury, and neurolysis was performed.

During the initial operation, the residual soft-tissue defect was covered with an acellular dermal matrix (AlloDerm), and negative-pressure wound therapy was applied. At re-exploration on postoperative day 7, the wound was free of infection and the acellular dermal matrix demonstrated granulation, with no remaining exposure of the arterial graft, tendon, bone, or hardware. A full-thickness skin graft harvested from the ipsilateral groin was applied over the incorporated matrix/the vascularized wound bed. Graft take was approximately 95%, and no additional coverage procedure was required.

Follow-up and outcomes

The postoperative course was uneventful. A conservative antiplatelet regimen was selected; aspirin 100 mg once daily was administered for 4 weeks postoperatively. Cefazolin and gentamicin were administered according to the institutional protocol for type III open fractures, with gentamicin dosing adjusted for renal function. Antibiotic prophylaxis was discontinued after 3 days. Postoperative three-dimensional computed tomography angiography, performed on postoperative day 3 after reassessment of renal function, confirmed patency of the interposition graft (Fig. 2C), with no deterioration in renal function. Clinical examination demonstrated a warm, well-perfused hand with a capillary refill time of 1 second. The dorsal spanning plate was removed at 2 months postoperatively. Ulnar nerve-related symptoms persisted for up to 3 months postoperatively, but gradually improved and had resolved by 6 months. At the 1-year follow-up, bony union had been achieved, and the patient demonstrated a favorable functional outcome, with a Disabilities of the Arm, Shoulder and Hand score of 6.7 and a modified Mayo wrist score of 85. Objective sensory assessment using Semmes-Weinstein monofilament testing demonstrated 2.83 at the ring and small finger pulps. At 1 year, wrist flexion and extension were 50° and 70°, respectively, and forearm pronation and supination were 80° and 80°. Grip strength was 72% of that

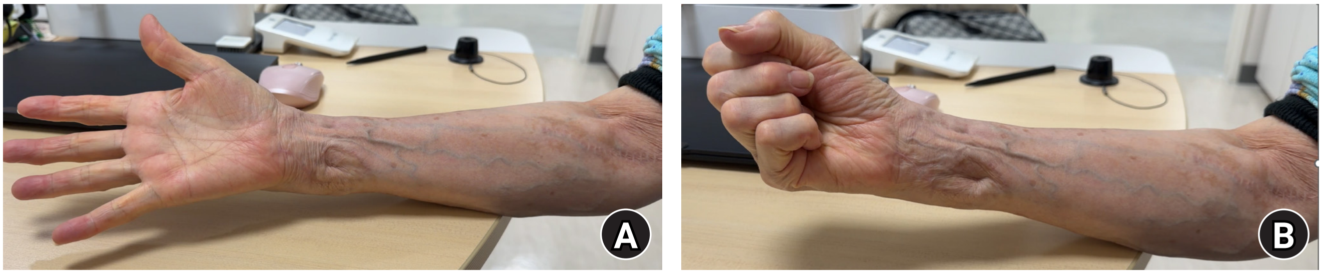

Fig. 4. Clinical photographs obtained 1 year postoperatively. (A, B) Full finger range of motion without stiffness, no residual ulnar nerve-related symptoms, and a well-healed skin graft site are shown.

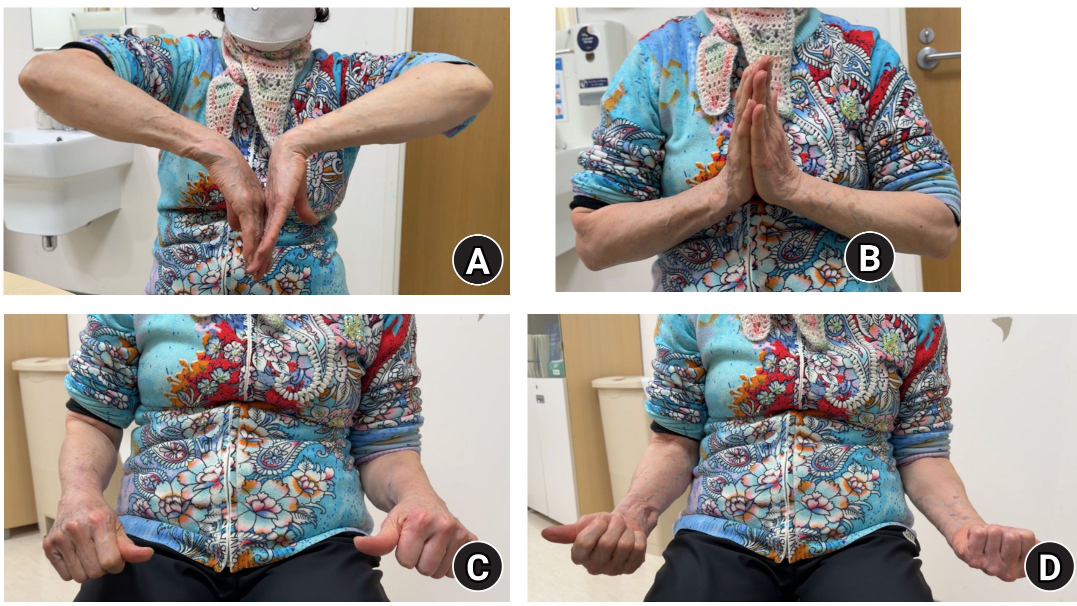

Fig. 5. Clinical photographs obtained at final follow-up demonstrating wrist and forearm range of motion: (A) flexion, (B) extension, (C) pronation, and (D) supination. Mild limitation of wrist flexion is noted, whereas wrist extension and forearm rotation are full.

of the contralateral hand. Finger range of motion was full without stiffness (Figs. 4, 5). The hand remained warm and well-perfused, with a palpable radial pulse and palpable ulnar pulse and a capillary refill time of 1 second. No postoperative vascular complication, infection, or graft-related adverse event occurred. The clinical timeline from injury through final follow-up is summarized in Table 1.

Table 1. Clinical timeline from injury to final follow-up

Timepoint	Event
Injury	Fall from stairway
Within 6 hr	Surgery initiated
Approximately 7 hr	Skeletal stabilization completed (dorsal spanning plate + volar lunate facet plate)
Approximately 8 hr	Ulnar arterial flow restored (reversed basilic vein interposition graft)
Day 0	Acellular dermal matrix + negative-pressure wound therapy applied
Day 3	Postoperative computed tomography angiography confirms graft patency
Day 7	Full-thickness skin graft
2 Months	Dorsal spanning plate removed
3 Months	Peak ulnar nerve-related symptoms
6 Months	Ulnar nerve symptoms resolved
1 Year	Final functional and perfusion assessment

Discussion

Rationale for vascular reconstruction vs. ligation

The clinical challenge in our patient was the need to coordinate skeletal stabilization, arterial reconstruction, nerve evaluation, and staged soft-tissue reconstruction within a single treatment plan in an elderly patient with significant

https://doi.org/10.12671/jmt.2026.00164

comorbidities. Several case-specific factors guided our decision-making. First, the presence of impaired distal perfusion, including cold sensation and delayed capillary refill, indicated that the residual radial artery inflow alone was unlikely to provide adequate perfusion, and that arterial reconstruction rather than simple ligation should be considered. Second, the markedly comminuted intra-articular fracture pattern (AO/OTA 23-C3) with a small volar lunate facet fragment required a combined fixation strategy capable of restoring overall length and alignment while also addressing the articular fragment. Third, because definitive soft-tissue coverage could not be achieved primarily, a staged reconstructive approach was planned from the outset. The following discussion focuses on how each of these decisions was made and how they were integrated into the overall treatment sequence. Although single-artery injury at the wrist can often be managed with ligation when the hand remains well perfused through the remaining intact artery, this principle did not fully apply in our patient [2]. Unlike the ligation cases reported by de Witte et al. [2], our patient demonstrated evidence of distal hypoperfusion, delayed capillary refill, and a nonpalpable ulnar pulse. In addition, debridement resulted in a 2-cm segmental ulnar arterial defect that precluded tension-free primary repair. Although ligation may be acceptable for an isolated single-artery injury in a well-perfused hand, these two factors—persistent hypoperfusion and a defect too large for primary repair—supported reconstruction as a case-specific strategy to restore adequate hand perfusion. This case does not establish the superiority of reconstruction over ligation in a well-perfused hand; rather, it is consistent with the observation by de Witte et al. [2] that interpositional vein grafting may be necessary in the unusual patient with a dysvascular hand, particularly when crush injury or thrombosis involves a several-centimeter arterial segment.

Characteristics of ulnar neurovascular injury

The pattern of ulnar neurovascular injury in our case also deserves attention. Sahin et al. [3] reported a delayed case of combined ulnar artery and ulnar nerve injury after comminuted distal radius fracture, in which scar entrapment, thrombosis, and a segmental arterial defect were identified during secondary exploration and treated with basilic vein grafting. In contrast, our patient underwent urgent exploration at the index procedure because the fracture was open and accompanied by impaired distal perfusion. The ulnar nerve remained in continuity and was therefore treated with neurolysis alone. Ulnar nerve-related symptoms gradually improved and recovery occurred during the follow-up period.

Sequencing of fixation and coordinated salvage strategy

Stable skeletal fixation and coordinated staged treatment were also essential. Severe metaphyseal comminution in elderly patients may occur even after a fall from standing height [4], and dorsal spanning plate fixation can serve as an internal bridge construct that restores length and alignment through distraction and ligamentotaxis [5]. In our case, provisional restoration of length and coronal alignment provided a stable framework for vascular reconstruction and subsequent soft-tissue management. Completing skeletal stabilization before arterial anastomosis also allowed accurate determination of the required vein graft length and minimized the risk of disrupting the microvascular repair during subsequent fracture manipulation. Because hand perfusion was reduced but not completely absent, rapid skeletal stabilization was completed first to restore alignment and protect the subsequent vascular repair. Skeletal stabilization required approximately 60 minutes, after which arterial reconstruction was performed. More broadly, this case illustrates the feasibility of coordinated management of debridement, skeletal stabilization, revascularization, and soft-tissue coverage in a patient with combined orthopedic and vascular injury [7]. Shahien et al. [7] reported high complication and amputation rates in patients with combined orthopedic and vascular injuries presenting with ischemia and emphasized the importance of an individualized salvage strategy.

Throughout management, the patient's advanced age and chronic kidney disease were taken into account in key decisions, including antibiotic dosing, staged soft-tissue reconstruction, and selection of a conservative antiplatelet regimen. At 1 year postoperatively, bony union was achieved, postoperative computed tomography angiography confirmed graft patency, and the patient had no perfusion-related symptoms such as cold intolerance. Although this is a single case, it suggests that satisfactory results can be achieved in severe open distal radius fractures with combined ulnar neurovascular injury when arterial reconstruction is selected appropriately based on perfusion status and defect morphology, and when fixation, revascularization, and soft-tissue reconstruction are carefully coordinated.

Limitations

This report has several limitations: it is a single case without a comparison group, and the 1-year follow-up may be insufficient to detect late vascular or neurologic complications. Given the rarity of this injury pattern, additional cases, multicenter registries, and longer vascular surveillance would help clarify optimal management.

Article Information

Author contributions

Conceptualization: KEK, JSK. Data curation: KEK, HYL, SWL. Investigation: KEK, HYL, SWL, JSK. Methodology: KEK, JSK. Project administration: KEK, JSK. Resources: JSK. Supervision: JSK. Visualization: KEK, JSK. Writing-original draft: KEK. Writing-review & editing: KEK, HYL, SWL, JSK. All authors read and approved the final manuscript.

Conflicts of interest

No potential conflict of interest relevant to this article was reported.

Funding

None.

Data availability

Not applicable.

Acknowledgments

This case report was presented in the Case Discussion section of the 2026 Annual Congress of the Korean Orthopaedic Trauma Association (KOTA).

Supplementary materials

None.

References

1. Wang AA, Strauch RJ, Moore JA. Pseudoaneurysm of the ulnar artery occurring after fracture of the distal radius and ulna: a case report. J Hand Surg Am 1998;23:933-7.
2. de Witte PB, Lozano-Calderon S, Harness N, Watchmaker G, Green MS, Ring D. Acute vascular injury associated with fracture of the distal radius: a report of 6 cases. J Orthop Trauma 2008;22:611-4.
3. Sahin MS, Gokkus K, Sargin MB. Ulnar nerve and ulnar artery injury caused by comminuted distal radius fracture. J Orthop Case Rep 2020;10:25-30.
4. Cha SM. The clinical outcome of treating elderly distal radius fractures by long volar locking plate with the elimination of irreducible metaphyseal comminuted volar cortical fragments: a retrospective case series. J Musculoskelet Trauma 2025;38:13-25.
5. Calem D, Weintraub M, Vosbikian M, Ahmed I. Radiographic outcomes of dorsal spanning plate with and without volar plate fixation for comminuted intra-articular distal radius fractures. J Clin Orthop Trauma 2025;64:102949.
6. Park HJ, Kim JH. Hook plate versus periarticular-type volar locking plate for distal radius fractures involving the volar lunate facet in Korea: a retrospective cohort study. J Musculoskelet Trauma 2025;38:221-8.
7. Shahien AA, Sullivan M, Firoozabadi R, et al. Combined orthopaedic and vascular injuries with ischemia: a multicenter analysis. J Orthop Trauma 2021;35:512-6.

https://doi.org/10.12671/jmt.2026.00164

JMT Journal of Musculoskeletal Trauma

pISSN 3058-6267 · eISSN 3058-6275
J Musculoskelet Trauma 2026;39(3):269-274
https://doi.org/10.12671/jmt.2026.00185

Radiocarpal subluxation after volar plating due to an insufficiently supported dorsal key fragment: a case report

Yeongyoon Koh[1], Kanghun Yu[2], Jong Woong Park[2], In Cheul Choi[2]

[1]Department of Orthopedic Surgery, Soonchunhyang University Seoul Hospital, Soonchunhyang University College of Medicine, Seoul, Korea
[2]Department of Orthopedic Surgery, Korea University Anam Hospital, Korea University College of Medicine, Seoul, Korea

Distal radius fractures are commonly managed using volar locking plate fixation, which provides stable fixation in most cases. However, certain fracture patterns involving dorsal key fragments may not be adequately stabilized with a volar approach alone, even when intraoperative reduction appears satisfactory. We report the case of a 58-year-old male patient with a complex intra-articular distal radius fracture involving a dorsoulnar corner (DUC) fragment. Preoperative computed tomography revealed a dorsal fragment associated with subtle dorsal radiocarpal subluxation. Despite this finding, the fragment was considered amenable to fixation through a volar approach because it was relatively large. Although satisfactory reduction was achieved intraoperatively, early postoperative imaging demonstrated progressive dorsal radiocarpal subluxation due to displacement of the DUC fragment, while overall alignment parameters remained preserved. Revision surgery with additional dorsal buttress fixation successfully restored stability. This case highlights the critical importance of recognizing dorsal key fragments and achieving adequate dorsal support during fixation, as failure to provide sufficient support may result in delayed instability despite acceptable initial reduction.
Level of evidence: V.

Keywords: Radius fractures; Bone plates; Joint instability; Wrist joint; Case reports

Case Report

Received: April 28, 2026
Revised: May 13, 2026
Accepted: May 20, 2026

Correspondence to:
In Cheul Choi
Department of Orthopedic Surgery, Korea University Anam Hospital, 73 Koryeodae-ro, Seongbuk-gu, Seoul 02841, Korea
Tel: +82-2-920-5924
Email: indolldr@korea.ac.kr

Introduction

Background

Distal radius fractures are among the most common injuries encountered in orthopedic practice [1]. With the advancement of volar locking plate (VLP) systems and fixation techniques, most of these fractures can now be effectively managed through a volar approach alone, providing stable fixation and favorable clinical outcomes [2-4]. However, this technical progress has also introduced a potential pitfall. Even experienced surgeons may underestimate the need for a dorsal approach in certain fracture patterns or may be tempted to rely solely on volar fixation when the fracture appears adequately reducible intraoperatively.

The concept of key fragments, defined as osteoligamentous units that determine fracture stability and carpal alignment, emphasizes the biomechanical importance of specific fracture components [5]. Fractures involving the dorsoulnar corner (DUC) may represent a dorsal key fragment requiring mechanical support rather than simple fixation.

Objectives

We present a case that highlights this pitfall and emphasizes the importance of recognizing dorsal key fragments in surgical decision-making.

Case presentation

Ethics statement

This case report was approved by the Institutional Review Board (IRB) of Korea University Anam Hospital (IRB No. K2025-0977-001). Written informed consent was obtained from the patient for publication of this case report and accompanying images.

Patient information

A 58-year-old male patient presented with a left wrist injury following a fall from a height of approximately 1.5 m.

Clinical findings

Initial physical examination revealed swelling, tenderness, and limited range of motion without gross neurovascular deficit. The patient was right-hand dominant and had a medical history significant only for hypertension. He was independent in activities of daily living prior to the injury.

Diagnostic assessment

Preoperative radiographic and computed tomography (CT) evaluation demonstrated a complex intra-articular distal radius fracture classified as AO/OTA type 23-C3. Quantitative parameters measured on initial radiographs were as follows: radial height 12 mm, radial inclination 25°, volar tilt –30° (dorsal tilt), ulnar variance 9 mm, and articular step-off 3 mm (Fig. 1). A DUC fragment associated with subtle dorsal radiocarpal subluxation was identified. Although recognized, the fragment appeared relatively large on plain radiographs; however, CT imaging revealed dorsal cortical comminution. Nonetheless, stable fixation was anticipated using a volar approach based on the overall fragment size.

Surgical intervention and timeline

Open reduction and internal fixation were performed using a VLP (Medartis Aptus Volar Rim Plate, Medartis AG). Intraoperative fluoroscopy demonstrated satisfactory restoration of radial height, inclination, and volar tilt, with acceptable articular congruity. Immediate postoperative radiographs confirmed maintained reduction with no gross malalignment (Fig. 2).

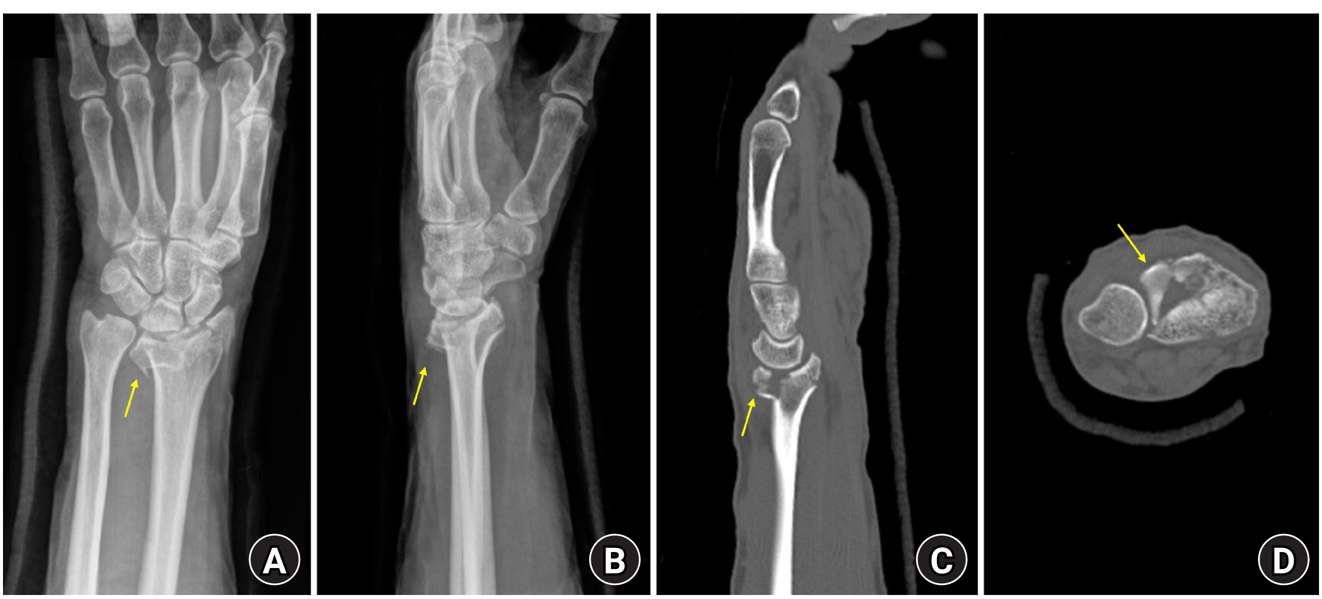

Fig. 1. Preoperative imaging. Preoperative radiographs (A, B) and computed tomography images (C, D) of the left wrist demonstrating a complex intra-articular distal radius fracture. Axial and sagittal computed tomography images revealed a dorsoulnar corner fragment associated with subtle dorsal radiocarpal subluxation. Yellow arrows indicate the dorsoulnar corner fragment.

https://doi.org/10.12671/jmt.2026.00185

Follow-up and outcomes

Following surgery, the wrist was immobilized with a short arm splint, and the patient was instructed to avoid active wrist motion and loading. At 1-week follow-up, radiographs demonstrated dorsal radiocarpal subluxation despite this immobilization (Fig. 3). CT imaging confirmed displacement of the DUC fragment and loss of dorsal support, while conventional radiographic alignment parameters—including radial height, radial inclination, and volar tilt—remained within acceptable ranges; however, radiocarpal congruity was progressively compromised, as evidenced by worsening dorsal carpal translation.

Revision surgery was performed via a dorsal approach, and dorsal buttress fixation was applied to stabilize the

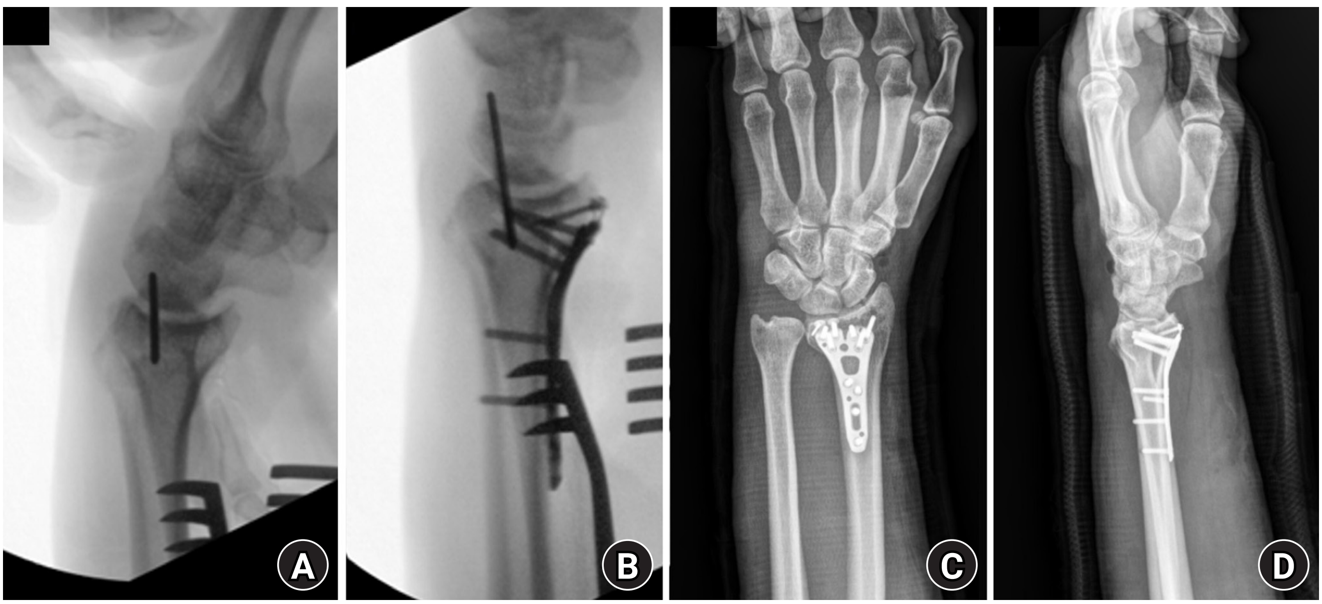

Fig. 2. Intraoperative and immediate postoperative imaging. Intraoperative fluoroscopic images (A, B) demonstrated apparent restoration of radial height, inclination, and volar tilt following volar locking plate fixation. Immediate postoperative radiographs (C, D) demonstrated acceptable reduction without obvious dorsal translation or carpal malalignment.

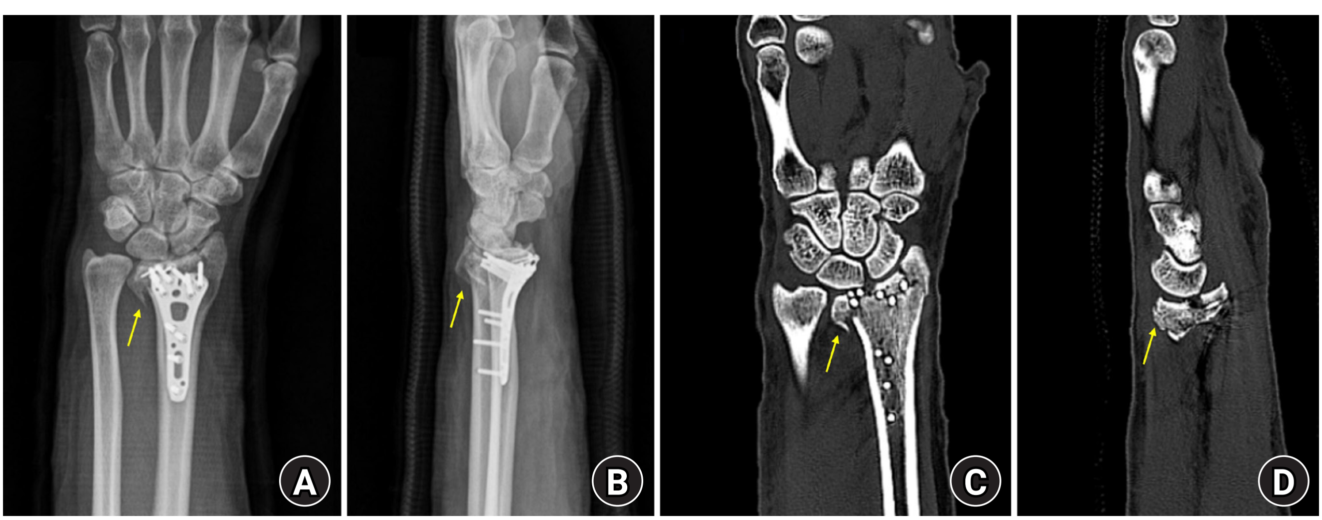

Fig. 3. Early postoperative failure. Radiographs (A, B) and computed tomography images (C, D) obtained 1 week postoperatively demonstrated dorsal radiocarpal subluxation. Displacement of the dorsoulnar corner fragment was evident, resulting in loss of dorsal support despite preservation of overall alignment parameters. Yellow arrows indicate the dorsoulnar corner fragment.

DUC fragment. Postoperative imaging demonstrated restoration of radiocarpal alignment without residual subluxation (Fig. 4). The patient showed improved pain and functional recovery during follow-up.

At the 14-month postoperative follow-up, the patient had undergone removal of both the volar locking plate and the dorsal buttress plate via their respective approaches. Radiographic evaluation demonstrated complete bony union with maintained radiocarpal alignment. Clinically, the patient reported minimal pain with a visual analog scale score of 1. Grip strength was 65 pounds (29.5 kg) on the operated side compared to 70 pounds (31.8 kg) on the contralateral side. The Patient-Rated Wrist Evaluation score was 8. Wrist range of motion was as follows: flexion 50°, extension 70°, radial deviation 10°, ulnar deviation 30°, pronation 65°, and supination 80° (Fig. 5). The patient expressed a high level of satisfaction with the surgical outcome and was able to return to his pre-injury level of daily activity without significant limitation.

Discussion

This case highlights a key pitfall in distal radius fracture management in the era of VLP fixation. While VLP systems provide reliable fixation in most cases, certain fracture patterns require biomechanical consideration beyond alignment restoration [2-4]. Despite satisfactory intraoperative reduction, this case demonstrated delayed dorsal instability. This suggests that anatomical alignment alone does not ensure mechanical stability.

The DUC fragment represents a key osteoligamentous unit that contributes to radiocarpal stability. Displacement of this fragment may result in instability patterns not controlled by volar fixation alone. Previous studies have suggested that sufficiently large dorsal key fragments may be amenable to indirect reduction and fixation through a volar approach alone [5]. However, in our experience, dorsal key fragments are frequently associated with comminution, which limits the effectiveness of volar fixation. Therefore, even in cases where indirect reduction appears achievable, surgeons should exercise caution when considering volar fixation alone. Fragment-specific fixation principles support addressing such critical fragments directly [6].

A key distinction highlighted in this case is between fragment capture and fragment support. Although the fragment was captured by volar screws—as confirmed on intraoperative fluoroscopic imaging demonstrating screw tips engaging the DUC fragment (Fig. 2)—the absence of dorsal buttress support led to failure under physiological loading conditions [7].

Fig. 4. Revision surgery and outcome. Postoperative radiographs obtained following revision surgery demonstrated restoration of radiocarpal alignment after additional dorsal fixation. (A) Posteroanterior view showing restored radial height and inclination with the dorsal buttress plate in situ. (B) Lateral view confirming restoration of volar tilt and absence of dorsal radiocarpal subluxation. (C) Radial oblique view demonstrating adequate fragment stabilization and articular congruity. (D) Ulnar oblique view confirming restoration of the dorsoulnar corner with no residual subluxation.

https://doi.org/10.12671/jmt.2026.00185

Fig. 5. Final follow-up findings. (A) Clinical photographs demonstrating recovery of wrist range of motion, including flexion, extension, pronation, and supination. (B) Radiographs obtained at the final follow-up evaluation, showing complete bony union with maintained joint congruency and satisfactory radiocarpal alignment.

While slight residual deformity may not significantly impact functional outcomes, this concept does not apply to cases involving structural instability [8]. Dorsal fixation using low-profile plates can effectively restore stability while minimizing complications.

The failure of volar fixation in this case should be interpreted in the context of two potentially coexisting mechanisms. First, technical factors related to screw purchase—including screw length and the ability to achieve adequate cortical purchase in a comminuted fragment—may have contributed to construct instability. In cases involving small or comminuted dorsal fragments, achieving reliable screw purchase through a volar approach is inherently challenging, and this limitation should not be overlooked. Second, and arguably more fundamentally, the failure reflects an underlying biomechanical limitation of volar-only fixation in the setting of a DUC fragment associated with carpal subluxation. Even with optimal screw placement, volar screws provide fragment capture rather than true buttress support; without direct dorsal support, the construct remains vulnerable to failure under physiological loading. Therefore, rather than attributing the failure to either technical or biomechanical factors alone, this case underscores the importance of recognizing both dimensions when planning fixation strategy. Stability in such cases is not achieved by screw purchase alone but requires restoring structural support through appropriate dorsal buttressing—particularly when the fragment is comminuted or associated with carpal subluxation.

This case has several limitations. As a single case report, the findings cannot be generalized to all fracture patterns involving dorsal key fragments. The relative contributions of technical and biomechanical factors to the observed failure could not be definitively determined, and the size threshold beyond which dorsal buttress fixation is required remains undefined.

In conclusion, dorsal key fragments must be carefully identified in distal radius fractures. Even when they appear amenable to volar fixation, they may require dorsal buttress support. Fluoroscopy alone cannot assess mechanical stability, and failure to address these fragments may result in delayed instability.

Article Information

Author contributions

Conceptualization: YK, JWP, ICC. Data curation: YK, KY. Formal analysis: JWP. Investigation: YK. Methodology: ICC. Supervision: ICC. Validation: YK, KY. Writing–original draft: YK. Writing–review & editing: KY, JWP, ICC. All authors read and approved the final manuscript.

Conflicts of interest

No potential conflict of interest relevant to this article was reported.

Funding

None.

Data availability

Not applicable.

Acknowledgments

This case report was presented in the Case Discussion section of the 2026 Annual Congress of the Korean Orthopaedic Trauma Association (KOTA).

Supplementary materials

None.

References

1. Chung KC, Spilson SV. The frequency and epidemiology of hand and forearm fractures in the United States. J Hand Surg Am 2001;26:908-15.
2. Drobetz H, Kutscha-Lissberg E. Osteosynthesis of distal radial fractures with a volar locking screw plate system. Int Orthop 2003;27:1-6.
3. Orbay JL, Fernandez DL. Volar fixation for dorsally displaced fractures of the distal radius: a preliminary report. J Hand Surg Am 2002;27:205-15.
4. Simic PM, Robison J, Gardner MJ, Gelberman RH, Weiland AJ, Boyer MI. Treatment of distal radius fractures with a low-profile dorsal plating system: an outcomes assessment. J Hand Surg Am 2006;31:382-6.
5. Hintringer W, Rosenauer R, Pezzei C, et al. Biomechanical considerations on a CT-based treatment-oriented classification in radius fractures. Arch Orthop Trauma Surg 2020;140:595-609.
6. Rikli DA, Regazzoni P. Fractures of the distal end of the radius treated by internal fixation and early function: a preliminary report of 20 cases. J Bone Joint Surg Br 1996;78:588-92.
7. Harness NG, Jupiter JB, Orbay JL, Raskin KB, Fernandez DL. Loss of fixation of the volar lunate facet fragment in fractures of the distal part of the radius. J Bone Joint Surg Am 2004;86:1900-8.
8. Falk SS, Mittlmeier T, Gradl G. Residual dorsal displacement following surgery in distal radial fractures: a cause for trouble. Eur J Trauma Emerg Surg 2023;49:843-50.

 https://doi.org/10.12671/jmt.2026.00185

JMT Journal of Musculoskeletal Trauma

Instructions for authors

Enacted from January 1, 1988
Last revision: December 1, 2025

1. GENERAL INFORMATION

The *Journal of Musculoskeletal Trauma* is the official publication of the Korean Orthopaedic Trauma Association (KOTA), and is published in academic collaboration with the Thai Orthopaedic Trauma Society (TOTS) and the Taiwan Orthopaedic Trauma Association (TOTA) as Affiliated Societies. It is an international, peer-reviewed, open-access journal dedicated to advancing the science, education, and clinical care of musculoskeletal trauma. The journal was first launched in 1988 and is published quarterly on the 25th of January, April, July, and October. As of October 2024, the official language of the journal has been changed to English.

The journal covers a wide range of topics related to musculoskeletal injuries, including but not limited to: prevention, diagnosis, treatment, and rehabilitation of fractures, dislocations, and soft tissue injuries of both the extremities and the axial skeleton; advances in surgical techniques, implants, and prosthetic devices; biomechanical and biological research related to trauma and tissue healing; rehabilitation strategies for functional recovery; and clinical and translational research bridging basic science and clinical practice.

We invite submissions of original articles, reviews, case reports, technical notes, letters to the editor, and editorials that contribute to the advancement of musculoskeletal trauma care. Manuscripts submitted to JMT should be prepared according to the following instructions. The journal adheres to the Recommendations for the Conduct, Reporting, Editing, and Publication of Scholarly Work in Medical Journals (http://www.icmje.org/icmje-recommendations.pdf) from the International Committee of Medical Journal Editors (ICMJE).

2. ARTICLE PROCESSING CHARGE

There are no author fees for manuscript processing or publication in the journal, as all costs are covered by the publisher, the Korean Orthopaedic Trauma Association, unless the policy changes. Therefore, it is a platinum open-access journal.

3. RESEARCH AND PUBLICATION ETHICS

The journal adheres to the guidelines for research and publication described in the Committee on Publication Ethics (COPE) Guidances (https://publicationethics.org/resources/guidelines) the ICMJE Recommendations (https://www.icmje.org), and the Good Publication Practice Guideline for Medical Journals (https://www.kamje.or.kr/board/view?b_name=bo_publication&bo_id=14). Furthermore, all processes addressing research and publication misconduct shall follow the flowcharts of COPE (https://publicationethics.org/resources/flowcharts). Any attempts to duplicate publications or engage in plagiarism will lead to automatic rejection and may prejudice the acceptance of future submissions.

Statement of Human and Animal Rights

Clinical research should be conducted in accordance with the World Medical Association's Declaration of Helsinki (https://www.wma.net/what-we-do/medical-ethics/declaration-of-helsinki/). Any investigations involving humans and animals should be approved by the Research Ethics Committee (REC) or the Institutional Review Board (IRB) and Animal Care Committee, respectively, of the institution where the experiment was performed. JMT will not consider any studies involving humans or animals without appropriate approval. Such approval, along with the approval number and the name of the IRB or REC institution, should be stated in the Methods section of the manuscript. Informed consent must be obtained from patients participating in clinical investigations, unless waived by the IRB. In the case of an animal study, a statement should be provided indicating that the experimental procedures, such as the breeding and the use of laboratory animals, was approved by the REC of the institution where the experiment was performed or that it does not violate the rules of the REC of the institution or the National Institutes of Health (NIH) Guide for the Care and Use of Laboratory Animals (Institute of Laboratory Animal Resources, Commission on Life Sciences, National Research Council). The authors should preserve raw experimental study data for at least 1 year after the publication of the paper and should present this data if required by the Editorial Board.

Protection of Privacy, Confidentiality, and Written Informed Consent

The ICMJE has recommended the following statement for the protection of privacy, confidentiality, and written informed consent: The rights of patients should not be infringed without written informed consent. Identifying details (patients' names, initials, hospital numbers, dates of birth, or other personal or identifying information, protected healthcare information) should not be published in written descriptions. Images of human subjects should not be used unless the information is essential for scientific purposes and explicit permission has been given as part of the consent. For individuals who cannot provide consent independently, including those from vulnerable populations—such as minors, the elderly, racial or ethnic minorities, individuals with certain health conditions, or those who are socioeconomically disadvantaged—consent should be obtained from a legally authorized representative or parent/guardian. Even where consent has been given, identifying details should be removed if they are not essential. If identifying characteristics are altered to protect anonymity, authors should provide assurances that such alterations do not distort scientific meaning. If consent has not been obtained, it is generally not sufficient to anonymize a photograph simply by using eye bars or blurring the face of the individual concerned.

Conflict of Interest

Authors are responsible for disclosing any financial support or benefit that might affect the content of the manuscript or might cause a conflict of interest. When submitting the manuscript, the author must attach a conflict of interest statement (https://e-jmt.org/authors/copyright_transfer_agreement.php). All authors should disclose their conflicts of interest, i.e., (1) financial relationships (such as employment, consultancies, stock ownership, honoraria, or paid expert testimony), (2) personal relationship, (3) academic competition, and (4) intellectual passion. These conflicts of interest must be included as a footnote on the title page. Each author should certify the disclosure of any conflict of interest with their signature.

Originality, Plagiarism, and Duplicate Publication

Redundant or duplicate publication refers to the publication of a paper that overlaps substantially with one already published. Upon receipt, submitted manuscripts are screened for possible plagiarism or duplicate publication using Crossref Similarity Check. If a paper that might be regarded as duplicate or redundant had already been published in another journal or submitted for publication, the author should notify the fact in advance at the time of submission. Under these conditions, any such work should be referred to and referenced in the new paper. The new manuscript should be submitted together with copies of the duplicate or redundant material to the editorial committee. If redundant or duplicate publication is attempted or occurs without such notification, the submitted manuscript will be rejected immediately. If the editor was not aware of the violations and of the fact that the article had already been published, the editor will announce in the journal that the submitted manuscript had already been published in a duplicate or redundant manner, without seeking the author's explanation or approval.

Secondary Publication

It is possible to republish manuscripts if the manuscripts satisfy the conditions for secondary publication of the ICMJE Recommendations, available from: https://www.icmje.org/ as follows:

(1) Certain types of articles, such as guidelines produced by governmental agencies and professional organizations, may need to reach the widest possible audience. In such instances, editors sometimes deliberately publish material that is also published in other journals with the agreement of the authors and the editors of those journals.

(2) Secondary publication for various other reasons, in the same or another language, especially in other countries, is justifiable and can be beneficial provid-

ed that the following conditions are met. The authors have received approval from the editors of both journals (the editor concerned with secondary publication must have a photocopy, reprint, or manuscript of the primary version). The priority of the primary publication is respected by a publication interval of at least one week (unless specifically negotiated otherwise by both editors).

(3) The paper for secondary publication is intended for a different group of readers; therefore, an abbreviated version could be sufficient. The secondary version faithfully reflects the data and interpretations of the primary version. The footnote on the title page of the secondary version informs readers, peers, and documenting agencies that the paper has been published in whole or in part and states the primary reference. A suitable footnote might read: "This article is based on a study first reported in the [title of a journal, with full reference]."

Authorship

Authorship credit should be based on substantial contributions to all four categories established by the ICMJE: (1) substantial contributions to conception or design of the work, acquisition of data, and analysis and interpretation of data; (2) drafting the work or revising it critically for important intellectual content; (3) final approval of the version to be published; and (4) agreement to be accountable for all aspects of the work in ensuring that questions related to the accuracy or integrity of any part of the work are appropriately investigated and resolved.

- The contributions of all authors must be described. JMT has adopted the CRediT Taxonomy (https://credit.niso.org/) to describe each author's individual contributions to the work. The role of each author should be addressed on the title page.
- Correction of authorship: Requests for corrections in authorship (such as adding or removing authors, or rearranging the order of authors) after the initial manuscript submission and before publication should be explained in writing to the editor, in a letter or email signed by all authors. A completed copyright assignment form must be submitted by every author.
- Role of corresponding author: The corresponding author takes primary responsibility for communication with the journal during the manuscript submission, peer review, and publication process. The corresponding author typically ensures that all of the journal's administrative requirements, such as providing the details of authorship, ethics committee approval, clinical trial registration documentation, and conflict of interest forms and statements, are properly completed, although these duties may be delegated to one or more co-authors. The corresponding author should be available throughout the submission and peer-review process to respond to editorial queries in a timely manner, and after publication, should be available to respond to critiques of the work and cooperate with any requests from the journal for data, additional information, or questions about the article.
- Contributors: Any researcher who does not meet all four ICMJE criteria for authorship discussed above but contributes substantively to the study in terms of idea development, manuscript writing, conducting research, data analysis, and financial support should have their contributions listed in the Acknowledgments section of the article.

Process for Managing Research and Publication Misconduct

When the journal faces suspected cases of research and publication misconduct, such as redundant (duplicate) publication, plagiarism, fraudulent or fabricated data, changes in authorship, undisclosed conflict of interest, ethical problems with a submitted manuscript, appropriation by a reviewer of an author's idea or data, and complaints against editors, the resolution process will follow the flowcharts provided by COPE (http://publicationethics.org/resources/flowcharts). The discussion and decision on the suspected cases are carried out by the Editorial Board.

Editorial Responsibilities

The Editorial Board will continuously work to monitor and safeguard publication ethics: guidelines for retracting articles; maintenance of the integrity of academic records; preclusion of business needs from compromising intellectual and ethical standards; publishing corrections, clarifications, retractions, and apologies when needed; and excluding plagiarized and fraudulent data. The editors maintain the following responsibilities: responsibility and authority to reject and accept articles; avoid any conflict of interest with respect to articles they reject or accept; promote the publication of corrections or retractions when errors are found; and preserve the anonymity of reviewers.

Artificial Intelligence (AI) Guideline

JMT adheres to the following guidelines specified by the ICMJE regarding the use of AI tools. These measures are essential to ensuring academic integrity and ethical standards.

- AI cannot be listed as an author: AI tools cannot be listed or cited as authors due to their inability to take responsibility for errors.
- Reliability, responsibility, and permissible use of AI: Authors are fully responsible for the reliability, accuracy, originality, and integrity of their manuscripts when using AI tools. They must take complete responsibility for any plagiarism or false information generated by AI. AI-generated content cannot be cited as a primary source. The use of AI tools is permissible only for language editing or formatting assistance, and such use must be transparently disclosed.
- Data privacy and confidentiality: Authors must ensure that no confidential, sensitive, or personally identifiable data are entered into AI tools.
- Disclosure of AI use: Authors must disclose the use of AI tools at the time of manuscript submission. This disclosure should include the specific tools used, their model names, versions, manufacturers, and the role of the AI in the process. This information should be included in the Methods or Acknowledgments section, with detailed prompts included where relevant.
- Prohibition on AI-generated images and videos: AI-generated images or videos, which lack societal consensus on copyright, cannot be included in submitted manuscripts. However, exceptions may be made if AI is essential to the research design or methodology, in which case it must be explained in the Methods section.
- Restrictions for peer reviewers: Peer reviewers are prohibited from uploading manuscripts to external AI tools during the review process. If AI tools are used to support any part of the review, reviewers must transparently disclose this in their peer review reports.
- Editor's authority: the editor may refuse to proceed with the review of a paper if inappropriate use of AI is detected. Additionally, this policy may evolve in response to advancements in technology and societal agreements.

4. EDITORIAL POLICY

Copyright

Copyright in all published material is owned by the Korean Orthopaedic Trauma Association. Authors must agree to transfer copyright (https://e-jmt.org/authors/copyright_transfer_agreement.php) during the submission process. The corresponding author is responsible for submitting the copyright transfer agreement to the publisher. In addition, if excerpts from other copyrighted works are included, the authors must obtain written permission from the copyright owners and credit the sources in the article.

Open-Access License

JMT is an open-access journal. Articles are distributed under the terms of the Creative Commons Attribution License (https://creativecommons.org/licenses/by-nc/4.0/), which permits unrestricted non-commercial use, distribution, and reproduction in any medium, provided the original work is properly cited. Authors do not need permission to use tables or figures published in JMT in other journals, books, or media for scholarly and non-commercial purposes. For any commercial use of material from this open-access journal, permission must be obtained from Korean Orthopaedic Trauma Association (email: office@e-jmt.org).

Article Sharing (Author Self-Archiving) Policy

JMT is an open-access journal, and authors who submit manuscripts to JMT may share their research in several ways, including on preprint servers, social media platforms, at conferences, and in educational materials, in accordance with our open-access policy. Authors may deposit the accepted manuscript or published version in institutional repositories, provided that the original source (JMT, DOI, and publisher information) is clearly cited. All shared versions must include a link to the official publication on the JMT website. Commercial use of the published content is not permitted unless explicitly authorized by the publisher. Submitting the same manuscript to multiple journals is strictly prohibited. This policy may be updated in response to changes in copyright law, licensing agreements, or publisher requirements.

Registration of Clinical Trial Research

It is recommended that any research that deals with a clinical trial be registered with a clinical trial registration site, such as http://cris.nih.go.kr, or other primary national registry sites accredited by the World Health Organization (https://www.who.int/clinical-trials-registry-platform/network/primary-registries) or clinicaltrial.gov (http://clinicaltrials.gov/), a service of the United States National Institutes of Health.

Data Sharing Policy

JMT encourages data sharing wherever possible unless this is prevented by ethical, privacy, or confidentiality matters. Authors wishing to do so may deposit their data in a publicly accessible repository and include a link to the DOI within the text of the manuscript.

- Clinical Trials: JMT accepts the ICMJE Recommendations for data sharing statement policy. Authors may refer to the editorial, "Data Sharing Statements for Clinical Trials: A Requirement of the International Committee of Medical Journal Editors," in the Journal of Korean Medical Science (https://dx.doi.org/10.3346/jkms.2017.32.7.1051).

Archiving Policy

In accordance with the Korean Library Act, the full text of the JMT can be archived in the National Library of Korea. JMT provides electronic archiving and preservation of access to the journal content in the event the journal is no longer published, by archiving in the National Library of Korea (https://www.nl.go.kr/archive/search.do) and the National Library of Korea can permanently preserve submitted JMT papers.

Preprint Policy

A preprint can be defined as a version of a scholarly paper that precedes formal peer review and publication in a peer-reviewed scholarly journal. JMT allows authors to submit preprints to the journal. It is not treated as duplicate submission or duplicate publication. JMT recommends that authors disclose the existence of a preprint with its DOI in the letter to the editor during the submission process. Otherwise, a plagiarism check program—Similarity Check (Crossref) or Copy Killer—may flag the results as containing excessive duplication. A preprint submission will be processed through the same peer-review process as a usual submission. If a preprint is accepted for publication, the authors are recommended to update the information on the preprint site with a link to the published article in JMT, including the DOI at JMT. It is strongly recommended that authors cite the article in JMT instead of the preprint in their next submission to journals.

5. MANUSCRIPT SUBMISSION AND PEER-REVIEW PROCESS

Online Submission

All manuscripts should be submitted online via the journal's website (https://submit.e-jmt.org/) by the corresponding author. Once you have logged into your account, the online system will lead you through the submission process in a step-by-step manner. In case of any trouble, please contact the editorial office (Email: office@e-jmt.org).

Screening after Submission

The screening process will be conducted after submission. If the manuscript does not fit the aims and scope of the Journal or does not adhere to the Instructions to authors, it may be returned to the author immediately after receipt and without a review. Before review, all submitted manuscripts are inspected using "Similarity Check powered by iThenticate (https://www.crossref.org/services/similarity-check/), a plagiarism-screening tool. If an excessively high similarity score is found, the Editorial Board will do a more profound content screening. The criterion for similarity rate for further screening is usually 25%; however, the excess amount of similarity in specific sentences may be also checked in every manuscript. The settings for Similarity Check screening are as follows: It excludes quotes, a bibliography, small matches of 6 words, small sources of 1%, and the Methods section.

Peer-Review Process

All papers, including those invited by the Editor, are subject to peer review. Manuscripts will be peer-reviewed by two accredited experts in the musculoskeletal trauma care with one additional review by a prominent member of our Editorial Board. The editor is responsible for the final decision whether the manuscript is accepted or rejected.

- The journal uses a single-blind peer-review process: the reviewers are aware of the identity of the authors, but the authors do not know the identity of the reviewer. During the peer-review process, reviewers may interact directly or exchange information (e.g., via submission systems or email) only with the editor, which is known as "independent review."
- JMT's average turnaround time from submission to decision is 6 weeks.
- Decision letter will be sent to corresponding author via registered email. Reviewers can request authors to revise the content. The corresponding author must indicate the modifications made in their item-by-item response to the reviewers' comments. Failure to resubmit the revised manuscript within 4 weeks of the editorial decision is regarded as a withdrawal.
- The editorial committee has the right to revise the manuscript without the authors' consent unless the revision substantially affects the original content.
- After review, the Editorial Board determines whether the manuscript will be accepted for publication. Once rejected, the manuscript does not undergo another round of review.
- All articles in JMT include the dates of submission, revision, acceptance, and publication on their article page. No information about the review process or editorial decision process is published on the article page.

Submission by Editors

All manuscripts from editors, employees, or members of the Editorial Board are processed in the same way as other unsolicited manuscripts. During the review process, submitters will not engage in the selection of reviewers or the decision process. Editors will not handle their manuscripts even if the manuscripts are commissioned.

The conflict of interest declaration should be added as follows.

Conflicts of Interest: OOO has been an Editorial Board member of Journal of Musculoskeletal Trauma since OOO but has no role in the decision to publish this article. No other potential conflicts of interest relevant to this article were reported.

Feedback after Publication

If the authors or readers find any errors or contents that should be revised, it can be requested from the Editorial Board. The Editorial Board may consider erratum, corrigendum, or a retraction. If there are any revisions to the article, there will be a CrossMark description to announce the final draft. If there is a reader's opinion on the published article with the form of Letter to the editor, it will be forwarded to the authors. The authors can reply to the reader's letter. Letter to the editor and the author's reply may be also published.

Appeals of Decisions

Any appeal against an editorial decision must be made within 2 weeks of the date of the decision letter. Authors who wish to appeal a decision should contact the Editor-in-Chief, explaining in detail the reasons for the appeal. All appeals will be discussed with at least one other associate editor. If consensus cannot be reached thereby, an appeal will be discussed at a full editorial meeting. The process of handling complaints and appeals follows the guidelines of COPE. JMT does not consider second appeals.

6. MANUSCRIPT PREPARATION

Authors are required to submit their manuscripts after reading the following instructions. Any manuscript that does not conform to the following requirements will be deemed inappropriate and may be returned.

General Requirements

- All manuscripts should be written in English.
- The manuscript must be written using Microsoft Word and saved as ".doc" or ".docx" format. The font size should be 11 points. The body text must be left-aligned, double-spaced, and presented in a single column. The left, right, and bottom margins must be 3 cm, but the top margin must be 3.5 cm.
- The page numbers should be placed in Arabic numerals at the center of the bottom margin, starting from the abstract page.
- Only standard abbreviations should be used. Abbrevi-

ations should be avoided in the title of the manuscript. Abbreviations should be spelled out when first used in the text and the use of abbreviations should be kept to a minimum.

- The names of manufacturers of equipment and non-generic drugs should be given.
- Authors should express all measurements in conventional units, using International System (SI) units.
- P-value from statistical testing should be expressed as capital P.

Reporting Guidelines for Specific Study Designs

For the specific study design, it is recommended that authors follow the reporting guidelines, such as CONSORT (http://www.consort-statement.org) for randomized controlled trials, STROBE (http://www.strobe-statement.org) for observational studies, and PRISMA (http://www.prisma-statement.org) for systematic reviews and meta-analyses. A good source of reporting guidelines is the EQUATOR Network (https://www.equator-network.org/) and NLM (https://www.nlm.nih.gov/services/research_report_guide.html).

Types of Manuscripts

- The manuscript types are divided into original articles, review articles, case reports, technical notes, letters to the editor, editorial, and other types.
- Original Articles: Original articles should be written in the following order: title page, abstract (within 300 words), keywords, main body (introduction, methods, results, discussion, and conclusions), acknowledgments (if applicable), references (up to 30), tables, figure legends, and figures.
- Review Articles: Review articles should focus on a specific topic. The format of a review article is flexible. Publication of these articles will be decided upon by the Editorial Board.
- Case Reports: Case reports should be a report on a single case or an analysis of a few cases to add to the clinical spectrum. Case reports should be written in the following order: title page, abstract (within 200 words), keywords, main body (introduction, case report, and discussion), acknowledgments (if applicable), references (up to 10), tables, figure legends, and figures.
- Technical Notes: Technical notes should be written in the following order: title page, abstract (within 200 words), keywords, main body (introduction, technique, and discussion), acknowledgments (if applicable), references (up to 20), tables (if applicable), figure legends, and figures. The total word count should not exceed 1,500 words.
- Letters to the Editor: The journal welcomes readers' comments on recently published articles or orthopedic topics of interest. Letters to the editor should not exceed 1,000 words, excluding references, tables, and figures. A maximum of 5 references and total 4 figures or tables are allowed.
- Editorials: Editorials are invited by the editors and should be commentaries on articles recently published in the journal. Editorial topics could include active areas of research, fresh insights, and debates in the field of orthopedic surgery. Editorials should not exceed 1,000 words, excluding references, tables, and figures. A maximum of 10 references and total 4 figures or tables are allowed.
- Systematic Reviews and Meta-Analyses: Systematic reviews and meta-analyses should provide a comprehensive and structured overview of published material on a clearly defined subject. Authors must describe in detail how the evidence was identified, including the sources searched and the inclusion and exclusion criteria applied. Meta-analyses should quantitatively synthesize the results of two or more studies to address a specific research question or association. All systematic reviews and meta-analyses submitted to JMT must adhere to the PRISMA guidelines (http://www.prisma-statement.org).

Table 1. Recommended maximums for articles submitted to JMT[a)]

Type of article	Abstract (word)	Text (word)[b)]	References	Tables & Figures
Original Article	Structured, 300	NL	30	NL
Review	Unstructured, 300	NL	NL	NL
Systematic Review	Structured, 300	NL	NL	NL
Case Report	Unstructured, 200	1,500	10	NL
Technical Note	Unstructured, 200	1,500	20	NL
Letter to the Editor	-	1,000	5	4
Editorial	-	1,000	10	4

[a)]The requirements for the number of references, tables and figures and length of the main text can be consulted with the Editorial Office; [b)]Excluding abstract, tables, figures, acknowledgments, and references.

Format of Manuscript Title page

- The title page must include the title, the authors' names, affiliations, and the corresponding author's name and contact information. The corresponding author's contact information must include their name and email. In addition, a running title must be provided, with a maximum of 50 characters, including spaces.

Abstract and keywords

Each paper should begin with an abstract not exceeding 300 words (for original articles and reviews). The abstract for original articles should state the background, methods, results, and conclusions in each paragraph in a brief and coherent manner. Relevant numerical data should be included. Below the abstract, keywords should be provided (maximum of 5). Authors are encouraged to use the MeSH database to find Medical Subject Headings at http://www.nlm.nih.gov/mesh/meshhome.html. The structured abstract should be divided into the following sections.

- Background: The rationale, importance, or objectives of the study should be described briefly and concisely in one to two sentences. The objective should be consistent with that stated in the Introduction.
- Methods: The procedures conducted to achieve the study objective should be described in detail, together with relevant details concerning how data were obtained and analyzed and how research bias was adjusted.
- Results: The most important study results and analysis should be presented in a logical manner with specific experimental data.
- Conclusions: The conclusions drawn from the results should be described in one to two sentences and must align with the study objective.
- Level of evidence: Author should make the final determination of the study design and level of evidence based on the Centre for Evidence Based Medicine guidelines. Authors may refer to the definitions in the Level of Evidence table (https://www.cebm.ox.ac.uk/files/levels-of-evidence/cebm-levels-of-evidence-2-1.pdf).

Main Body

- All articles using clinical samples or data and those involving animals must include information on the IRB/IACUC approval or waiver and informed consent. An example is shown below. "We conducted this study in compliance with the principles of the Declaration of Helsinki. The study protocol was reviewed and approved by the Institutional Review Board of OO (No. OO). Written informed consent was obtained / Informed consent was waived."
- Description of participants: Ensure the correct use of the terms "sex" (when reporting biological factors) and "gender" (identity, psychosocial, or cultural factors), and, unless inappropriate, report the sex and/or gender of study participants, the sex of animals or cells, and describe the methods used to determine sex and gender. If the study was done involving an exclusive population, for example, in only one sex, authors should justify why, except in obvious cases (e.g., ovarian cancer). Authors should define how they determined race or ethnicity and justify their relevance.
- Introduction: State the background or problem that led to the initiation of the study. Introduction is not a book review, rather it is best when the authors bring out controversies which create interest. Lead systematically to the hypothesis of the study, and finally, to a restatement of the study objective, which should match that in the Abstract. Do not include conclusions in the Introduction.
- Methods: Describe the study design (prospective or retrospective, inclusion and exclusion criteria, duration of the study) and the study population (demographics, length of follow-up). Explanations of the experimental methods should be concise, yet enable replication by a qualified investigator.
- Results: This section should include detailed reports on the data obtained during the study. All data in the text must be presented in a consistent manner throughout the manuscript. All issues which the authors brought up in the method section need to be in result section. Also, it is preferred that data be in figures or tables rather than a long list of numbers. Instead, numbers should be in tables or figures with key comments on the findings.
- Discussion: The first paragraph of the discussion should deal with the key point in this study. Do not start with an article review or general comment on the study topic. In the Discussion, data should be interpreted to demonstrate whether they affirm or refute the original hypothesis. Discuss elements related to the purpose of the study and present the rationales that support the conclusion drawn by referring to relevant literature. Discussion needs

some comparison of similar papers published previously, and discuss why your study is different or similar from those papers. Care should be taken to avoid information obtained from books, historical facts, and irrelevant information. A discussion of study weaknesses and limitations should be included, followed by a brief conclusion that clearly states the answer to the research question or hypothesis. Conclusions must be drawn only from the study results, and authors should verify that their data firmly support these conclusions. The conclusions in the text and those in the abstract must be consistent.

- Article Information: This section should include details on Author Contributions, Conflicts of Interest, Funding, Data Availability, Acknowledgments, and Supplementary Materials. If any of these items are not applicable, authors must indicate "None."
- The contributions of all authors must be described using the CRediT (https://credit.niso.org/) taxonomy of author roles.
- References must be numbered with superscripts according to their quotation order. When more than two quotations of the same authors are indicated in the main body, a comma must be placed between a discontinuous set of numbers, whereas a dash must be placed between the first and last numerals of a continuous set of numbers: "Kim et al. [2,8,9] insisted..." and "However, Park et al. [11-14] showed opposing research results."
- Figures and tables used in the main body must be indicated as "Fig." and "Table." For example, "Magnetic resonance imaging of the brain revealed... (Figs. 1-3).
- ORCID: We recommend that the open researcher and contributor ID (ORCID) of all authors be provided. To have an ORCID, authors should register in the ORCID website (http://orcid.org/).

References

- References are recommended as 30 for original articles, 10 for case reports, and 20 for technical notes.
- All references must be cited in the text. The number assigned to the reference citation is according to the first appearance in the manuscript. References in tables or figures are also numbered according to the appearance order. Reference numbers in the text, tables, and figures should in a bracket ([ ]).
- List all authors when there are six or fewer. When there are seven or more authors, list only the first three authors followed by "et al."
- Authors should be listed by surname followed by initials.
- The journals should be abbreviated according to the style used in the list of journals indexed in the NLM Journal Catalog (http://www.ncbi.nlm.nih.gov/nlmcatalog/journals).
- Overlapping page numbers (e.g., 2025-2026) should omit the repeated numerals (e.g., 2025-2026 should be written as 2025-6).
- References to unpublished material, such as personal communications and unpublished data, should be noted within the text and not cited in the References. Personal communications and unpublished data must include the individual's name, location, and date of communication.
- Examples of references are as follows: Journal article

① Journal

1. Song HK, Cho WT, Choi WS, Sakong SY, Im S. Acute compartment syndrome of thigh: ten-year experiences from a level I trauma center. J Musculoskelet Trauma 2024;37:171-4.
2. MacKechnie MC, Shearer DW, Verhofstad MH, et al. Establishing consensus on essential resources for musculoskeletal trauma care worldwide: a modified Delphi study. J Bone Joint Surg Am 2024;106:47-55.
3. Raats JH, Ponds NH, Brameier DT, et al. Agreement between patient- and proxy-reported outcome measures in adult musculoskeletal trauma and injury: a scoping review. Qual Life Res 2024 Aug 23 [Epub]. https://10.1007/s11136-024-03766-1

② Book & Book chapter

4. Townsend CM, Beauchamp RD, Evers BM, Mattox K. Sabiston textbook of surgery. 21st ed. Elsevier; 2021.
5. Meltzer PS, Kallioniemi A, Trent JM. Chromosome alterations in human solid tumors. In: Vogelstein B, Kinzler KW, eds. The genetic basis of human cancer. McGraw-Hill; 2002. p. 93-113.

③ Homepage/Web site

6. World Health Organization (WHO). World health statistics 2021: a visual summary [Internet]. WHO; 2021 [cited 2023 Feb 1]. Available from: https://www.who.int/data/stories/world-health-statistics-2021-a-visual-summary

④ Preprint

7. Sharma N, Sharma P, Basu S, et al. The seroprevalence

and trends of SARS-CoV-2 in Delhi, India: a repeated population-based seroepidemiological study [Preprint]. Posted 2020 Dec 14. medRxiv 2020.12.13.20248123. https://doi.org/10.1101/2020.12.13.20248123

For more on references, refer to the NLM's "Samples of Formatted References for Authors of Journal Articles." https://www.nlm.nih.gov/bsd/uniform_requirements.html#journals

Figures and Figure Legends

Figures should be cited in the text and numbered using Arabic numerals in the order of their citation (e.g., Fig. 1). Figures are not embedded within the text. Each figure should be submitted as an individual file. The figure legends should begin on the next page after the last table. Every figure has its own legend. Abbreviations and additional information for any clarification should be described within each figure legend. Footnotes below the figure should follow the order of abbreviation first, followed by symbols. Symbols should be marked with small alphabet letters in the order of their usage, such as [a)], [b)], [c)], or asterisks (*) for statistical significance. Figure files are submitted in EPS, TIFF, or PDF formats. The requirement for minimum resolutions is dependent on figure types. For line drawings, 1,200 dpi are required. For grey color works (i.e., pictures of gel or blots), 600 dpi is required. For color or half-tone artwork, 300 dpi is required. The files should be named according to the figure number.

- Staining techniques used should be described. Photomicrographs with no inset scale should have the magnification of the print in the legend.
- Papers containing unclear photographic prints may be rejected.
- Remove any writing that could identify a patient.
- If any tables or figures are taken or modified from other papers, authors should obtain permission through the Copyright Clearance Center (https://www.copyright.com/) or from the individual publisher, unless they are from open-access journals under the Creative Commons License. For tables or figures from an open-access journal, simply verify the source of the journal precisely in the accompanying footnote. Please note the distinction between a free access journal and an open-access journal: it is necessary to obtain permission from the publisher of a free-access journal for using tables or figures published therein. Examples are shown below:

  Reprinted (Modified) from Tanaka et al. [48], with permission of Elsevier.

  Reprinted (Modified) from Weiss et al. [2], according to the Creative Commons License.

Tables

- Tables should be numbered sequentially with Arabic numerals in the order in which they are mentioned in the text.
- If an abbreviation is used in a table, it should be defined in a footnote below the table.
- Additional information for any clarification should be designated for citation using alphabetical superscripts [a)], [b)], [c)] or asterisks (*) for statistical significance. The explanation for superscript citation should follow these examples: [a)]Not tested.

  *$P< 0.05$, **$P< 0.01$, ***$P< 0.001$.
- Tables should be understandable and self-explanatory, without references to the text.
- If a table has been previously published, it should be accompanied by the written consent of the copyright holder, and the footnote must acknowledge the original source.

7. MANUSCRIPT PROCESSING AFTER ACCEPTANCE

Final Version

After the paper has been accepted for publication, the authors should submit the final version of the manuscript. The names and affiliations of the authors should be double-checked, and if the originally submitted image files were of poor resolution, higher-resolution image files should be submitted at this time. Symbols (e.g., circles, triangles, squares), letters (e.g., words, abbreviations), and numbers should be large enough to be legible on reduction to the journal's column widths. All symbols must be defined in the figure caption. If references, tables, or figures are moved, added, or deleted during the revision process, renumber them to reflect such changes so that all tables, references, and figures are cited in numeric order.

Manuscript Corrections
Before publication, the manuscript editor will correct the manuscript such that it meets the standard publication format. The authors must respond within two days when the manuscript editor contacts the corresponding author for revisions. If the response is delayed, the manuscript's publication may be postponed to the next issue.

Proof
The authors will receive the final version of the manuscript as a PDF file. Upon receipt, the authors must notify the editorial office (or printing office) of any errors found in the file within two days. Any errors found after this time are the responsibility of the authors and will have to be corrected as an erratum.

Errata and Corrigenda
To correct errors in published articles, the corresponding author should contact the journal's Editorial Office with a detailed description of the proposed correction. Corrections that profoundly affect the interpretation or conclusions of the article will be reviewed by the editors. Corrections will be published as corrigenda (corrections of the author's errors) or errata (corrections of the publisher's errors) in a later issue of the journal.

NOTICE: These recently revised instructions for authors will be applied beginning with the January 2026 issue.

Checklist

- ☐ Manuscript in MS-WORD (DOC, DOCX) format.
- ☐ Double-spaced typing with 12-point font.
- ☐ Sequence of title page, abstract and keywords, introduction, methods, results, discussion, and conclusions, acknowledgments, references, tables, and figure legends. All pages and manuscript text with line should be numbered sequentially, starting from the abstract.
- ☐ Title page with article title, authors' full name(s) and affiliation(s), address for correspondence (including telephone number, and email address), running title (less than 50 characters), and acknowledgments, if any.
- ☐ Abstract in structured format up to 300 words for original articles. Keywords (up to 5) from the MeSH.
- ☐ All table and figure numbers are found in the text.
- ☐ Figures as separate files, in TIFF, JPG, GIF, or PPT format.
- ☐ References listed in proper format. All references listed in the reference section are cited in the text and vice versa.

JMT Journal of Musculoskeletal Trauma

Copyright transfer agreement and COI disclosure

Manuscript Title ____

I. Copyright Transfer Form

The authors hereby transfer all copyrights in and to the manuscript titled above, in all forms and media, whether now known or hereafter developed, to the Korean Orthopaedic Trauma Association effective upon the manuscript's acceptance for publication in the *Journal of Musculoskeletal Trauma*. The authors retain all proprietary rights other than copyright, such as patent rights.

Everyone listed as an author on this manuscript has made a substantial, direct, and intellectual contribution to the work and assumes public responsibility for its content. This manuscript represents original work that has not previously published and is not currently under consideration for publication in any other journal.

List the names of all authors in the correct order.

____

____

____

The corresponding author signs this copyright agreement on behalf of all the co-authors.

Name(s) of the corresponding author(s): ______________________________

Signature: ______________________________ Date: ______________________

JMT Journal of Musculoskeletal Trauma

Conflict of interest form

Manuscript Title ____

____

As an integral part of the online submission process, Journal of Musculoskeletal Trauma policy requires that each author confirms whether he or she has any conflicts of interest or financial support to declare and to provide any such details.

Signature

By signing this conflict of interest form, each and every undersigned author agrees to the following: To the best of my knowledge, I have no relevant financial relationships except as follows (please list any possible exceptions below the author name).

Author Name__________________ Signed______________ Date______________(DD/ MM/ YY)

____

Author Name__________________ Signed______________ Date______________(DD/ MM/ YY)

____

Author Name__________________ Signed______________ Date______________(DD/ MM/ YY)

____

Author Name__________________ Signed______________ Date______________(DD/ MM/ YY)

____

Author Name__________________ Signed______________ Date______________(DD/ MM/ YY)

____

Author Name__________________ Signed______________ Date______________(DD/ MM/ YY)

____